สมบัติเชิงกลของคอมพอสิตยางธรรมชาติเสริมแรงด้วยกระดองปลาหมึก

นาย พนธวิชญ์ คลังสุวรรณ์

MECHANICAL PROPERTIES OF CUTTLEBONE REINFORCED NATURAL RUBBER COMPOSITES

Mr. Pontawit Klungsuwan

A Thesis Submitted in Partial Fulfillment of the Requirements

for the Degree of Master of Science Program in Petrochemistry and Polymer Science

Faculty of Science

Chulalongkorn University

Academic Year 2010

Thesis Title   MECHANICAL PROPERTIES OF CUTTLEBONE

         REINFORCED NATURAL RUBBER COMPOSITES

By   Mr.Pontawit Klungsuwan

Field of Study   Petrochemistry and Polymer Science

Thesis Advisor   Assistant Professor Sirilux Poompradub, Ph.D.

Accepted by the Faculty of Science, Chulalongkorn University in Partial
Fulfillment of the Requirements for the Master's Degree

…………………………………………….. Dean of the Faculty of Science

(Professor Supot Hannongbua, Dr.rer.nat.)

THESIS COMMITTEE

………………………………………….. Chairman

(Professor Pattarapan Prasassarakich, Ph.D.)

………………………………………….. Thesis Advisor

(Assistant Professor Sirilux Poompradub, Ph.D.)

………………………………………….. Examiner

(Associate Professor Wimonrat Trakarnpruk, Ph.D.)

………………………………………….. External Examiner

(Assistant Professor Chanchai Thongpin, Ph.D.)

พนธวิชญ์ คลังสุวรรณ์ : สมบัติเชิงกลของคอมพอสิตยางธรรมชาติเสริมแรงด้วยกระดอง
ปลาหมึก. (MECHANICAL PROPERTIES OF CUTTLEBONE REINFORCED
NATURAL RUBBER COMPOSITES) อ. ที่ปรึกษาวิทยานิพนธ์หลัก: ผศ.ดร.ศิริลักษณ์
พุ่มประดับ, 118 หน้า

กระดองปลาหมึกเป็นสารชีวมวลที่สำคัญซึ่งสามารถนำมาใช้เป็นสารตัวเติมเสริมแรงให้กับ
ยางธรรมชาติ องค์ประกอบที่สำคัญที่มีอยู่ในกระดองปลาหมึกคือแคลเซียมคาร์บอเนต ซึ่งเป็น
สารประกอบอนินทรีย์ประมาณ 89 - 94 % ในส่วนขององค์ประกอบที่เหลือประกอบไปด้วย
สารประกอบอินทรีย์ประเภทโปรตีน (3 – 7 %) และไคติน (3 – 4 %) ไคตินที่ได้จากการสกัดกระดอง
ปลาหมึกถูกนำมาพิสูจน์เอกลักษณ์โดยเทคนิคฟูเรียร์ทรานฟอร์มอินฟราเรดสเปกโทรสโกปี พบว่า
โครงสร้างทางเคมีของไคตินที่มีอยู่ในกระดองปลาหมึกอยู่ในรูปของเบต้าฟอร์ม คอมพอสิตยาง
ธรรมชาติถูกเตรียมโดยผ่านกระบวนการวัลคาไนเซชันในระบบซัลเฟอร์ทั้งสามประเภทคือ ระบบวัล
คาไนซ์แบบปกติ แบบกึ่งประสิทธิภาพ และแบบประสิทธิภาพ จากการศึกษาสมบัติการคงรูปของ
ยางคอมปาวด์ที่อัตราส่วนการเติมสารเสริมแรงที่อัตราส่วนต่าง ๆ กัน พบว่าเวลาที่ยางเกิดการคงรูป
ก่อนกำหนดและเวลาที่เหมาะสมในการวัลคาไนเซชันของยางคอมปาวด์มีแนวโน้มลดลง เมื่อ
ปริมาณของสารเสริมแรงเพิ่มขึ้น ผลการทดสอบสมบัติเชิงกลของคอมพอสิตยางธรรมชาติพบว่า
การใช้อนุภาคกระดองปลาหมึกเป็นสารเสริมแรงในยางธรรมชาติผ่านระบบวัลคาไนซ์แบบซัลเฟอร์
ทั้งสามประเภท สามารถปรับปรุงสมบัติเชิงกลด้านต่าง ๆ ของยางธรรมชาติได้และให้ผลการทดลอง
เทียบเท่ากับแคลเซียมคาร์บอเนตที่ใช้ในทางการค้า อย่างไรก็ตามการใช้สารเสริมแรงประเภท
แคลเซียมคาร์บอเนตมิได้ส่งผลต่อการปรับปรุงความต้านทานต่อการฉีกขาดและความต้านทานต่อ
การสึกหรอของคอมพอสิตยางธรรมชาติ เมื่อคอมพอสิตยางธรรมชาติถูกนำไปบ่มเร่งด้วยความร้อน
พบว่ายางธรรมชาติที่มีการเสริมแรงด้วยแคลเซียมคาร์บอเนตมีความเสถียรทางความร้อนที่ดีกว่า
เมื่อเทียบกับยางธรรมชาติที่ไม่มีการเติมสารเสริมแรง อย่างไรก็ตาม สารเสริมแรงประเภทแคลเซียม
คาร์บอเนตไม่สามารถป้องกันการเสื่อมสภาพของยางธรรมชาติเนื่องมาจากโอโซน สมบัติเชิงพลวัต
ของยางธรรมชาติที่มีอนุภาคกระดองปลาหมึกเป็นสารเสริมแรงสามารถให้ผลที่ใกล้เคียงกับยาง
ธรรมชาติที่ใช้แคลเซียมคาร์บอเนตเกรดการค้า นอกจากนี้จากการศึกษาลักษณะทางสัณฐานวิทยา
โดยใช้กล้องจุลทรรศน์อิเล็กตรอนแบบส่องกราด พบว่าการมีอยู่ของสารประกอบอินทรีย์ส่งผลให้
ความสามารถในการเกิดอันตรกิริยาของอนุภาคกระดองปลาหมึกกับตัวกลางยางธรรมชาติได้ดี

สาขาวิชา..ปิโตรเคมีและวิทยาศาสตร์พอลิเมอร์.. ลายมือชื่อนิสิต.......พนธวิชญ์ คลังสุวรรณ์

ปีการศึกษา................2553.....................ลายมือชื่อ อ.ที่ปรึกษาวิทยานิพนธ์หลัก......

5172370523   : MAJOR PETROCHEMISTRY AND POLYMER SCIENCE

KEYWORDS : CALCIUM CARBONATE / COMPOSITES MATERIAL / CUTTLEBONE / NATURAL RUBBER / REINFORCING FILLER

PONTAWIT KLUNGSUWAN: MECHANICAL PROPERTIES OF CUTTLEBONE REINFORCED NATURAL RUBBER COMPOSITES. ADVISOR: ASST.PROF. SIRILUX POOMPRADUB, Ph.D., 118 pp.

Cuttlebone is an important biomass which can be incorporated in natural rubber (NR) as a reinforcing filler. The main composition in cuttlebone particles was inorganic calcium carbonate ($CaCO_3$) about 89 – 94 % and the remained contents were protein (3 - 7 %) and chitin (3 - 4 %). The obtained chitin extracted from cuttlebone had been characterized by fourier transform infrared spectroscopy (FTIR). The results indicated that the characteristic absorption peaks were corresponding to the chemical structure of chitin in β-form. The composites were prepared via three kinds of sulfur vulcanizations, i.e., conventional vulcanization (CV), semi-efficiency vulcanization (semi-EV) and efficiency vulcanization (EV) systems. From the results of cure characteristics, the scorch time and cure time of NR compounding trended to be decreased with increasing filler loading. The mechanical properties of NR composites via three kinds of sulfur vulcanizations were improved by addition of cuttlebone particles and the mechanical properties were found to be comparable with those of the NR filled with commercial $CaCO_3$. However, the $CaCO_3$ did not improve the tear and abrasion resistances of the NR composites. When the NR composites were subjected to thermal aging, it was found that the incorporation of the $CaCO_3$ filler could improve the thermal stability of composite materials, compared with NR vulcanizate without the reinforcing filler. Nevertheless, the incorporation of $CaCO_3$ filler could not prevent the surface cracking caused by ozone. Dynamic mechanical properties of cuttlebone particles filled NR vulcanizates were comparable with those of the commercial $CaCO_3$ filled ones. In addition, the presence of organic component such as chitin was affected to give a good rubber-filler interaction of cuttlebone particles to NR matrix as supported by scanning electron microscopy (SEM).

Field of Study:..Petrochemistry and Polymer Science..Student's Signature.P. Klungsuwan

Academic Year:...............2010..........................Advisor's Signature...Sirilux P.

ACKNOWLEDGEMENTS

CONTENTS

LIST OF TABLES

LIST OF FIGURES

FIGURE   PAGE

LIST OF SCHEMES

ศูนย์วิทยทรัพยากร

จุฬาลงกรณ์มหาวิทยาลัย

LIST OF ABBREVIATIONS

ASTM	: American Society for Testing and Materials
$^{\circ}$C	: Degree Celsius
CA	: Commercial calcium carbonate
CBS	: *N*-cyclohexylbenzothiazole-2-sulfenamide
CTB	: Cuttlebone Particle
CV	: Conventional Vulcanization
DMA	: Dynamic Mechanical Analysis
EV	: Efficient Vulcanization
FTIR	: Fourier Transform Infrared Spectroscopy
MPa	: Mega Pascal
NR	: Natural Rubber
phr	: Part per hundred part of rubber
SEM	: Scanning Electron Microscope
semi-EV	: Semi-Efficient Vulcanization
TGA	: Thermo Gravimetric Analysis
ZnO	: Zinc Oxide

CHAPTER I

INTRODUCTION

1.1 Statement of Problems

Natural rubber (NR) is one of the most important elastomers, which widely used in many applications and products such as rubber band, gloves, rubber tubes, conveyor belts and vehicle tires, because it has many excellent unique physical and chemical properties. In fact, the growing industrial activities create a continual demand to improve materials that satisfy more stringent requirements, such as higher tensile strength, modulus and thermal properties. These requirements, which often involve a combination of many difficult-to-attain properties, can be satisfied by utilizing a composite material. Therefore, the reinforcement of elastomers by particulate fillers has been extensively studied. The reason is naturally the drastic changes in mechanical properties that induce fillers reinforcement.

In rubber industry, there are much kind of the filler, the whole of inert filler, semi-reinforcing filler and reinforcing filler, such as carbon black, silica (SiO_2), talc, china clay and calcium carbonate ($CaCO_3$). In general, a carbon black and silica reinforced natural rubber have been commonly used as reinforcing filler in the various rubber applications. The reinforcement is expressed by the enhancement of the modulus, tensile properties, hardness, tear resistance and abrasion resistance. However, the carbon black and silica are non-renewable material that obtained from incomplete combustion of hydrocarbon feedstock and chemical process, respectively [1]. Furthermore, $CaCO_3$ is also utilized as filler for rubber for many years. It has been used as filler for rubber and plastics not only to improve the mechanical properties of the composites but also to reduce the cost of products. Nevertheless, $CaCO_3$ also obtained from the chemical process that involves precipitation. According to these reasons, there has been a growing interest in the use of reinforcing filler from renewable resources such as bamboo, coir, rice husk, wood flour and chitin as a reinforcing element in rubbery matrix [2-6]. Polymers from renewable resources have attracted an increasing amount of attention due to two major reasons: firstly environmental concerns and secondly the realization that our petroleum resources are finite. The specific benefits of these natural product are low cost, easy availability,

lightweight, renewable character, high specific strength and modulus, without residue after burning at the end of their life-cycle and biodegradability [7].

In this research, cuttlebone, is an interesting abundant natural material from food industrial, was used as a reinforcing filler in NR composites. It was mainly composed of $CaCO_3$ and the organic component such as protein and chitin [8]. In the previous study, Poompradub *et al*. [9] studied the reinforcement effect of cuttlebone particles on the mechanical properties of NR vulcanizates in the peroxide vulcanization system. The results revealed that the efficiency of the cuttlebone filled NR could be comparable with the commercial $CaCO_3$ filled ones. Probably, the presence of the organic component brought to the good reinforcement of cuttlebone in NR. Generally, the sulfur vulcanization is commonly used for vulcanizing rubber compound in various industries owing to the superior mechanical properties compared with peroxide vulcanization. Therefore, the effect of cuttlebone on the curing characteristic, mechanical, and thermal properties of NR vulcanizates in sulfur vulcanization system was investigated and all results were compared with commercial $CaCO_3$ filled NR vulcanizates. Furthermore, the dynamic mechanical properties and the morphology of the cuttlebone filled NR vulcanizates were also examined. Additionally, the organic compounds in the cuttlebone particles were identified and characterized by Fourier Transform Infrared Spectroscopy (FTIR). Finally, the mechanism of reinforcement effect of cuttlebone in NR vulcanizates was also proposed.

1.2 Objectives

The objectives of this research are as follows:

    1.2.1   To determine the organic components containing in the cuttlebone.

    1.2.2   To study the effect of cuttlebone particles on the mechanical, thermal, dynamic mechanical, morphological properties and ozone stability of sulfur crosslinked NR.

1.3 Scope of Work

1.3.1   Review related previously published research.

1.3.2   Design and prepare experimental procedure and chemical substances.

1.3.3   Study the characteristic of the cuttlebone and characterize the organic component by following methods:

      a) demineralization was carried out in dilute hydrochloric acid solution (1 M HCl) at ambient temperature for 3 h with a ratio of the solution to cuttlebone of 40 ml/g.

      b) deproteinization was performed by using alkaline treatments with 1 M sodium hydroxide solutions.

1.3.4   Prepare the formulation for rubber compounding with various three curing systems, including:

      a) Conventional vulcanization (CV).

      b) Semi-efficient vulcanization (semi-EV).

      c) Efficient vulcanization (EV).

1.3.5   Determine cure characteristic such as scorch time, optimum cure time and maximum torque.

1.3.6   Study the mechanical properties of cuttlebone filled NR vulcanizates as follows:

      a) Tensile properties by using Universal Testing Machine.

      b) Hardness by using Shore type A Durometer.

      c) Tear strength by using Tear Resistance Tester.

      d) Abrasion resistance by using DIN Abrasion Tester.

1.3.7   Study the thermal resistance, ozone stability and dynamic mechanical analysis (DMA) of cuttlebone filled NR vulcanizates.

1.3.8   Investigate the morphology of cuttlebone particles filled NR vulcanizates by using Scanning Electron Microscope (SEM).

1.3.9   Compare all results with commercial $CaCO_3$ filled NR vulcanizates.

1.3.10 Analyze data, summarize the results and write thesis.

CHAPTER II

THEORY AND LITERATURE REVIEWS

2.1 Natural Rubber (NR)

Natural rubber (NR) is an elastic hydrocarbon polymer which occurs as a milky emulsion (known as *latex*) in the sap of a number of plants but can also be produced synthetically. The major commercial source of the latex used to create rubber is the Para rubber tree, *Hevea brasiliensis*. NR also contains small amounts of non-rubber substances, notably amino acid, protein, lipid and inorganic constituents. Proteins and lipids are the major non-rubber substances in NR. They are believed to cover the surface of rubber particles and yield substantial effect on some properties of NR; for example, alanine, ethanolamine and arginine increase the formation of chemical crosslinks or increase the efficiency of sulfur vulcanization [10]. This naturally occurring polymer is known chemically as cis-1,4-polyisoprene (Figure 2.1). Recently, several million tonnes of NR are still produced annually, and is still essential for many industrials and technological areas, including automotive and military [11].
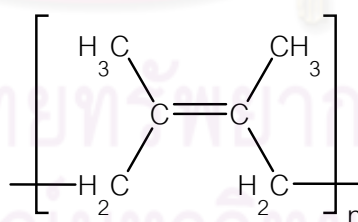
Figure 2.1 Structure of NR (cis-1,4-polyisoprene).

The repeating unit in NR has the cis-configuration (with chain extensions on the same side of the ethylene double bond), which is essential for elasticity. If the configuration is trans- (with chain extensions on opposite sides of the ethylene double bond), the polymer is either a hard plastic (naturally occurring gutta-percha) [12]. The possibility that the NR molecule might contain a mixture of cis- and tran- groups was

considered to be unlikely because such a mixed polymer would have an irregular structure and be unable to crystallize in the manner of natural rubber. In addition, infrared studies have indeed shown that NR was at least 97% cis-1, 4-polyisoprene. The absence of any peak corresponding to a vinyl group precluded the presence of measurable amounts of 1,2- structure but an infrared band at 890 cm^{-1} was at one time thought to be due possibly to the products of a 3,4- structure as shown in Figure 2.2 [13].

(a)   (b)   (c)
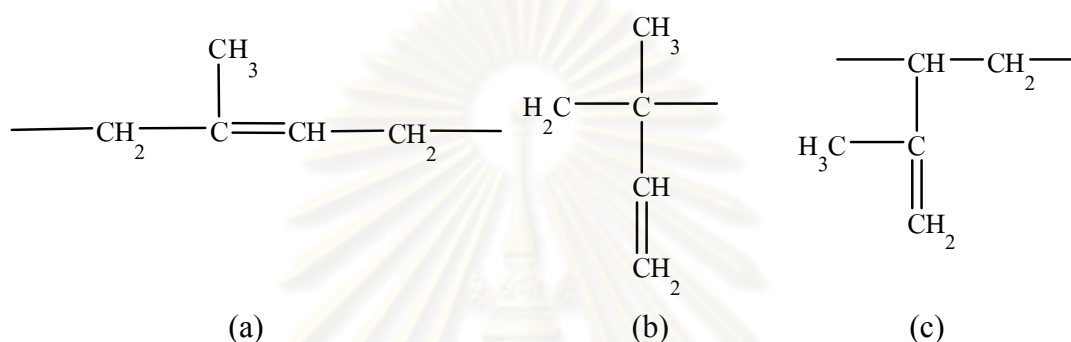
Figure 2.2 Structure of polyisoprene isomer (a) 1,4-polyisoprene, (b) 1,2-polyisoprene and (c) 3,4-polyisoprene [13].

On account of its unique chemical and physical properties, NR is widely used in many industrial especially in tire manufacture. Other important applications include: the production of thin-walled, soft products with a high strength such as balloons, surgical gloves, or sanitary rubber products. Due to its strain crystallization and thus, self-reinforcing properties, NR still dominates in these applications [14-15].

2.2 Mixing Machinery for Rubber Compounding

Mixing is defined as a process which reduces the composition nonuniformity or inhomogeneity of a mixture of two or more components. In conjunction with the chemicals used in a rubber formulation to ensure acceptable product characteristics, a number of ingredients may be incorporated to allow or improve processing with the manufacturing equipment available in the plant.

Historically [16], rubber compounding is almost simultaneously with Goodyear's discovery of sulfur vulcanization, it was found that kneading, or softening, the elastomer was useful in increasing its receptivity to incorporation of

powders. During mixing in the internal mixer or open mill the additives should facilitate homogeneous blending of difference polymers and enable faster incorporation of fillers and other compounding materials. Mixing must provide two basic functions to give a well-mixed rubber compound, both equally important: intensive or dispersive mixing and high uniformity or distributive mixing. In many cases the piece of equipment used most often by the rubber technologist is a two-roll mill (Figure 2.3)
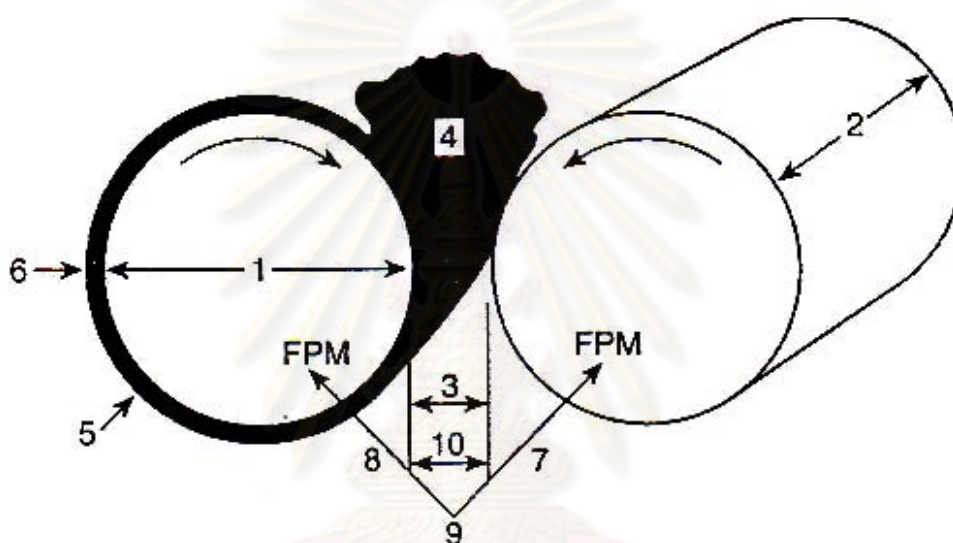
Figure 2.3 Two-roll mill: 1. Diameter (D) 2. Face length (L) 3. Roll gap 4. Bank size 5. Banded roll 6. Front roll 7. Slow roll 8. Fast roll 9. Friction roll 10. Separating force [16].

The two-roll mill was consisted of two horizontal cylindrical rolls rotating in opposite directions with an adjustable gap between them (nip gap) and varying roll frequency. Two-roll mills are important mixing equipment in almost all rubber industries. In large-capacity plants, although mixing is carried out in an internal mixer like Banbury mixer and the mills are used for sheeting out and warming up of the master-batches, yet in small and medium capacity industries, and for specialty rubber mixing, two-roll mills still constitute the main mixing equipment. The completeness and ease of mixing depend on the physical properties of the rubber and other

ingredients, process temperature, rheological behavior of gum rubbers and filled compounds and the machine parameter including: roll speed, speed ratio or friction ratio, nip gap, roll diameter and length. Although, the two-roll mill has been the oldest mixing equipment in use in the rubber industry, rubber mixing on the roll mill is still more of an art than science, and an expert mill operator is the key to efficient mixing [17].

2.3 Vulcanization

Vulcanization is the process of treating an elastomer with a chemical to decrease its plasticity, tackiness, and sensitivity to heat and cold and to give it useful properties such as elasticity, strength and stability. Ultimately, this process chemically converts thermoplastic elastomer into three-dimensional elastic networks. This process converts a viscous entanglement of long-chain molecules into a three-dimensional elastic network by chemically joining (cross-linking) these molecules at various points along the chain. The process of vulcanization is depicted graphically in Figure 2.4. In this diagram, the polymer chains are represented by the lines and the cross-links by the black circles [18]. In addition, the comparison between raw natural rubber and vulcanised natural rubber are summarized in Table 2.1.

Raw Rubber   Vulcanized Rubber
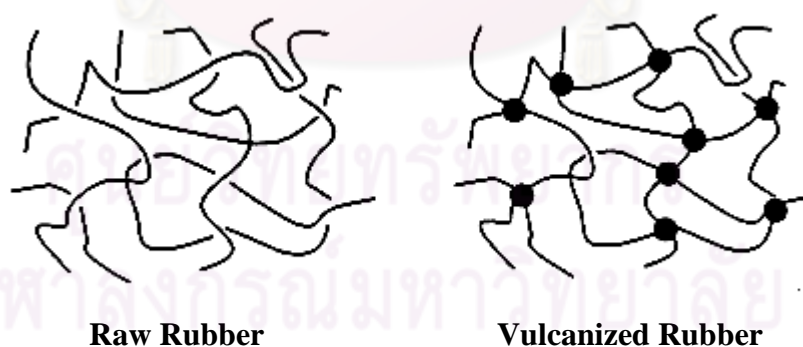
Figure 2.4 The formation of a cross-linked network [18].

Table 2.1 Comparison between raw natural rubber and vulcanized natural rubber
[19].

Raw Natural Rubber	Vulcanized Natural Rubber
- Soft and sticky	- Comparatively hard and non-sticky
- Low tensile strength and not very strong	- High tensile strength and very strong
- Low elasticity	- High elasticity
- Can be used over a narrow range of temperature from 10 to 60 degrees centigrade	- Can be used over a wide range of temperature from -40 to 100 degrees centigrade
- Low abrasion resistance	- High abrasion resistance
- Absorbs a large amount of water	- Absorbs a small amount of water
- Soluble in solvents like ether, carbon disulfide, carbon tetrachloride, and petrol	- Insoluble in all the usual solvents

2.3.1 Terminology of Curing Parameters

The following is a short list of terminology commonly used within rubber industry discussion of vulcanization of general-purpose elastomers [18, 20] and the result of rheometer cure curve is presented in Figure 2.5.

Scorch is the initial formation of an extensive three-dimensional network rendering the compound elastic. The compound is thus no longer plastic or deformable and cannot be shaped or further processed. Scorch safety is the length of time for which the compound can be maintained at an elevated temperature and still remain plastic. This time marks the point at which the plastic material begins the chemical conversion to the elastic network. Thus, if the compound scorches before it

is formed into the desirable shape or composite structure it can no longer be used. Time to scorch is thus importance because it indicates the amount of time the compound may be exposed to heat during shaping and forming operations before it becomes an intractable mass.

Rate of cure is the rate at which cross-links form. After the point of scorch, the chemical cross-linking continues providing more cross-links and thus greater elasticity or stiffness (modulus). The rate of cure determines how long a compound must be cured in order to reach "optimum" properties.

Cure time is the time required to reach a desired state of cure. Most common lab studies use the t_{90} cure time, which is the time required to reach 90% of the maximum cure.

State of cure refers to the degree of cross-linking (or cross-link density) of the compound. State of cure is commonly expressed as a percentage of the maximum attainable cure (or cross-link density) for a given cure system. The elastic force of retraction, elasticity, is directly proportional to the cross-link density or number of cross-links formed in the network.

Reversion refers to the loss of cross-link density as a result of non-oxidative thermal aging. Reversion occurs in isoprene-containing polymers to the extent that the network contains polysulfidic cross-links. Reversion converts a polysulfidic network into a network rich in monosulfidic and disulfidic cross-links and, most important, one that has a lower cross-link density than the original network. Reversion does not occur or hardly occurs in isoprene polymers cured with vulcanization systems designed to produce networks rich in monosulfidic and disulfidic cross-links. Reversion is commonly characterized by the time required for a defined drop in torque in the rheometer as measured from the maximum observed torque.

Over cure A cure which is longer than optimum is an "overcure." Overcure may be in two types. In one type, the stock continues to harden, the modulus rises, and tensile and elongation fall. In other cases, including most natural rubber compound, reversion occurs with overcure and the modulus and tensile strength decrease.
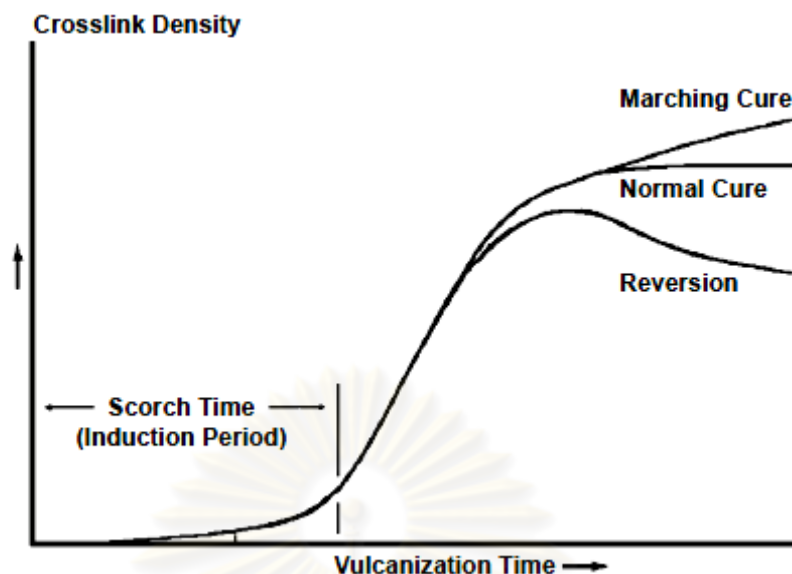
Figure 2.5 Rheometer cure curve.

The kinetic of vulcanization are studied using curemeters or rheometers that measure the development of torque as a function of time at a given temperature. An idealize cure curve is given in Figure 2.6. Several important values derived from the rheometer characterize the rate and extent of vulcanization of a compound. Critical values include the following.

M_L or R_{min} The minimum torque in the rheometer. This parameter often correlates well with the Mooney viscosity of a compound.

M_{HR} or R_{max} The maximum torque achieved during the cure time.

t_{s2} The time required for the state of cure to increase to two torque units above the minimum at the given cure temperature. This parameter often correlates well with the Mooney scorch time.

t_{c90} The time required to reach 90% of full cure defined as M_{HR} - M_L. t_{90} is generally the state of cure at which the most physical properties reach optimum results.
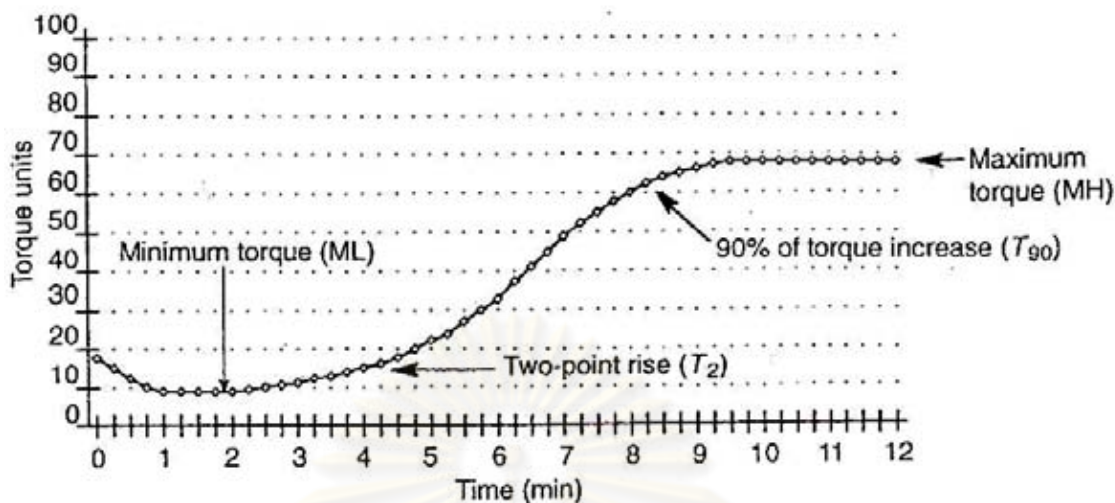
Figure 2.6 Typical rheometer curve [18].

2.3.2 Vulcanization Condition

In vulcanization processes, consideration must be made for the difference in the thickness of the objects involved, the vulcanization temperature, and the thermal stability of the rubber compound [20].

Effect of thickness. Rubbers are poor heat conductors, thus it is necessary to consider the heat conduction, heat capacity, geometry of the mold, heat exchange system, and the curing characteristic of a particular compound when articles thicker than about one-quarter of an inch are being vulcanized. This effect is best shown by immersing thermocouples at various depths in a rubber compound and measuring the time required to reach the vulcanization temperature as indicated by the press temperature. Since these effects are complicated, generally an estimate of the time required can be determined by adding an additional 5 minutes to the cure time for every one-quarter inch of thickness. In exceptionally thick or complicated articles, the item may be built up using sections with different curing characteristics, or by controlling the rate at which the mold is heated or cooled.

Effect of temperature. The vulcanization temperature must be chosen in order to produce a properly cured product having uniform physical properties in the shortest possible molding time. The "temperature coefficient of vulcanization" is a term used to identify the relationship that exists between different cure times at different temperatures. With information of this type, optimum cure times at higher or lower temperatures can be estimated for many rubber compounds with known coefficients of vulcanization. For example, most rubber compounds have a coefficient of approximately 2. This indicated that the cure time must be reduced by a factor of 2 for each 18 ^{0}F (10 ^{0}C) increase in cure temperature, or, if the temperature is reduced 18 ^{0}F, the cure time must be doubled.

Effect of thermal stability. Each type of rubber has a definite range of temperatures which may be used for vulcanization. These temperatures may vary somewhat but it is quite important not to exceed the maximum for each, as some form of deterioration will occur. This effect is either shown by the appearance of the finished product or its physical properties.

2.3.3 Effects of Vulcanization on Vulcanizates Properties

Vulcanization causes profound changes at the molecular level. The long rubber molecules (molecular weight usually between 100,000 and 500,000 daltons) become linked together with junctures (crosslinks) spaced along the polymeric chains, with the average distance between junctures corresponding to a molecular weight between crosslinks of about 4,000 to 10,000 daltons. As a result of this network formation, the rubber becomes essentially insoluble in any solvent, and it cannot be processed by any means which requires it to flow, e.g., in a mixer, in an extruder, on a mill, on a calender, or during shaping, forming, or molding.Thus, it is essential that vulcanization occur only after the rubber article is in its final form [21].

Major effects of vulcanization on use-related properties are illustrated by the idealization of Figure 2.6. It should be noted that static modulus increases with vulcanization to a greater extent than does the dynamic modulus. (Here, static modulus is more correctly the equilibrium modulus, approximated by a low strain, slow-strain-rate modulus. Dynamic modulus is generally measured with the imposition of a sinusoidal, small strain at a frequency of 1–100Hz.) The dynamic

modulus is a composite of viscous and elastic behavior, whereas static modulus is largely a measure of only the elastic component of rheological behavior [22-24].

Hysteresis is reduced with increasing crosslink formation. Hysteresis is the ratio of the rate-dependent or viscous component to the elastic component of deformation resistance. It is also a measure of deformation energy that is not stored (or borne by the elastic network) but that is converted to heat. Vulcanization then causes a trade-off of elasticity for viscous or plastic behavior. Tear strength, fatigue life, and toughness are related to the breaking energy. Values of these properties increase with small amounts of crosslinking, but they are reduced by further crosslink formation. Properties related to the energy-to-break increase with increases in both the number of network chains and hysteresis. Since hysteresis decreases as more network chains are developed, the energy-to-break related properties are maximized at some intermediate crosslink density [24]. It should be noted that the properties given in Figure 2.7 are not functions only of crosslink density. They are also affected by the type of crosslink, the type of polymer, and type and amount of filler, etc.
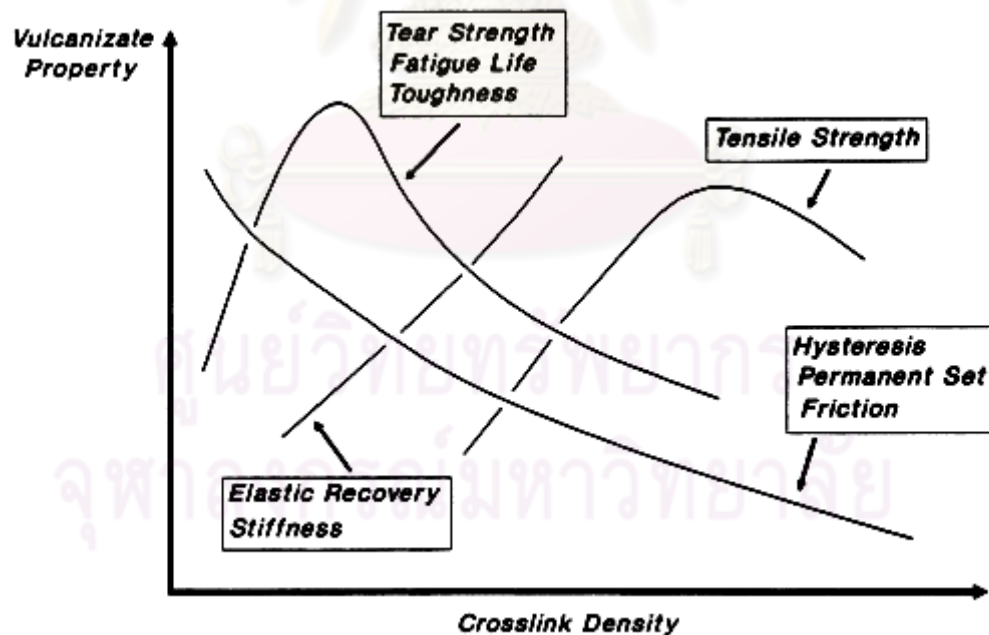
Figure 2.7 Vulcanizate properties as a function of the extent of vulcanization [25].

2.3.4 Sulfur Vulcanization and Acceleration

Initially, vulcanization was accomplished by using elemental sulfur at a concentration of 8 parts per 100 parts of rubber (phr). It required 5 hours at 140 °C. The addition of zinc oxide reduced the time to 3 hours. The use of accelerators in concentrations as low as 0.5 phr has since reduced the time to as short as 1 to 3 minutes. As a result, elastomer vulcanization by sulfur without accelerator is no longer of much commercial significance. (An exception to this is the use of about 30 or more phr of sulfur, with little or no accelerator, to produce molded products of hard rubber or "ebonite.") Even though unaccelerated sulfur vulcanization is not of commercial significance, its chemistry has been the object of much research and study. The chemistry of unaccelerated vulcanization is controversial. Many slow reactions occur over the long period of vulcanization. Some investigators have felt that the mechanisms involved free radicals as illustrated in Scheme 2.1 [25]:
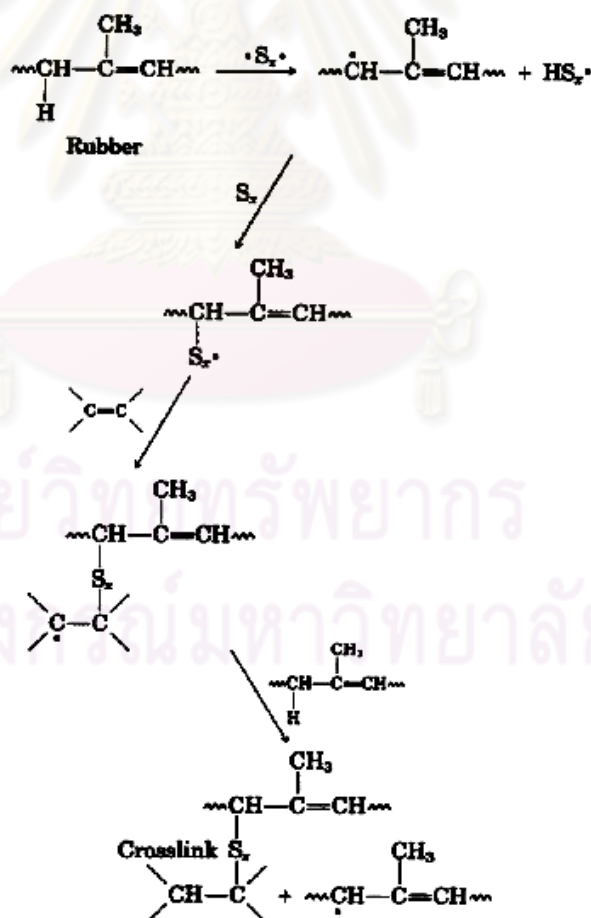
Scheme 2.1 Mechanism of unaccelerated sulfur vulcanization of rubber.

Although vulcanization takes place by heat and pressure in the presence of sulfur, the process is relatively slow, inefficient process. A faster process is normally achieved by the addition of small amounts of chemicals known as accelerators. For this reason over a century of research efforts have been directed toward the development of materials to improve the efficiency of this process. The activators, accelerators, and retarders are associated with the sulfur vulcanization of polydienes, e.g. NR, as shown in Table 2.2 [18, 26].

Table 2.2 Classification of accelerators [15].

Class	Acronyms	Response speed
Mercapto-accelerators:		
2-Mercaptobenzothiazole	MBT	Semi-fast
Dibenzothaizyl disulfide	MBTS	
Sulfenamide-accelerators:		
N-cyclohexyl-2-benzothiazylsulfenamide	CBS	Fast, delayed action
N,N-dicyclohexyl-2- benzothiazylsulfenamide	DCBS	
Thiuram-accelerators:		
Tetramethythiuram disulfide	TMTD	Very fast
Tetraethythiuram disulfide	TETD	
Dithiocabamate-accelerators:		
Zinc dimethyldithiocarbamate	ZDMC	Very fast
Zinc dibutyldithiocarbamate	ZDBC	
Guanidine-accelerators:		
Diphenylguanidine	DPG	Medium
Di-o-tolylguanidine	DOTG	
Sulfur donors:		
2-Benzothiazole-N-morpholyldisulfide	MBSS	
Dimorpholine disulfide	DTDM	-
Vulcanization retarders:		
Benzoic acid	BES	
Salicylic acid	SCS	-
Phtalic anhydride	PTA	

Accelerated-sulfur vulcanization is the most widely used method. For many applications, it is the only rapid crosslinking technique that can, in a practical manner, give the delayed action required for processing, shaping, and forming before the formation of the intractable vulcanized network. It is used to vulcanize NR, synthetic

isoprene rubber (IR), styrene-butadiene rubber (SBR), nitrile rubber (NBR), butyl rubber (IIR), chlorobutyl rubber (CIIR), bromobutyl rubber (BIIR), and ethylene-propylene-diene-monomer rubber (EPDM) [26].

Realization of the full potential of most organic accelerators and cure systems requires the use of inorganic and organic activators. Zinc oxide (ZnO) is the most important inorganic activator, but other metallic oxides such as magnesium oxide (MgO), calcium hydroxide (Ca(OH)$_2$) and lead oxide (PbO) are also used. Although zinc has long been termed an activator, zinc or another divalent metal ion should be considered to be an integral and required part of the cure system. As shown in Figure 2.8, zinc has a profound effect on the extent of cure achievable in accelerated sulfur vulcanization and thus should be expected to be inherently active at the sulfuration step. The most important organic activators are fatty acid, although weak amines, guanidines, ureas, thioureas, amides, polyalcohols, and amino alcohols are also used [18]. The large preponderance of rubber compounds today use a combination of ZnO and stearic acid as the activating system. Several studies [27-29] have been published on the effects of variations in the concentrations of these activators. In general, the use of the activator ZnO and stearic acid improves the rate and efficiency of accelerated sulfur vulcanization. Rheographs obtained on stocks containing various combinations of cure system components are shown in Figure 2.8.
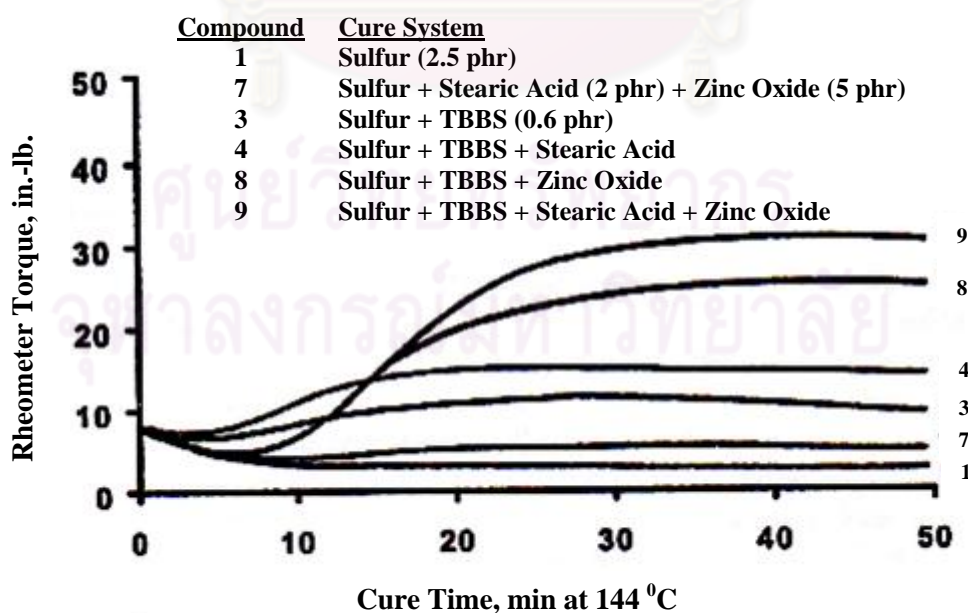
Figure 2.8 Effect of activator on cure rate (100 NR) [18].

According to Figure 2.8, the addition of ZnO to the accelerated stock as the only activator produces a dramatic effect and well-cured stock. The boost in efficiency suggests that zinc should be considered an integral component of the intermediate responsible for the attachment of sulfur to the rubber in the cross-link reactions. Thus, ZnO is furthermore activated by the addition of fatty acid (normally stearic acid) as zinc stearate. However, most NR and some synthetic rubbers contain enough fatty acids to form soluble zinc salts that interact with the accelerators. Sulfenamide-accelerated cures will release free amine, which produces a soluble zinc amine complex from the zinc oxide. The use of fatty acid soaps permits full development of cross-links by the organic accelerator as shown for compound 9 in Figure 2.8.

2.3.5 Vulcanizing System

As mentioned above, sulfur is used in combination with one or more accelerators and activators. The ratio of accelerator to sulfur determines the efficiency with which sulfur is converted into cross-links and upon it will depend on the nature of cross-links and the extent of main chain modification. There are three generally classifications for sulfur vulcanization including: conventional vulcanized system (CV), semi-efficient vulcanized system (semi-EV) and efficient vulcanized system (EV) [30-31]. The level of sulfur, accelerator, the ratio of accelerator to sulfur and the crosslinking efficiency (E) are shown in Table 2.3. The crosslinking efficiency defined as the network-combined sulfur atoms present per physically-effective chemical crosslink [31].

Table 2.3 Classification of sulfur vulcanizing systems [31-32].

Class	Sulfur concentration (phr)	Accelerator concentration (phr)	Accelerator/Sulfur ratio	Approximate rang of E* values
EV	0.3-1.0	6.0-2.0	2.5-12	1.5-4.0
semi-EV	1.0-2.0	2.5-1.0	0.7-2.5	4.0-8.0
CV	2.0-3.5	1.0-0.5	0.1-0.6	10.0-25.0

* The crosslinking efficiency

2.3.5.1 Network Structure of Sulfur Cross-links

The various types of chemical grouping (crosslinks formed) which have so far been deduced to be presented in sulfur vulcanizates of NR are shown in Figure 2.9. The quantity and kinds of crosslinks formed during vulcanization are determined by the relative amounts of accelerator and sulfur used in the compound formulation, and also by the time, temperature and pressure conditions in the cure process. Sulfur is combined in the vulcanization network in the number of ways as monosulphide (C-S-C), disulphide (C-S-S-C) or polysulphide (C-S_x-C, X>2) (Figure 2.9 (a)), but it may also be present as pendent sulphide (Figure 2.9 (b)), or cyclic monosulphides and disulphides (Figure 2.9 (c)) [33].
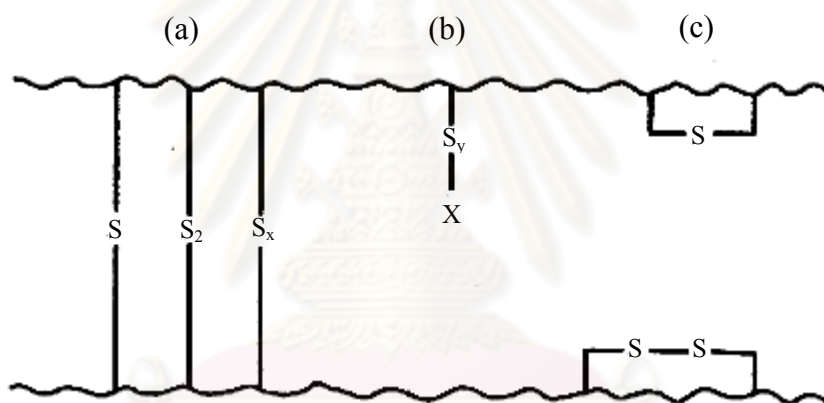
Figure 2.9 Structural features of vulcanizates network [33].

2.3.5.2 Influence of Network Structure on Vulcanizates Properties

The length of the sulfide crosslinks formed during vulcanization affect rubber properties, as shown in Table 2.4. Mono- and disulfide crosslinks are more stable (less prone to scission) than polysulfide links and so promote better thermal and aging characteristics. Due to the sulfur to sulfur bonds (34 kcal mole^{-1}) are weaker than carbon to carbon link (80 kcal mole^{-1}); the conventionally cured system is therefore, less heat resistance than a Semi EV or EV systems as seen the bonding energy values in Table 2.5. Polysulfide links, on the other hand, provide somewhat

better molecular flexibility. This can result in better dynamic fatigue resistance. Physical properties aside, the more stable crosslinks are often preferred to provide reversion resistance. Reversion is the cleavage of sulfide crosslinks during vulcanization which results from extending the cure beyond the time required to obtain the desired optimized balance of vulcanizates properties. When overcured in this way, certain elastomers, particularly NR will revert to the soft, more plastic, less elastic condition characteristic of the uncured compound [30, 34-35].

The choice of accelerator will influence the length of crosslinks, but this can be further controlled by adjusting the accelerator: sulfur ratio. Increasing this ratio progressively favors shorter crosslinks. This can be alternatively accomplished by using sulfur donors in place of most or all of the elemental sulfur for vulcanization. The thiuram accelerators, particularly the disulfides, and dithiodimorpholine are commonly used for this purpose [35].

Table 2.4 Influence of di- and polysulfide crosslinks on properties [31].

Property	Change with increase in proportion of di- and polysulfides
Creep, stress relaxation	Increase
Permanent set	Increase
Incremental swelling	Increase
Tensile strength, tear strength	Increase
Resilience	Increase
Fatigue failure	Decrease
Heat resistance	Decrease
Thermal aging resistance	Decrease

Table 2.5 Bonding energy [18].

Linkage Type	Bond energy (kcal mole^{-1})
Polysulfide (-S$_x$-)	34
Disulfide (-S-S-)	54
Monosulfide (-S-)	74
Carbon to carbon (-C-C)	80

2.3.6 Non-Sulfur Cross-links [36-37]

2.3.6.1 Peroxide Vulcanization

During peroxide vulcanization, direct carbon-carbon cross links are formed between elastomer molecules as shown in Figure 2.10.

Figure 2.10 Peroxide initiated vulcanization [37].

The peroxides decompose under vulcanization conditions forming free radicals on the polymer chains, thus facilitating direct cross link formations. Peroxides can be used to cross link a wide variety of both saturated and unsaturated elastomers, where as sulfur vulcanization will occur only in unsaturated species. A wide range of organic peroxides is available, including products such as benzoil peroxide and dicumyl peroxide.

2.3.6.2 Vulcanization with Resin

Epoxy resins are used with nitrile, quirone dioximes, and phenolic resins with butyl and dithiuls, or dramines with fiuorocarbons. The most important resin to cure butyl rubber is phenolic resin. The low level of unsaturation of butyl requires resin cure activation using halogen-containing materials.

2.3.6.3 Metal Oxide Vulcanization

Metal oxides, usually zinc oxide but on occasion lead oxide for improved water resistance, are used as crosslinking agent for halogenated elastomers such as neoprene, halobutyl rubber, and chlorosulfonated polyethylene. The metal oxide abstracts the allylic halogen of adjacent polymer chains to form an oxgen crosslink plus the metal chloride salt.

2.3.6.4 Difunctional Compounds

Certain difunctional compounds are used to crosslink elastomers by reacting to bridge polymer chains. For example, diamines (e.g., hexamethylenediamine carbamate) are used as crosslinks for fluoroelastomers; p-quinone dioxime is oxidized to p-dinitrosobenzene as the active crosslink for bridging at the polymer double bonds of butyl rubber; and methylol terminated phenol-formaldehyde resins will likewise bridge butyl rubber chains (with $SnCl_2$ activation) as well as other unsaturated elastomers.

2.3.6.5 Urethane Vulcanization

The vulcanizing agents in these systems are derived from p-benzoquinone monoxime (p-nitrosophenol) and a di-orpolyisocianate. Accelerators as used in sulfur vulcanization are not necessary, but the efficiency of the process is improved by the presence of free diisocyanate and by ZMDC. The latter catalyzes the reaction between the nitrosophend and the polymer. The principal advantage of these systems lies in the high stability of the cross links that give very little modulus reversion even on extreme over-cure. Problems can occur with their lower scorch, rate of cure, and modulus. However, modulus and fatigue are very good.

2.4 Reinforcement of Rubber by Fillers

2.4.1 Concept of Reinforcement

The additives, which are used to fill up the void volume of the polymers, generally define as fillers. Initially, these types of fillers are used just to increase the volume of polymers and thereby the cost per unit volume of the articles is decrease. However, the concept now is completely changed and fillers are used mainly to improve the bulk properties of polymers in most of cases. Although all such fillers can be categorized into two main classes depending on their functions towards the polymers into which these are incorporated. These are (i) reinforcing and (ii) non-reinforcing or so called inert fillers. The reinforcing filler are very important as they significantly improve many bulk properties, especially the mechanical properties of

the polymers like tensile strength, compressive strength, tear strength, abrasion resistance, hardness, etc., as illustrated in Figure 2.11.

According to Figure 2.11, the certain properties will only either increase or decrease, for instance viscosity, hardness, but other ones will pass through extremes in the case of the reinforcing filler. Thus immediately suggests that there will be optimum loadings, for given filler, in a given polymer, for a specific application. Therefore, to establish the optimum filler level is the most important task for the compounder.
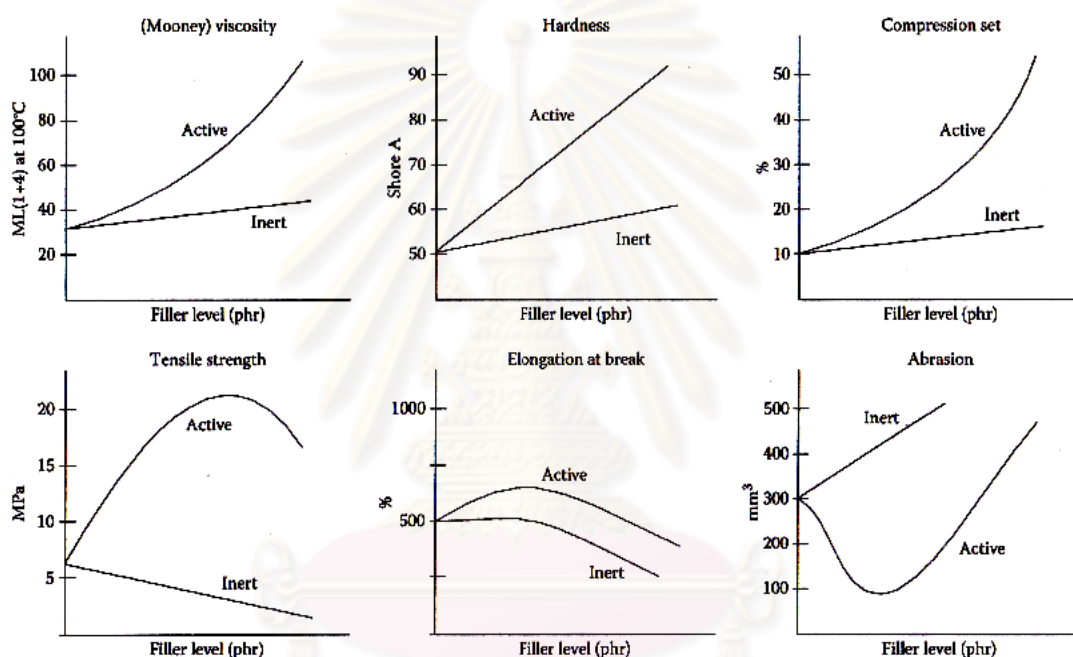
Figure 2.11 Relative variation of rubber compound properties as imparted by active (reinforcing) or inert filler [39].

Fillers for polymers exhibit in fact a stunning variety of chemical nature, particle sizes and shapes. Essentially three basic shapes can be distinguished: either spheres, or plaques (disks, lamellas) or rods (needles, fibers), as illustrated in Figure 2.12. Such basic shapes can be further combined to result in quite complex geometrical objects to which specific (reinforcing) properties can be associated [38-39].

Essentially, there are four types of filler with respect to fabrication process and reinforcing activity including: organic fillers of natural origin, organic fillers obtained by chemical synthesis, mineral fillers of natural origin and mineral fillers obtained through chemical processes in broad sense, as illustrated in Figure 2.13. As mentioned above, the fillers used in rubber industry can be classified as reinforcing, semi-reinforcing and non-reinforcing or inert fillers, depending how they boost, improve or do not affect certain mechanical properties of interest, for instance stiffness, tensile or flexural strength, and abrasion resistance, to name a few [39].

Spheres   Scales, flakes lamellas   Cylinders, rods, needles, fibers

Partial fusion elementary particles => aggregates

Complex tri-dimensional object
⇨ Structure effect of the filler
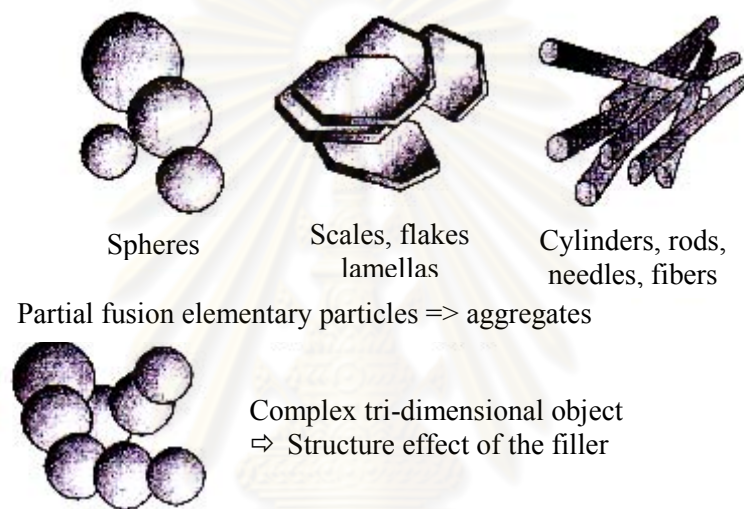
Figure 2.12 Fillers basic shapes and structure [39].

Filler

Organic   Inorganic

Natural   Synthetic   Natural   Synthetic

- Inactive
- Semiactive
- Active
Liege
Wood flour
Fibers (jute, sisal,...)

- Inactive
- Semiactive
- Active
Synthetic Resin
Cellulose derivatives

- Inactive
- Semiactive
- Active
Minerals
($CaCO_3$, talc, clays,..)

- Inactive
- Semiactive
- Active
Carbon blacks
Silica (fumed, precipitated)
Metal oxides (TiO_2, ZnO,…)
Metal salts ($BaSO_4$,…)

Figure 2.13 Classifying fillers with respect to fabrication process and
reinforcing activity [39].

Another approach consists of paying attention to particle size, as illustrated in Figure 2.14. There is a clear relationship between this characteristic and the reinforcing capabilities. Essentially, no reinforcement is obtained when particles are larger than 10^3 nanometer (nm) and too large particles deteriorate mechanical properties of vulcanized rubber.
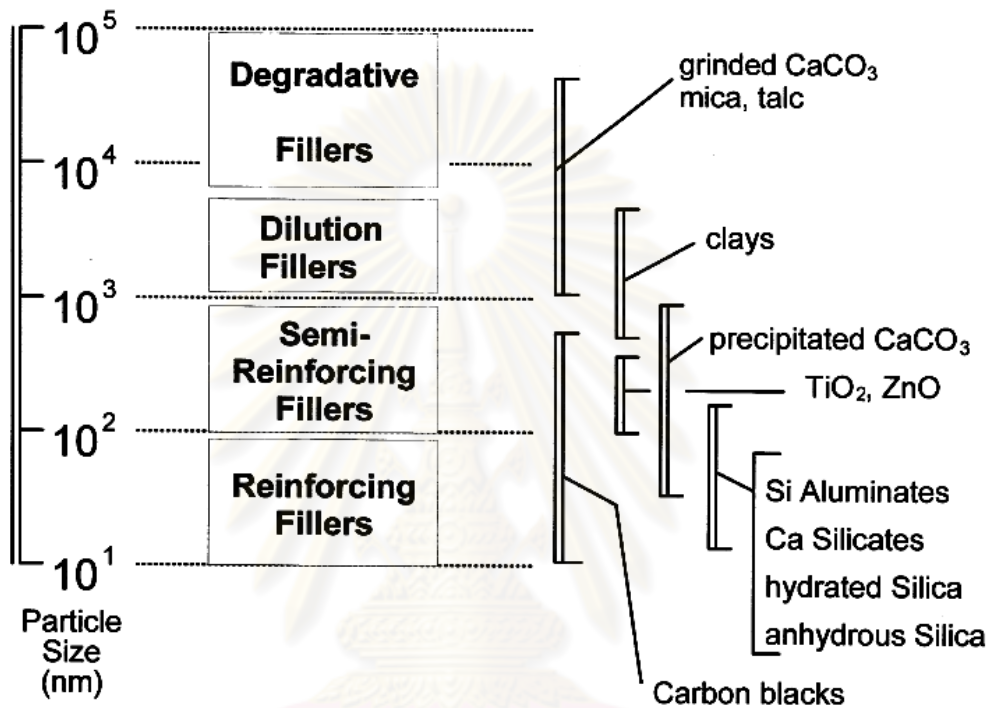
Figure 2.14 Classifying fillers with respect to particle sizes [39].

2.4.2. Factors that Influence Reinforcement of Rubber by Filler

In general, the reinforcing activity of filler depends on at least four criteria including: the particle size, the structure, the specific surface area and the surface activity [39-41].

2.4.2.1 Particle Size

Fillers with primary particle sizes greater than 10 μm act as flaws, which can initiate rupture during flexing, bending, or stretching. Filler with primary particle sizes between 1 and 10 μm are diluents, usually having only small effects on vulcanizates properties. Semi-reinforcing fillers, with primary particle sizes ranging

between 0.1 and 1 μm (between 100 and 1000 nm), can improve the strength of vulcanizates and increase modulus and hardness. Fillers of primary particle sizes ranging between 10 and 100 nm greatly improve strength, tearing resistance, wearing resistance, and other qualities.

2.4.2.2 Surface Area

The primary particle size of the filler has the most significant influence on reinforcement. This assumes, of course, that the filler in question is adequately dispersed. Particle size has a direct influence on the specific surface area of the filler and it is the increase in reinforcement. It can be argued that reducing particle size simply leads to a greater influence of polymer-filler interaction. In consequence, the presence of large particle or agglomerates in rubber bring to detract from strength, not only because of the reduced surface contact, but through localization of stresses which would thus lead to premature failure by functioning as failure initiation sites. According to the nitrogen adsorption method developed by Brunauer, Emmett and Teller, one obtained the so-called BET-value of surface area, expressed as m^2/g. As might be expected, there is a correlation between the BET surface area and the activity (or reinforcing capability) of filler:

- BET < 10 m^2/g: inert filler
- BET = 10-60 m^2/g: semi-active filler
- BET > 60 m^2/g: active filler
- BET > 100 m^2/g: very active filler

2.4.2.3 Structure

Structure can be thought of as degree of difference from a spherical shape. It is similar to shape factor. High structure aggregates are in the form of chains, branched chains, and so on. Some of this aggregate structure can break down during processing due to the development of high stress on the structures. High-structure fillers give rise to reduce elasticity in the uncured state. Unfilled elastomers, when extruded in the uncured state expand or swell when they leave the extruded die. It is

called extrusion shrinkage. Extrusion shrinkage is greatly reduced by fillers, especially those of high structure. Also, as the structure of the filler increases, the viscosity of the uncured composition or the stiffness of the vulcanizates increases. This is because the higher-structure fillers immobilize more of the elastomer during its straining in either the cured or uncured state. Structure also affects the processability of the compound with high structures giving ease of incorporation, high compound viscosity and low die swelling, and the cured compound will have high modulus, high hardness and good wear resistance [42]. In simplest term, the more an aggregate deviates from a solid spherical shape and the larger its size, the higher is its structure. The higher its structure, in turn, the greater its reinforcing potential [36] as exhibited in Figure 2.15. Types of structures formed from primary particles are also illustrated by Figure 2.16. Additionally, the amount of structure is measured by using dibutyl phthalate (DBP) absorption method. Small amounts of DBP (a nonvolatile liquid) are added to dry filler until a non-crumbling paste is obtained. The DBP absorption is expressed in ml of DBP per 100 g filler.
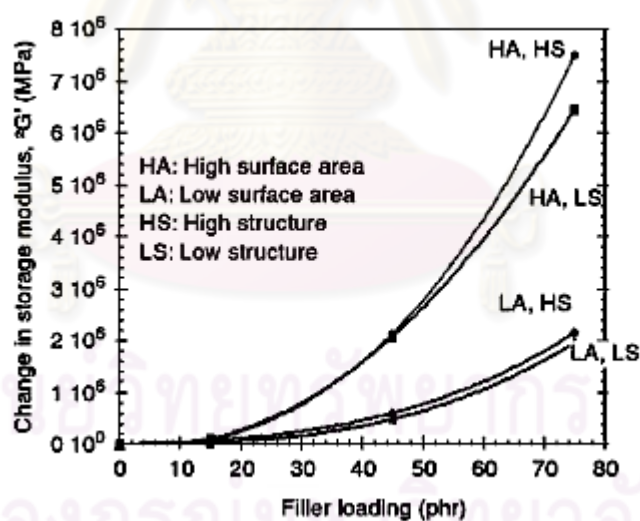
Figure 2.15 Influence of the filler content on the storage modulus (MPa) of carbon black filled elastomers [43].

Large Particles, Low Surface Area, High Structure (High DBP Absorption)

Small Particles, High Surface Area, High Structure (High DBP Absorption)

Large Particles, Low Surface Area, Low Structure (Low DBP Absorption)

Small Particles, High Surface Area, Low Structure (Low DBP Absorption)
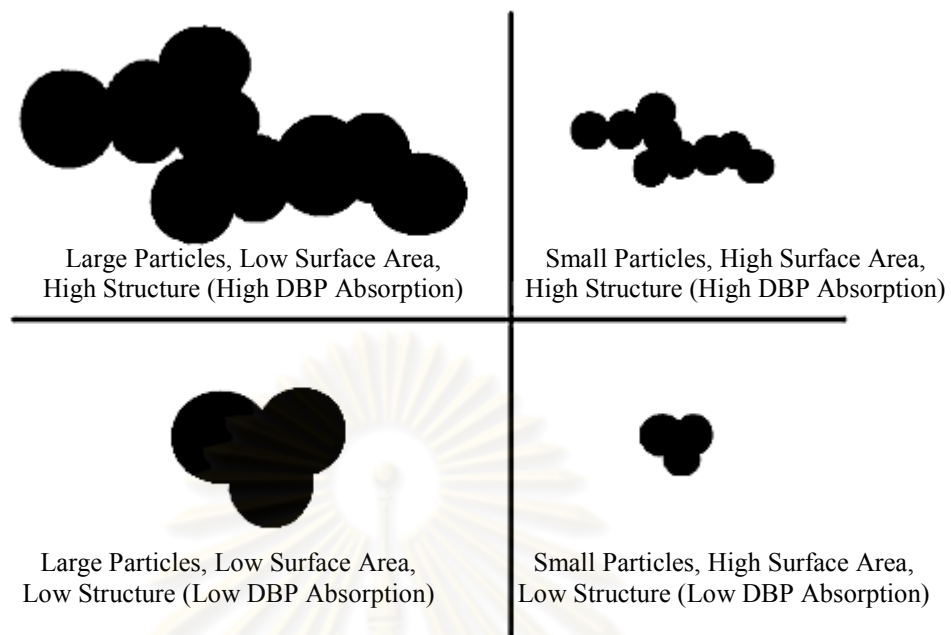
Figure 2.16 Particle size and structure [41].

2.4.2.4 Surface Activity

Filler can have high surface area and high structure and still give poor reinforcement if its surface does not interact at all with the elastomeric matrix. For example, carbon black, which is highly effective reinforcing filler, loses much of its reinforcing effect if it is graphitized. During the graphitization processing (high-temperature heating in the absence of reactive gases such as air), most of the reactive chemical functional groups are removed from the particulate surfaces.

A way to infer the activity of filler toward an elastomer is to measure so-called "bound rubber." When an uncured elastomer-filler mixture is extracted with a solvent (e.g., toluene), then the gel-like elastomer, which is bound to filler, cannot be dissolved, whereas the rest of the elastomer is soluble and is extracted away from the gel-like mixture. The more the bound rubber, the more active the filler is assumed to be.

2.5 Composite Material [44-45]

A composite is a heterogeneous substance consisting of two or more materials which does not lose the characteristics of each component. This combination of materials brings about new desirable properties. Naturally occurring composites include tendon, bone, bamboo, rock, and many other biological and geological materials. For composites engineering applications, we restrict ourselves to synthetic polymer matrices which are used with naturally occurring mineral fillers such as wollastonite, silica, mica, and calcium carbonate, and synthetic fibers like glass fibers and carbon fibers. Composites have many engineering advantages over synthetic polymers and copolymers. Some of these advantages are as follows:

- Reinforcement of the resin resulting in increase tensile strength, flexural strength, compression strength, rigidity and combination of these properties.
- Increased size stability.
- Improved fire retardancy.
- Corrosion protection.
- Improved processibility; controlled viscosities, good mixing.

Filler particles are commonly used in composites for a variety of reasons, such as weight reduction, flame and smoke suppression and prevention of ultraviolet degradation due to exposure to sunlight. The need for fiber placement in different directions according to the particular application has led to various types of composites, as shown in Figure 2.17. In the continuous fiber composites laminate (Figure 2.17 (a)) individual continuous fiber/matrix laminate are obtained in the required directions and bonded together to form a laminate. Although the continuous fiber laminate is used extensively, the potential for delamination, or separation of the laminae, is still a major problem because the interlaminar strength is matrix-dominated. Woven fiber composites (Figure 2.17 (b)) do not have distinct laminae and are not susceptible to delamination, but strength and stiffness are sacrificed due to the fact that the fibers are not so straight as in the continuous fiber laminate. Chopped fiber composites may have short fibers randomly dispersed in the matrix, as shown in

Figure 2.17 (c). Chopped fiber composites are used extensively in high-volume applications due to low manufacturing cost, but their mechanical properties are considerably poorer than those of continuous fiber composites. Finally, hybrid composites may consist of mixed chopped and continuous fibers, as shown in Figure 2.17 (d).

(a) Continuous fiber composite   **(b) Woven fiber composite**

(c) Chopped fiber composite   **(d) Hybrid fiber composite**
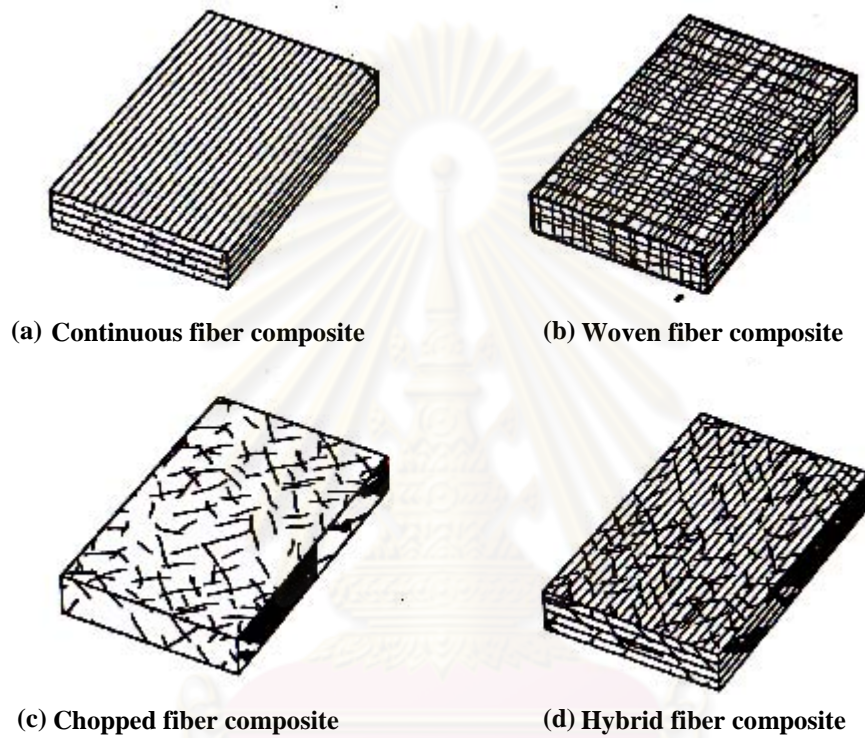
Figure 2.17 Types of fiber-reinforced composites [45].

2.6 Type of Filler

As mentioned earlier, there are various types of filler either a reinforcing or non-reinforcing filler in the elastomer. However, the most importance commercial filler, which are wildly used in rubber industry, are as follows:

2.6.1 Carbon Black

2.6.1.1 Chemical Structure of Carbon Black

The tradition reinforcing filler in modern industrial rubber and tire manufacture has been carbon black, an intensively black, finely divided form of amorphous carbon in the form of spheres and their fused aggregates with sizes below 1,000 nm. Carbon blacks are, in effect, soot produced by incomplete combustion of volatile organic materials, principally oil and gas. During this time, there have been four main processes resulting in products of different characteristics: furnace, channel, thermal and lamp blacks. As the name implies, carbon black is largely composed of carbon, although considerable quantities of hydrogen and oxygen can also be present. There are more than 100 commercial grades of carbon black characterized by spherical particles ranging from 10 to 100 nm, with surface areas in the range of 5-150 m^2/g.

Carbon black has very chemically active surfaces resulting from their production process, with hydrogen, oxygen and sulfur being the principal surface atoms combined with the carbon. The species of most importance are acidic and basic oxides, active hydrogen groups and highly reactive sulfur moieties as illustrated in Figure 2.18. These lead to strong, covalent bonds with many polymers, especially unsaturated elastomers. It is this strong bonding that helps make carbon blacks such good reinforcing agents for elastomeric compounds [40, 46].
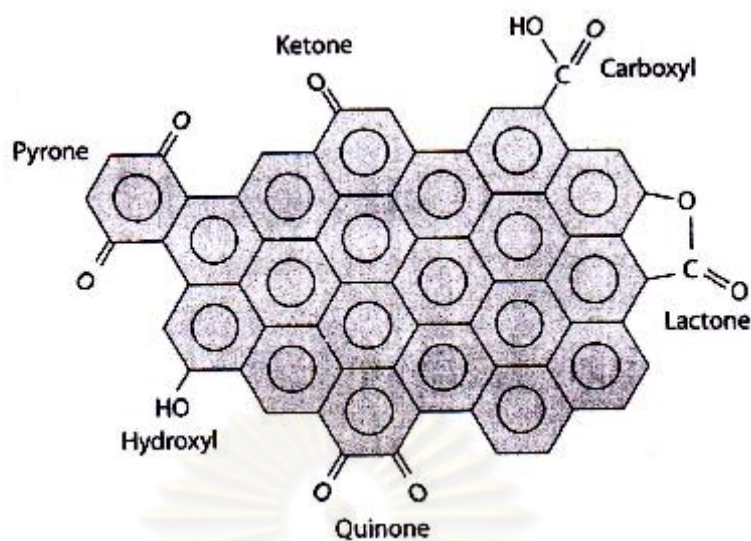
Figure 2.18 Chemical functions detected on carbon black surface [39].

2.6.1.2 Usages of Carbon Blacks

An estimated 70% of the world's consumption of carbon black is used in the production of tires and tire products for automobiles and other vehicles, with an additional 20% going into sundry rubber products such as hoses, belting, mechanical and molded goods, and footwear. In general, carbon black accounts for about one quarter of the weight of a standard automobile tire. Other applications include their use as conductive fillers, ink, thermoplastic, paper and paint [46].

2.6.2 Synthetic Silica

Two forms of synthetic silica find significant use in filled polymers. These are both very small particle, high specific surface area forms, and are known as precipitated and fumed silica. Long known as the "white carbon black" because of its reinforcing ability in elastomers.

2.6.2.1 Precipitated Silica

Traditionally, precipitated silicas are used as reinforcement fillers in rubber applications. These products are made from a mixture of sodium silicate, sulfuric or hydrochloric acid, and metallic ions agitated to form precipitated silica with high

brightness (97%), a 20 nm average particle size, and low porosity. Precipitated silica's ultimate fine particle size generates a high surface area (25-700 m^2/g) that allows for interaction with polymer chains [46]. In order to obtain reinforcing silica, much care must be taken in precipitated recipes (to obtain small rigid objects) and drying condition (to maintain high dispersibility).

2.6.2.2 Fumed (Pyrogenic) Silica

Fumed silica (silicon dioxide) is generally regarded as a unique material because of its unusual particle characteristics, enormous surface area and high purity. Formed from the hydrolysis of silicon tetrachloride in a hydrogen/oxygen flame reactor at 1000 ^{0}C. It is a fine white, extremely fluffy powder and composed of 7 to 20 nm spherical particles. This structure provides a high surface area ranging from 130 to 380 m^2/g, affects dispersibility, rheology control, thixotropic behavior, and reinforcement efficiency [46-47]. Various properties of fumed silica are compared with those of precipitated silica in Table 2.6. Fumed silica is used for thickening, viscosity control, thixotropy, and reinforcement purposes in the rubber and other industries.

The surface chemistry of silica can be regarded as polymers of silicic acid, consisting of interlinked SiO_4 tetrahedral. At the surface, the structure terminates in either a siloxane group (Si-O-Si) with the oxygen on the surface, or one of several forms of silanol groups (Si-OH). As shown in Figure 2.19, the silanol can be divided into isolated groups (or free silanols), where the surface of silicon atom has three bonds into the bulk structure and the fourth bond attached to a single OH group, and vicinal silanols (or bridged silanols), where two single silanol groups, attached to different silicon atoms, are close enough to hydrogen bond. A third type of silanols, germinal silanols, consists of two hydroxyl groups, which are attached to one silicon atom. The germinal silanols are too close to hydrogen bond each other, whereas the free hydroxyl groups are too far separated [48].

Isolated silanol   Geminal silanols   Vicinal silanols
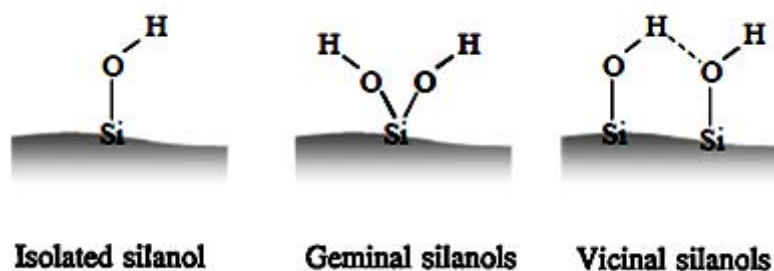
Figure 2.19 Surface chemistry of silica [48].

Table 2.6 Typical property ranges for synthetic silica [39].

Characteristic	Precipitated Silica	Fumed Silica
Particle size (μm)	10-12	0.007-0.3
N_2 specific surface area (m^2/g)	110-240	100-400
Moisture content at 105 ^{0}C, 1 h (max %)	5	0.5-2.0
Ignition loss at 1000 ^{0}C for 1 h (max %)	10	5-6
Bilk density (g/cm^3)	0.08-0.4	0.05-0.2
pH 5% Aqueous suspension	6.5-7.2	3.7-4.8
Water absorption (%)	175-250	-
Oil absorption (%)	180-270	250-320
Residue on 325 mesh, wet sieving (max %)	0.3	0.5
Soluble salt (%max)	0.5	-
R_2O_3 (max %)	0.3	-
SiO_2 (max %)	89	99.8
Specific gravity (g/cm^3)	1.95	2.0
Refractive index	1.46	-

2.6.3 Calcium Carbonate [47, 49-50]

Calcium carbonate ($CaCO_3$) is abundant, largely inert, low cost, white filler with cubic, block-shaped, or irregular particles of very low aspect ratio. Generally speaking, its usage reduces costs in a variety of thermoplastics and thermosets, with moderate effects on the mechanical properties. As filler in plastics, calcium carbonate leads to increased modulus with minimal effect on the impact strength. As value-added functional filler, $CaCO_3$ may act as a surface property modifier, as a processing aid and as a toughener. $CaCO_3$ contrasts sharply with other high volume fillers such as clay, talc, silica and asbestos, which may be much darker in color, stiffer in filled polymer compounds and in the case of silicates and clays, may contain water of crystallization or hydration. Removal of the water in clay, to form calcined clay, results in a more expensive product.

2.6.3.1 Production of $CaCO_3$

Precipitated $CaCO_3$ is also known as synthetic $CaCO_3$ since several chemical operations may be involved in its manufacturing. In the earlier synthetic processes, it was obtained as a by-product during the manufacture of Na_2CO_3 by the ammonia process (Scheme 2.2 (a)), or during the manufacture of NaOH by the soda-lime process (Scheme 2.2 (b)).

(a)
$$NH_3 + H_2O + CO_2 + NaCl \rightleftharpoons NaHCO_3 + NH_4Cl$$

$$2NaHCO_3 + heat \longrightarrow Na_2CO_3 + H_2O + CO_2$$
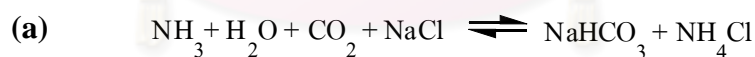
$CaCO_3$ is used in this process as follows:

$$CaCO_3 + heat \longrightarrow CaO + CO_2 \xrightarrow{H_2O} Ca(OH)_2$$

$$Ca(OH)_2 + 2NH_4Cl \longrightarrow 2NH_3 + 2H_2O + CaCl_2 \xrightarrow{CO_2} 2NH_4Cl + H_2O + CaCO_3$$

(b)
$$Na_2CO_3 + Ca(OH)_2 \rightleftharpoons 2NaOH + CaCO_3$$
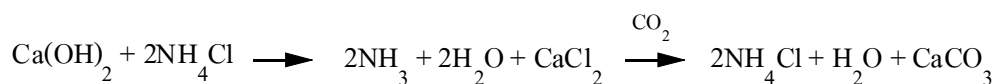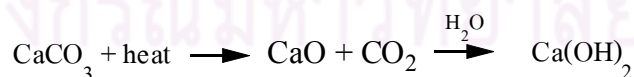
Scheme 2.2 A schematic of the manufacture of $CaCO_3$ by (a) Na_2CO_3 or (b) NaOH.

The particle size is controlled by conditions of precipitation: temperature, concentration, rate and order of addition of ingredients, and amount of agitation. Particles sizes are fairly uniform and can be varied from about 0.03-0.05 μm up to about 8-10 μm.

2.6.3.2 Structure and Properties

$CaCO_3$ occurs in different crystalline forms. The most widespread is calcite, which has either a trigonal-rhombohedral or a trigonal-scalenohedral crystal lattice. Another form is the orthorhombic aragonite, which is less stable and can be converted by heat to calcite. Vaterite, a third form is unstable and overtime will transform into the two forms. Aragonite has a higher density (2.8-2.9 g/cm^3), a higher single refractive index (1.7), and a somewhat higher Mohs hardness (3.5-4) than calcite. Its other properties are very similar. Both minerals are white and their refractive indices are not high enough to interfere with effective coloration.

2.6.3.3 Application

Precipitated $CaCO_3$ is used as semi-reinforcing filler shoe products and industrial polymer goods, particularly when resistance to alkali solutions is needs. The low moisture content and good reinforcement allow precipitated $CaCO_3$ to be used in wire and cable insulation applications. Typical $CaCO_3$ levels used in polymer compounds range from 20 to 300 phr.

2.6.4 Fillers from Renewable Resources

Organic fillers are attracting attention as fillers for various polymers mainly due to their low price, low density and renewable nature. Like fillers and reinforcements generally, the organic material additives affect many of the properties of the compounds into which they are incorporated. The natural materials are generally less expensive than the resins with which they are compounded. The reasons for using such organic materials, as with other types of additives, are varied. These include reduction of cost of the molding compound, improved processability, and improved physical, chemical, and electrical properties of the final compound. The

various organic materials have been used for reinforcement of the various polymers such as wood flour, cotton, cellulose fibers, sisal, rice husk, and starch etc [50].

2.6.4.1 Wood Flour

Wood flour is a finely ground, dried wood product fibrous in structure, which acts as a reinforcing material polymer. It is made mostly from softwoods, chiefly pine and spruce, but hard wood maple or ash flours are used where no wood resin content is desired. Wood flour is made from sawdust, chips and shavings by grinding in a buhrstone mill, and has the appearance of wheat flour. Particle sizes commonly used for polymer fillers are 40, 60 and 80 mesh, with sizes as fine as 140 mesh available [6, 50].

2.6.4.2 Cellulose Fibers

Cellulose fibers are derived from plant fibers by mechanical and chemical treatment to break up fiber bundles and remove some of the lignin or other compounds which may be present. All plant fibers are composed principally of cellulose, but the other materials present, and the structure and properties of the purified fibers, will depend upon the vegetable source used. Commonly used fibers are produced from wood, cotton or other plant sources. Cellulose fibers of high purity are readily made from cotton fiber by boiling with sodium hydroxide solution, neutralization with acetic acid, and prolonged washing with distilled water. Over the past decade there has been a growing interest in the use of lignocellulosic fibres as reinforcing elements in polymeric matrix. The specific properties of this natural product, namely low cost, lightweight, renewable character, high specific strength and modulus, availability in a variety of forms throughout the word, reactive surface and the possibility to generate energy, without residue, after burning at the end of their life-cycle, motivate their association with organic polymers to elaborate composite materials [50].

2.6.4.3 Hemp

Hemp fiber is obtained from the stalk of the plant Cannabis sativa, which is grown principally in Southern Russia, Central Europe, South America, United States

and Asia. The stalk is treated by a process called "retting" and yields fibers up to 75 in. long. They are coarse, strong and more durable than cotton. These fibers are composed of as much as 78% alpha cellulose. Hemp fibers are used chiefly for cordage, sacking and packing. They are also used as a reinforcing fillers for polymers [50].

2.6.4.4 Starch

Starches from corn, potatoes, rice, tapioca and wheat have recently been proposed as a filler for rendering polymer biodegradable. The starches are readily obtained from these plant sources as a fine powder consisting of spherical or ellipsoidal grains ranging in particle size from 3-100 millimicrons. In general, they are insoluble in cold water, alcohol, ether and form a jelly with hot water. Specific gravity is 1.499–1.513. It does not melt but decomposes or burns when heated.

A property that makes starches of interest as fillers for formulating biodegradable compounds is that they are subject to biological and oxidative attack. The action of enzymes and oxygen brings about their decomposition when buried in soil. Combining starches with polymers requires techniques adapted to avoiding degradation during processing. However, they resist dry heat in the normal plastics processing operations, and have been successfully compounded with low density polyethylene, polypropylene and polystyrene [50].

2.6.4.5 Cuttlefish Bone

The familiar internal shell or bone of the cuttlefish *(Sepia Officinalis L.)* appears to function both as a skeletal structure and as a rigid buoyancy tank, enabling the cuttlefish to become more or less dense than sea water. Since an animal fractionally denser than sea water can only preserve constant depth by the expenditure of significant energy, the variable buoyancy tank role of cuttlebone confers a considerable advantage to the cuttlefish which can maintain a fixed position in water with little effort. In the past, cuttlebones were used in making polishing powder. The powder was added to toothpaste, and used as an antacid or as an absorbent. Today, cuttlebones are commonly used as calcium-rich dietary supplements for caged birds, chinchillas, hermit crabs, snails, and turtles [8].

2.7 Literature Reviews

Ismail *et al*. [2] studied the effect of bamboo fiber and two types of bonding agent, phenol formaldehyde and hexamethylenetetramine, on the cure characteristic and the mechanical properties of NR in sulfur vulcanization system. Two series of composites were studied i.e. composites with and without the presence of a bonding agent. The curing characteristics of the composites were determined and the composites were vulcanized at 150 °C using a hot press. The properties of the composites such as tensile strength, tensile modulus, tear strength, elongation at break and hardness were studied. The results revealed that the adhesion between the bamboo fiber and the NR was enhanced by the addition of bonding agent as exhibited by the tensile fracture surfaces of the composites using Scanning Electron Microscopy (SEM). In addition, the presence of bonding agent also gave shorter curing time and enhanced mechanical properties.

Geethamma *et al*. [3] studied the dynamic mechanical behavior of NR and its composites reinforced with short coir fibers. Maxima in tan δ (loss tangent), E" (loss modulus) and the middle point of E' (storage modulus) vs. temperature curves of the gum NR compound at different frequencies almost coincided with one another. But the maxima in tan δ and E" did not coincide in the case of composites. It was observed that as frequency increased the values of tan δ and E" decreased whereas the values of E' increased in the case of both gum and the composites. The values of E" and tan δ increased with fiber incorporation, which indicated the lower heat dissipation in the gum. Two prominent peaks were observed in the tan δ vs. temperature curve of these composites due to the dynamic mechanical behavior of matrix and fiber. The additional small peak represented the dynamic mechanical behavior at the interface. The effect of chemical treatment of coir fiber on damping of composites was studied and it was found that composite with poor interfacial bonding tended to dissipate more energy than that with good interfacial bonding.

Ismail *et al*. [4] reported that the potential of white rice husk ash (WRHA) as a filler for NR compounds. The optimum loading of WRHA to obtain maximum physical properties was achieved at 10 phr after which there was deterioration in properties. The incorporation of multifunctional additive (n-fallow-1-3-propane

diamine salt of a carboxylic acid [RNH^+_2 (CH_2)$_3NH^+_3$] [$R'COO^-$]$_2$, MFA) reduced the scorch and cure times of the WRHA filled SMR-L compounds, but increased the torque difference, M_{HR}-M_L. Meanwhile, the tensile and tear strengths increased with increasing WRHA loading to a maximum level (10 phr of filler loading), after which there is a deterioration in both properties. However, the tensile modulus (M_{100} and M_{300}) and hardness increased with increasing WRHA loading. Furthermore, at 10 phr optimum loading, 3 phr of MFA was found to give maximum physical properties. SEM studies indicated that the incorporation of MFA improved filler dispersion.

Gopalan Nair *et al*. [5] prepared the nanocomposite materials which were obtained by using latex of either unvulcanized or prevulcanized NR as the matrix and a colloidal suspension of crab chitin whiskers as the reinforcing phase. The reinforcing effect of chitin whiskers strongly depended on their ability to form a rigid three-dimensional network, resulting from strong interactions such as hydrogen bonds between the whiskers. The results emanating from the successive tensile test experiments gave the clear evidence for the presence of a three-dimensional chitin network within the evaporated samples. Cross-linking of the matrix was found to interfere with the formation of this network.

Ismail *et al*. [6] studied the physico-mechanical properties of Oil Palm Wood Flour (OPWF) filled NR composites. The composites were prepared with a laboratory two roll mill and hot press. Increasing OPWP loading in NR compounds resulted in the reduction of tensile strength, tear strength and elongation at break but increased tensile modulus and hardness. The incorporation of OPWF had also resulted in the reduction of fatigue life. As the filler loading increased, the poor wetting of the OPWF by the rubber matrix gave rise to poor interfacial adhesion between the filler and rubber matrix (as evidenced by the SEM fatigue fracture surface).

Poompradub *et al*. [9] studied the effect of cuttlebone particles on NR vulcanizates in peroxide vulcanization. The results revealed that the cuttlebone particles did not prevent a peroxide cross-linking reaction of NR, and mechanical properties of peroxide cross-linked NR filled with cuttlebone particles were found to be comparable with those of peroxide cross-linked NR filled with commercial $CaCO_3$

filler. In addition, the presence of chitin on the surface of the cuttlebone particles was speculated to result in a good interaction between cuttlebone particles and NR, which may be ascribed to the mechanical properties of cuttlebone filled NR samples.

Jacob *et al*. [51] studied the effects of concentration and modification of fiber surface in sisal/oil palm hybrid fiber reinforced rubber composites. Composites were prepared using fibers treated with varying concentrations of sodium hydroxide solution and for different time intervals. The vulcanization parameters, processability characteristics, and stress–strain properties of these composites were analyzed as a function of fiber loading, ratio and treatment. The results revealed that the mechanical properties of the composites in the longitudinal direction are superior to those in the transverse direction. Addition of sisal and oil palm fibers led to decrease of tensile strength and tear strength but increased modulus. In addition, the extent of adhesion between fiber and rubber matrix was found to increase on alkali treatment of fibers. From the mechanical properties the alkali treated fibers exhibited better tensile properties than untreated composites. Subsequently, the processing characteristics were found to be independent of fiber loading and modification of fiber surface. Swelling studies revealed that composites containing bonding agents and alkali treated fibers showed higher crosslink density and better adhesion. Anisotropic swelling studies indicated that the presence of short fibers restricted the entry of solvent.

Wang *et al*. [52] investigated the morphology, thermal stability and mechanical properties of the starch/NR composite. The starch was modified by esterification, and the composite was prepared by blending the modified starch with NR latex. The results showed that the crystal structure of starch in the composite disappeared after modification with esterification, and the starch particles with an average size around 200 nm homogenously dispersed throughout the NR matrix. The thermal stability of composite was improved significantly after the modification with starch. The mechanical properties of composite were enhanced with the increase of starch loading. The composite possessed the best properties at the starch xanthate content of 20 parts per hundred rubber (phr). The enhanced thermal stability and

mechanical properties of modified starch/NR composite were mainly due to the improved phase interface interactions between rubber and starch.

Al Sagheer *et al*. [53] extracted chitin in the alpha (chitin-α) and the beta (chitin-β) forms from different marine crustacean from the Arabian Gulf by treatment with dilute HCl solution for demineralization, and dilute NaOH for deproteiniztion. The contents of the various exoskeletons have been analyzed and the percent of the inorganic salt (including the various elements present), protein and the chitin was determined. Deacetylation of the different chitin produced was conducted by the conventional thermal heating and by microwave heating methods. Microwave heating has reduced enormously the time of heating from 6–10 h to 10–15 min, to yield the same degree of deacetylation and higher molecular weight chitosan. This technique could save massive amount of energy when implemented on a semi-industrial or industrial scale. Moreover in FTIR spectra, the amide I band was split for α-chitin, and the amide I for β-chitin was a single peak. The XRD, SEM results indicated that α-chitin was a more crystalline polymorph because of its parallel structure.

Ravall *et al*. [54] extracted β-chitin from squid pens from Loligo sanpaulensis and Loligo plei, species found in the Brazilian coast, as the raw material. The squid pens were submitted to the usual sequence of treatments used for chitin extraction, demineralization and deproteinization. The extraction of β-chitin from the pens of L. plei and L. sanpaulensis resulted in polymers containing very low contents of inorganic compounds, even if the demineralization treatment was not carried out. It was attributed to the low content of inorganics found in these squid pens and also to a well designed experimental procedure. Indeed, the samples of β-chitin prepared in this work contained much lower contents of ash and metals than present in commercial a chitin, which was extracted from a biomass, namely the shells of crabs, whose content of inorganic was much more important. Additionally, other works reported higher contents of ash and metals for β-chitin extracted from squid pens. Excluding the demineralization treatment also allowed the extraction of more acetylated samples but the infrared spectroscopy and X-ray diffraction showed only minor differences among β-chitin samples extracted by employing different treatments, however α- and β-chitin are clearly distinguished.

CHAPTER III

EXPERIMENTALS

3.1 Chemicals

The chemicals and reagents used in this study are presented in Table 3.1

Table 3.1 List of chemicals and reagents.

Chemicals	Company
Natural rubber (STR-5L)	PI Industry Ltd.
Active zinc oxide	PI Industry Ltd.
Stearic acid	PI Industry Ltd.
N-cyclohexylbenzothiazole-2-sulfenamide	PI Industry Ltd.
Sulfur	PI Industry Ltd.
Hydrochloric acid	Ajax Finechem
Sodium hydroxide	Fisher Scientific Ltd.
Toluene	Earth Cheme Lab Ltd., Part.
Cuttlebone	Siam Ocean Food Ltd.
Calcium carbonate (Silver-W)	Shiraishi (Thailand) Co.,Ltd.

3.2 Instruments

The instruments used in the present study are summarized in Table 3.2

Table 3.2 List of instruments used in the present study.

Instrument	Manufacture
Laboratory two-roll mill	LabTech Engineering Thailand
Compression molding machine	LabTech Engineering Thailand
Vibratory Mill Machine	Fritsch Germany
Fourier Transform Infrared Spectrometer	Perkin Elmer 2000
X-Ray diffractrometer	Bruker AXS model D8 Discover
X-Ray fluorescence	Philips model PW 2400
Thermal gravimetric analysis	Perkin-Elmer Pyris Diamond TG/DTA
Surface Area and Porosity Analyzer	ASAP 2020, Micromeritics
Gas Pycnometer	Quantachrome / Ultrapycnometer 1000
Particle Size Analyzer	Malvern / Mastersizer X
Moving Die Rheometer	TECHPRO
Universal Testing Machine	LLOYD model LR 10 K Plus
Hardness Testing Machine	REX GAUGE 2000 & OS-2 Stand
Aging Oven	UESHIMA, AG103
Ozone resistance tester	HAMPDEN, Northampton, England
Scanning Electron Microscope	JEOL model JSM–6480 LV
Dynamic Mechanical Analysis	Mettler Toledo DMA/SDTA 861
Abrasion Tester	APH-40, England
Tear resistance tester	LS 500, England

3.3 Experimental Procedures

3.3.1 Preparation of the Cuttlebone

Cuttlebone was obtained from waste stock at commercial processor in Samutsakorn province. Samples were washed in plain water several times and left to dry under the sun. Then, the cuttlebone was crushed and sieved with a 37 μm-mesh sieve. Commercial $CaCO_3$ filler without any surface treatment was used as a reference. The $CaCO_3$ filler and the cuttlebone particles were dried at 120 ^{0}C for 2 h before use. The cuttlebone used in this study was classified into three parts (inner shell, outer shell and both inner and outer shell) as illustrated in Figure 3.1.

Cuttlebone

Inner shell   **Outer shell**   **Cuttlebone particles**
                                                  (Inner shell + outer shell)
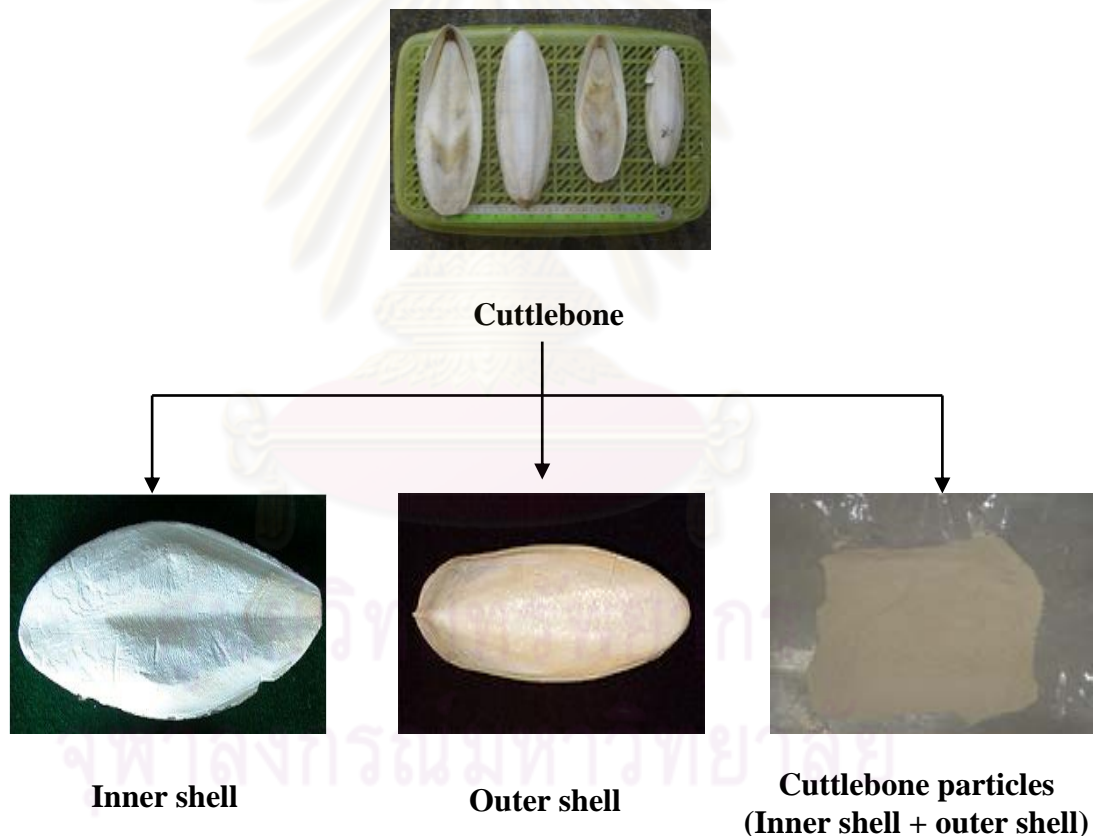
Figure 3.1 Classification of the cuttlebone part.

3.3.2 Characterization of the Cuttlebone

The commercial $CaCO_3$ and the cuttlebone particles filler were characterized by various techniques as follows:

3.3.2.1 Elemental Analysis

The elemental content in the commercial $CaCO_3$ and the cuttlebone particles was determined by using the Energy Dispersive X-ray Fluorescence Spectrometer (Philips PW-2400 ED-2000, England). The elemental content was calculated from the oxide form of each element by the theoretical formulas of "fundamental parameter calculations" method.

3.3.2.2 X-ray Diffraction Measurements

The crystal structure of the commercial $CaCO_3$, inner cuttlebone shell and outer cuttlebone shell were determined by using X-ray diffractometer (Bruker AXS model D8 Discover, Germany) using CuK_α. The filament was operated at 40 kv and 40 mA. The diffraction angle (2θ) was varied from 20^0 to 80^0 using the scanning speed of 0.3 sec/step.

3.3.2.3 Thermal Gravimetric Analysis

The degradation temperature was determined by thermogravimetric analysis (TGA) using a Perkin-Elmer Pyris Diamond TG/DTA, Japan. The sample of ca. 10 mg was placed in a platinum pan and heated up to 1000 ^0C under air at a heating rate of 10 ^0C/min. Degradation temperatures of the samples was calculated from TGA plot.

3.3.2.4 Surface Area Analyzer

The Brunauer–Emmett–Teller (BET) specific surface area was estimated by a ASAP 2020 surface area and porosity analyzer (Micromeritics Instrument Group, USA). The samples were weighed ca. 70 mg and per-treatment at 300 ^0C before each analytical.

3.3.2.5 True Density

The true density of the commercial $CaCO_3$ and the cuttlebone particles was measured by a Gas Pycnometer (Quantachrome / Ultrapycnometer 1000, USA). The porous of the samples was displaced by the helium gas (Archimedes' principle) to determine the volume of a sample. Then, the volume of the sample is translated into the absolute density, as the weight of the sample is known. The measurements were performed at least twenty times and the mean value was reported.

3.3.2.6 Particle Size Distribution

The particle size distributions of the commercial $CaCO_3$ and the cuttlebone particles were determined by using the Particle Size Analyzer (Malvern / Mastersizer X, England)

3.3.3 Extraction and Characterization of Organic Compound

The inner cuttlebone shell and outer cuttlebone shell were subjected to the demineralization and deproteinization in order to extract the organic compounds as demonstrated in scheme 3.1. Demineralization was carried out in dilute hydrochloric acid solution (1 M HCl) at ambient temperature for 3 h with a ratio of the solution to cuttlebone of 40 ml/g. The precipitate was then washed with distilled water, dried and weighed, respectively. The deproteinization was subsequently performed by using alkaline treatment with 1 M sodium hydroxide solution (20 ml/g) at 80-85 ^0C for 1 h. The treatment was repeated several times, which depended on the absence of the proteins at the last treatment. Chitin content was determined from the weight difference of the raw material after acid and alkaline treatments as illustrated in equations 3.1 − 3.3. Finally, the presence of characteristic functional groups of the resulting precipitated chitin was measured by Fourier transform infrared spectroscopy (FTIR).

$$\% \text{ CaCO}_3 = \frac{(A - B)}{A} \times 100 \qquad (3.1)$$

$$\% \text{ Protein} = \frac{(B - C)}{A} \times 100 \qquad (3.2)$$

$$\% \text{ Chitin} = \frac{C}{A} \times 100 \qquad (3.3)$$

where A is the initial weight of cuttlebone inner or cuttlebone shell.

B is the weight of sample after demineralization.

C is the weight of sample after deproteinization.

```
┌─────────────────────────────────┐
│      Cuttlebone particles       │
│   (CaCO₃ + proteins + chitin)   │
└─────────────────────────────────┘
```

Demineralization by   -CaCO₃
1 M HCl

```
┌─────────────────────────────────┐
│      Demineralized products     │
│        (Proteins + chitin)      │
└─────────────────────────────────┘
```

Deproteinization by   -protein
1 M NaOH, 80-85 °C,

```
┌─────────────────────────────────┐
│          Obtained chitin        │
└─────────────────────────────────┘
```

```
┌─────────────────────────────────┐
│   Fourier transform infrared    │
│      spectroscopy (FTIR)        │
└─────────────────────────────────┘
```
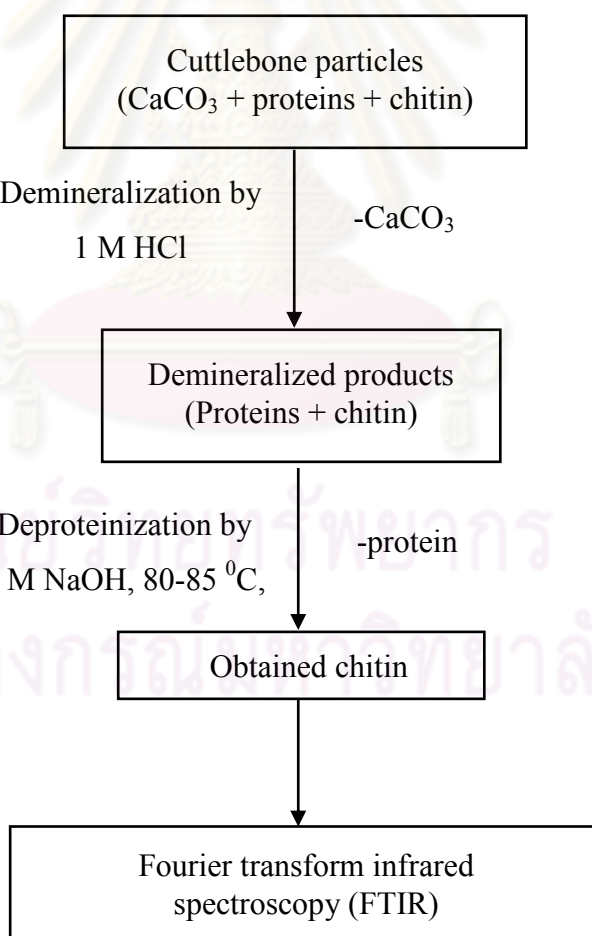
Scheme 3.1 Isolation of chitin from the cuttlebone shell.

3.3.4 Mixing and Determination of Cure Characteristic

The rubber compounding was prepared by a two- roll mill operated at room temperature. The three vulcanization systems, i.e. conventional vulcanization (CV), semi-efficiency vulcanization (semi-EV) and efficiency vulcanization (EV) were investigated. The formulations of rubber compounding are presented in Table 3.3.

Table 3.3 Formulation for NR compounding in the unit of phr[1].

Ingredients	Conventional vulcanized system (CV)	Semi-efficiency vulcanized system (semi-EV)	Efficiency vulcanized system (EV)
NR[2]	100	100	100
ZnO[3]	5	5	5
Stearic acid	2	2	2
CBS[4]	1	2	3
Sulfur	3	1.5	0.5
CA[5]	10,20,40,60,80,100	10,20,40,60,80,100	10,20,40,60,80,100
CTB[6]	10,20,40,60,80,100	10,20,40,60,80,100	10,20,40,60,80,100

[1] Part by weight per hundred part of rubber [2] Natural rubber [3] Active zinc oxide [4] *N*-cyclohexyl-2-benzothiazole sulfenamide [5] Commercial $CaCO_3$ (Silver-W) [6] Cuttlebone particles

The cure characteristics of the compounds were determined by using a TECHPRO: rheoTECH MDR at 155 ^{0}C according to ASTM D5289. The respective cure times as measured by t_{c90}, scorch times (t_{s2}), minimum torques (M_L), maximum torques (M_{HR}) and the torque difference (M_{HR}-M_L) were determined from the rheograph. The rubber compounding was compressed by a compression molding under the pressure of 150 kg/m^2 according to the cure time. In this research, the codes "CA" and "CTB" were represented the commercial $CaCO_3$ and cuttlebone particles reinforced NR vulcanizates, respectively, and the filler contents in a part by weight per hundred part of rubber (phr) were given by the number after the sample code.

3.3.5 Characterization of Composite Material

3.3.5.1 Equilibrium Swelling Measurement of the Vulcanizates

The vulcanized rubber sample was cut into 20 x 20 x 2 mm sized pieces and weight approximately 0.6-1.0 g. The samples were immersed in toluene until they reached the equilibrium (within 3 days) at room temperature. The swollen sample was then removed from the toluene and the excess toluene was rapidly removed by absorption paper. The swollen weight of the samples had been recorded for the determination of swelling ratio. At least 3 samples for each vulcanizates were tested and the average values were reported. The degree of swelling (Q) was calculated by using the equation 3.4.

$$Q = \frac{(W_2 - W_1)}{W_1} \tag{3.4}$$

where W_1 is the weight of the dry sample

W_2 is the weight of the swollen sample.

The variation of Q with crosslink density, for conventionally-cured NR in toluene, may be described as follows:

Unvulcanized rubber, Q_{UV} = >15

Lightly vulcanized, Q_{LV} = 7-15

Moderately vulcanized, Q_{MV} = 5-7

Fully vulcanized, Q_{FV} = <5

3.3.5.2 Tensile Properties

The mechanical properties in terms of modulus at 100% and 300% elongation, tensile strength and elongation at break of the NR vulcanizates were determined under an ambient condition. The tensile test was carried out by a Universal Testing Machine (LR 10K PLUS, England) at a cross-head speed of 500 mm/min according to ASTM D412. The vulcanized sheets having about 2 mm thick were cut by using a die C into the dumbbell shape specimens having dimension as illustrated in Figure 3.2. The specimen was symmetrically placed at the grips of the testing machine to achieve uniform tension distribution over the cross section. The elongation of the specimens was detected from the distance between the extensometer. All tests were considered at least five times and the mean value was reported.

Gauge length

25.0 mm
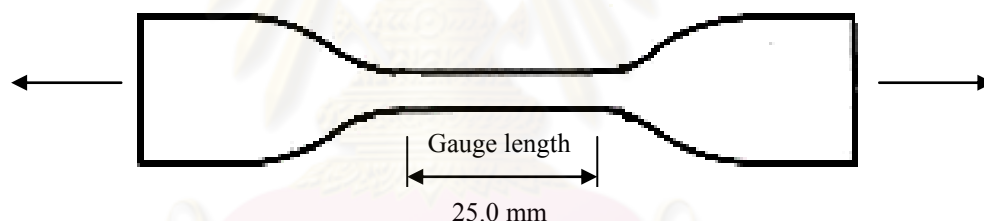
Figure 3.2 Dimensions of the tensile specimen.

To determine the effect of thermal ageing on the mechanical properties of the NR composites, a circulated air oven (UESHIMA - AG103, Japan) was used. The specimens were investigated in a hot air aging oven at 100 ^{o}C for 22 $\pm$ 2 h. At the termination of the aging interval, the dumbbell-shape specimens was removed from the oven and cooled at room temperature on a flat surface for at least 16 h before determination of the tensile properties according to ASTM D412. The thermal aging properties were calculated as percentage of properties retention following equation 3.5.

$$\% \text{ Retention} = \frac{\text{Mechanical properties after aging}}{\text{Mechanical properties before aging}} \text{ x } 100 \qquad (3.5)$$

3.3.5.3 Hardness

The hardness of the rubber vulcanizates was measured by using a Shore-type-A Lever Loader (REX GAUGE 2000 & OS Stand) according to ASTM D2240 at room temperature. The specimen having about 6 mm of thickness was placed on the platform. The durometer was held in a vertical position with point of the indenter at least 10 mm from any edge of the specimen. The measurements were taken from five different points distributed over the sample and the reported were based on an average of five measurements.

3.3.5.4 Tear Strength

Tear strength of rubber vulcanizates were measured by Lloyd Instruments materials testing machines (LS 500, England) according to ISO 34. The vulcanized sheets having about 2 mm thick were cut by using type C die having dimension as illustrated in Figure 3.3. The specimen was gripped in the testing machine. The machine was started until the test specimen was completely ruptured. At least 5 specimens were tested for these properties and the average values were reported. The tear strength was calculated from the maximum force required to cause a nick in the tested specimen with tab end to grow by tearing of rubber and the thickness of the specimen according to equation 3.6;

$$\text{Tear strength (N/mm)} = F/d \qquad (3.6)$$

where   F is the maximum force, (N)

d is the thickness of the specimen, (mm).
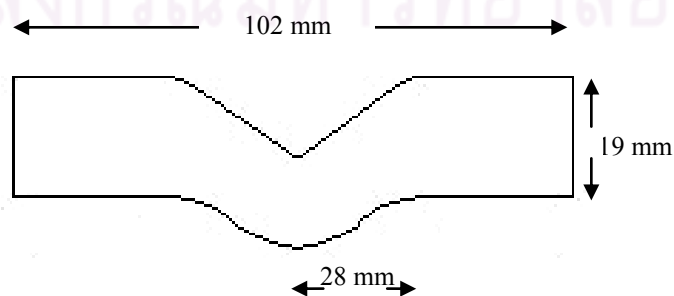
Figure 3.3 Dimensions of the tear specimen.

3.3.5.5 Abrasion Resistance

Abrasion tests use an abradant to be applied to the surface of a rubber sample. Tested compounds are usually compared with a "volume loss" basis which is calculated from the weight and density of the vulcanizates as illustrated in equation 3.7. In this research, DIN abrasion test was done by the DIN abrasion tester (APH-40, England) for determining the abrasion resistance of compounds of vulcanized rubber according to DIN 53516 at room temperature. The cylindrical in shape of samples used was 16 mm in diameter and had a minimum thickness of 6 mm.

$$\text{Volume loss (mm}^3) = \frac{\Delta m \times 200}{D \times 180} \qquad (3.7)$$

where Δm is mass loss, (original mass of the sample – final mass of the sample, mg)

D is the density, (mg/mm^3).

3.3.5.6 Dynamic Mechanical Analysis (DMA)

The dynamic mechanical properties such as storage modulus and loss modulus of each rubber vulcanizate were measured under shear mode at a frequency of 1 Hz by a dynamic mechanical analyzer, (Mettler Toledo DMA/STDA 861, Switzerland) rectangular sample of 5 x 5 x 2 mm was subjected to sinusoidal loading and heated from -120 to 80 ^{0}C at with a heating rate of 4 ^{0}C/min.

3.3.5.7 Ozone Resistance Test

The resistance to ozonolysis was investigated followed the standard method ISO 1431/1–2004 and the physical testing standards of rubbers was developed by Nishi and Nagano. The specimens were cut into a size of 25 mm x 80 mm x 20 mm. The rubber samples were exposed in an ozone cabinet (HAMPDEN, Northampton, England) at 40 ^{0}C to an ozone atmosphere of 50 pphm (part per hundred million). Before exposure to ozone, the specimens were stretched by 20% using a specimen holder for 48 h in the absence of light under an ozone-free

atmosphere. The results of ozone cracking were observed at 24 and 48 h. The cracking on rubber surface was examined by using a CCD camera. The classification of ozone cracking on the rubber surface was specified in terms of the size and depth of cracking as shown in Table 3.4.

Table 3.4 Classification of cracking on rubber surface [55].

Number of Cracking	Size and Depth of Cracking
A: a small number of cracking	1. That cannot be seen with eyes but can be confirmed with 10 times magnifying glass.
	2. That can be confirmed with naked eyes.
B: a large of number cracking	3. That the deep and comparatively long (below 1 mm).
	4. That the deep and long (above 1 mm and below 3 mm).
	5. That about to crack more than 3 mm
C: numberless cracking	or about to severe.

3.3.5.8 Morphology of the NR vulcanizates

The morphology of the commercial $CaCO_3$ or cuttlebone filled NR vulcanizates was examined by using Scanning electron microscopy (SEM), JEOL, JSM–6480, Japan, operated at 15 kV. The fracture surfaces after tensile testing were cut and stitched on a SEM stub using double-sided tape. The sample was then sputter–coated with gold before measuring.

CHAPTER IV

RESULTS AND DISCUSSION

4.1 Characterization of Cuttlebone Particles

Table 4.1 shows the elemental composition analysis of commercial $CaCO_3$ inner and outer cuttlebone shells by XRF spectroscopy. It is clearly seen that Ca^{2+} was the major elements in the cuttlebone not only in the inner part (57.22%) but also in outer part (56.11%), while the main composition of commercial $CaCO_3$ was about 67.21 %, which was higher than that of the both parts of cuttlebone. The other components such as Na_2O, MgO, SiO_2 and so on were appeared as trace elements.

Table 4.1 Elemental analysis by X-Ray Fluorescence.

| Element | Composition | | |
	Commercial $CaCO_3$ (%wt/wt)	Inner cuttlebone shell (%wt/wt)	Outer cuttlebone shell (%wt/wt)
Na_2O	-	1.86	1.47
MgO	0.46	0.24	0.22
Al_2O_3	0.09	0.01	0.04
SiO_2	0.16	0.01	0.14
P_2O_5	0.01	0.23	0.18
SO_3	0.14	0.40	0.35
Cl	0.03	1.65	0.98
K_2O	-	0.17	0.17
CaO	67.21 (98.56%)[*]	57.22 (92.34%)[*]	56.11 (93.68%)[*]
Fe_2O_3	0.08	0.02	0.05
ZnO	-	-	0.03
SrO	0.01	0.12	0.12
ZrO_2	-	0.04	0.03

[*] The normalized values

Crystalline structures of both $CaCO_3$ from inner and outer shells were confirmed by using XRD technique. Figure 4.1 shows the XRD patterns of the commercial $CaCO_3$, inner and outer cuttlebone shells, respectively. Their XRD patterns showed different crystalline peaks. Crystal form of commercial $CaCO_3$ was found to be a calcite form in a hexagonal-rhombohedral shape (Figure 4.1 (a)), while those of inner and outer cuttlebone shells were an aragonite one in an orthorhombic shape of crystal as shown in Figures 4.1 (b) and (c), respectively.

The thermal degradation characteristics of commercial $CaCO_3$ and cuttlebone particles are presented in Figure 4.2. The degradation temperature and percentage of weight loss are summarized in Table 4.2. From the thermogravimetric analysis, the degradation of the commercial $CaCO_3$ started around 713 ^{0}C, and was completed at 787 ^{0}C with a weight loss of 40 % due to the thermal decomposition of $CaCO_3$. In addition, the results revealed that the degradation of either inner cuttlebone shell or outer cuttlebone shell occurred in two steps and the behavior of degradation of both parts was almost similar. In the first step, approximately 266 ^{0}C to 330 ^{0}C and reduced the weight of 4 – 8 % was due to the decomposition of the organic materials. In the second step, approximately 650 ^{0}C to 825 ^{0}C with a weight loss of ca. 40 % was associated with the burning of $CaCO_3$ to produce calcium oxide (CaO) and carbon dioxide (CO_2), respectively. Birchall *et al*. [8] reported that one of the main components of cuttlebone is a chitin and the chitin is covalently linked to protein components in cuttlebone. Thus, the identification of the organic parts is necessary and will be reported in the later part of this thesis. Finally, both inner cuttlebone shell and outer cuttlebone shell were mixed together and subjected to TGA and the result was shown in Figure 4.2 (d). It is clearly seen that the thermogram of cuttlebone particles was similar to each part of shell, i.e., inner and outer cuttlebone shells. Accordingly, in this study we used both inner and outer parts of cuttlebone shell, which is so called "cuttlebone particles" to investigate the reinforcement effect in NR vulcanizates.

The average size, BET surface area and density of cuttlebone particles were measured for discussing their reinforcement effect for rubber, and they were 106 μm, 11 m^2/g and 2.50 g/cm^3, respectively. The such values were comparable with the values of inner cuttlebone particles (121 μm, 18 m^2/g and 2.60 g/cm^3) as illustrated in Table 4.3.
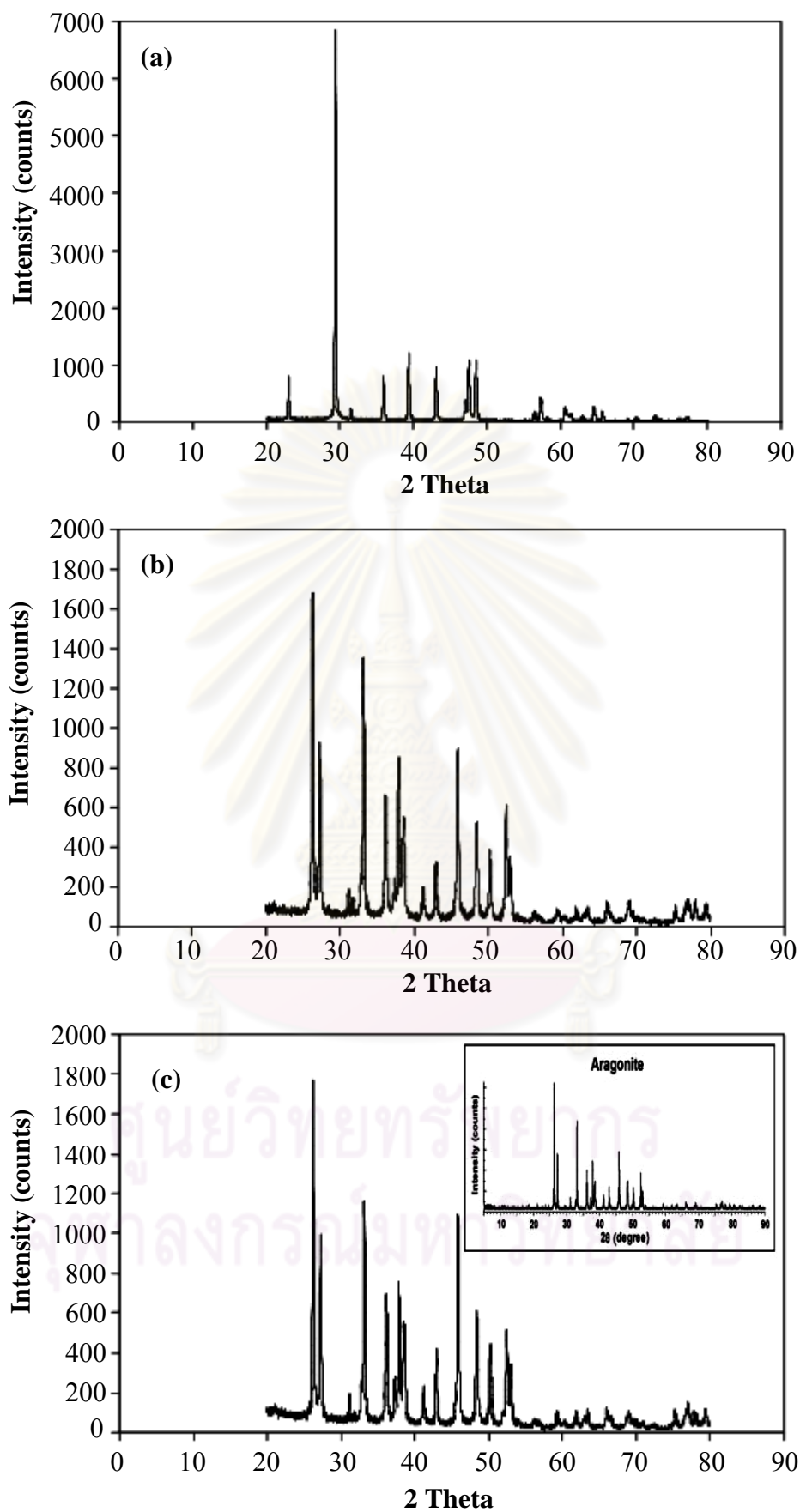
Figure 4.1 XRD patterns of (a) commercial CaCO₃ (b) inner cuttlebone shell and

(c) outer cuttlebone shell.
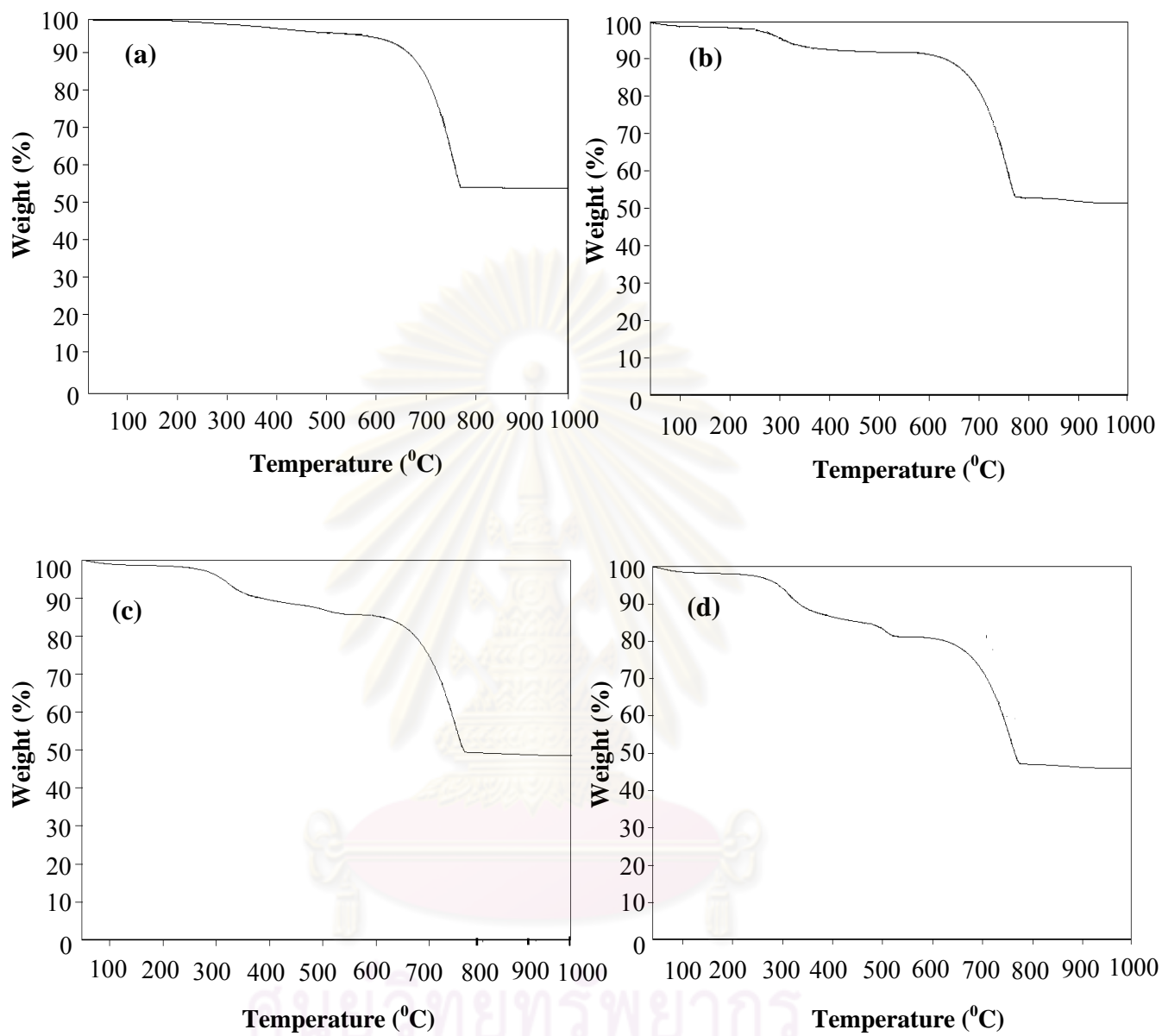
Figure 4.2 Thermogravimetric curves of (a) commercial $CaCO_3$ (b) inner cuttlebone shell
(c) outer cuttlebone shell and (d) cuttlebone particles.

Table 4.2 Degradation temperatures and % weight loss of commercial $CaCO_3$, inner cuttlebone shell, outer cuttlebone shell and cuttlebone particles.

Sample	Degradation temperature (^{o}C) (First stage)		Weight loss (%)	Degradation temperature (^{o}C) (Second stage)		Weight loss (%)
	T_{id}[a]	T_{fd}[b]		T_{id}[a]	T_{fd}[b]	
Commercial $CaCO_3$	713	787	39.9	-	-	-
Inner cuttlebone shell	266	331	4.3	696	771	38.8
Outer cuttlebone shell	282	338	6.3	683	756	34.9
Cuttlebone particles[*]	286	330	8.3	692	771	33.8

[a] Initial decomposition temperature

[b] Final decomposition temperature

[*] inner and outer cuttlebone shells

Table 4.3 Characteristics of commercial $CaCO_3$ and the cuttlebone particles.

Sample	Average particle size[*] (μm)	BET surface area (m^2/g)	Density (g/cm^3)
Commercial $CaCO_3$	1.5	5.5	2.54
Inner cuttlebone particles	121	18	2.60
Cuttlebone particles	106	11	2.50

[*] The average particle size was determined by laser technique

4.2 Determination of Organic Component

4.2.1 Isolation of Chitin

In this section, the determination of organic components in both inner and outer cuttlebone shells was examined. After the inner or outer cuttlebone shells were subjected to the demineralization and deproteinization processes, the obtained products were composed of the inorganic $CaCO_3$, protein and chitin [53-54, 56] as seen in Table 4.4. It is clearly seen that the main composition in cuttlebone particles was inorganic $CaCO_3$ about 89–94 % and the remained contents were protein (3-7 %) and chitin (3-4 %).

Table 4.4 Mineral content (% Composition) of raw shell cuttlebone.

Chitin source	$CaCO_3$ content (%)	Protein content (%)	Chitin content (%)
Inner cuttlebone shell	93.79	3.20	3.01
Outer cuttlebone shell	89.06	7.09	3.85

The values depicted above are the average value of 3 experiments.

4.2.2 Chitin Characterization

Chitin is a modified polysaccharide containing nitrogen. Three different polymorphs of chitin are found in the nature, α- , β- and γ-chitin. Figure 4.3 shows the FTIR spectra of commercial chitin in β-form (Figure 4.3 (a)) and extracted chitin from cuttlebone both of inner and outer parts (Figure 4.3 (b) and (c)). The broad peak at 3456 cm⁻¹ is due to the O–H stretch vibrations and the absorption of intra-hydrogen bonds. The absorption peaks at 1656 cm⁻¹ was commonly assigned to the stretching of the CO group hydrogen bonded to amide group of the neighboring intra-sheet chain. The absorption peaks appeared at 1628 cm⁻¹, 1560 cm⁻¹ and 1316 cm⁻¹ were assigned to the Amide I, Amide II and Amide III, respectively. These results indicated that the characteristic absorption peaks of extracted chitin from cuttlebone particles were corresponding to the chemical structure of chitin in β-form [53-54, 57].
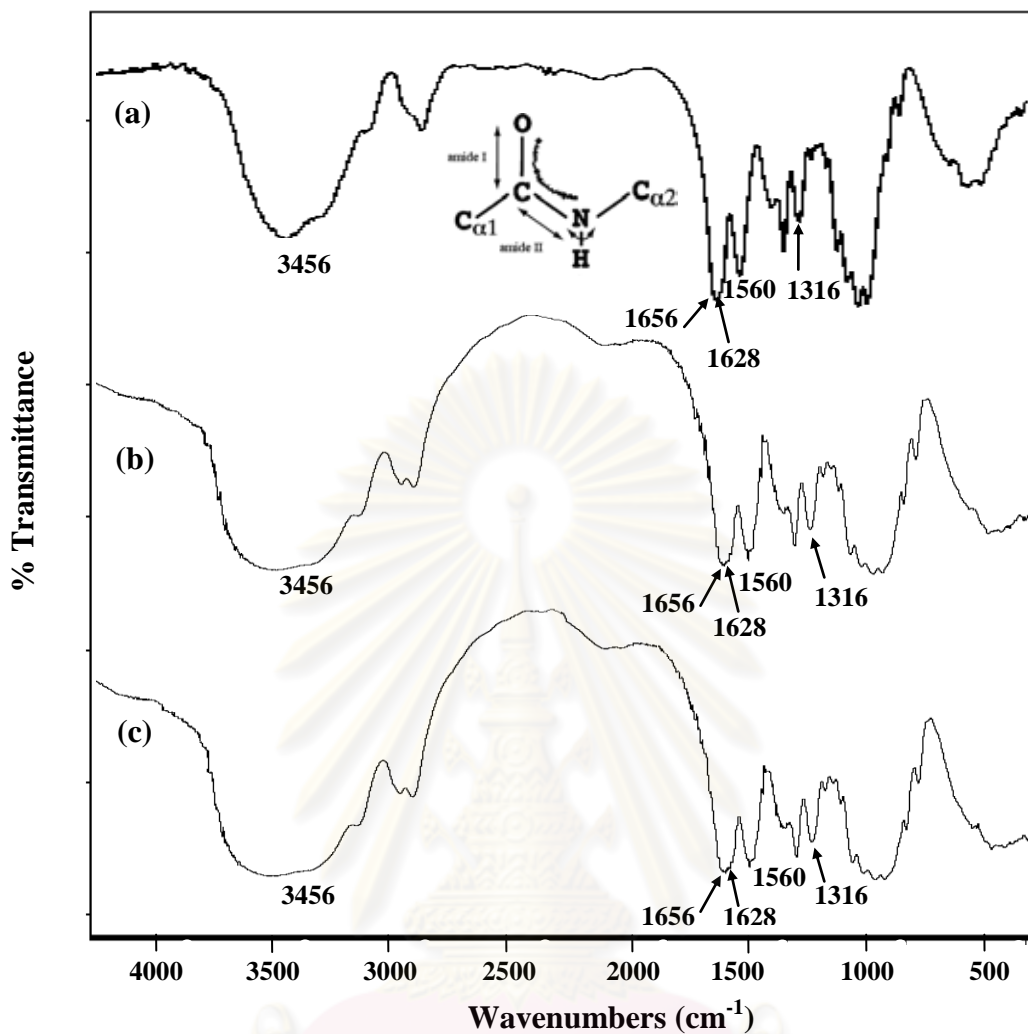
Figure 4.3 FTIR spectra of chitin (a) β-chitin (standard) (b) isolated chitin from inner cuttlebone shell and (c) isolated chitin from outer cuttlebone shell.

According to the results, it was also confirmed that the characteristics and the essential components of the inner cuttlebone shell were very similar to the outer cuttlebone shell. For this reason, the inner cuttlebone shell was combined with the outer cuttlebone shell by using the vibratory mill machine and the cuttlebone particles were used as a reinforcing filler in NR composites. The combined material would be beneficial to the process, which times in the system and cost of the products are very concerned in the industrial.

4.3 Cure Characteristics of the NR compounding

The cure characteristics of various NR vulcanizates filled with commercial $CaCO_3$ and the cuttlebone particles at 155 ^{0}C were examined. The effects of the curing system (CV, semi-EV and EV) on the curing properties of various NR compounding filled with commercial $CaCO_3$ and the cuttlebone particles are illustrated in Figures 4.4 - 4.6. The summarization of raw data of scorch time, optimum cure time, torque difference values, curing time and curing temperature was presented in Appendix B (Table B-1 - B-3). The results revealed that the scorch time or induction period and the optimum cure time decreased with increasing quantities of filler loadings. Accordingly, the cure time was found to be dependent of filler loading. This might possibly be because the nature of the $CaCO_3$ filler was basic and so can increase the curing rate, resulting in the decrease of curing time. In addition, the reduction in cure time of the filled rubber vulcanizates could be attributed to the longer time spent during the mixing process on the two-roll mill. This result was corresponding with the Jacob *et al*. [51] and Geethamma *et al*. [58] works. They studied the mechanical properties of NR composites filled with natural fiber and reported that when the filler loading increased, the time of incorporation of filler into the rubber matrix also increased and consequently generated more heat due to additional friction resulted in the formation of the partial cross-linking in the NR matrix.

The effect of commercial $CaCO_3$ and the cuttlebone particles loading on the torque difference, M_{HR}-M_L (maximum torque - minimum torque), of the commercial $CaCO_3$ or the cuttlebone particles filled NR compounding in various vulcanization systems are exhibited in Figures 4.4 (b) - 4.6 (b) and Table B-1 - B-3. The results showed that the torque difference was gradually increased with increasing fillers loading in the following order: CV > semi-EV > EV. This result indicated that the formation of rubber networks was increased when using the commercial $CaCO_3$ or the cuttlebone particles filler. Theoretically, it is known that in compounds the torque difference showed shear dynamic modulus which indirectly related to the crosslink density of the compounds [4]. Furthermore, the presence of the filler generates an increase in viscosity of the mixes. The increment in torque values with increasing filler loadings indicates that as more and more filler gets into the rubber matrix. The

mobility of the macromolecular chains of the rubber reduces resulting in more rigid vulcanizates [51]. The CV system in NR vulcanizates predominantly contained the polysulfidic networks, while the vulcanizates cured with the semi-EV and EV systems normally have mono- and di-sulfidic networks [59]. The difference types of crosslinks in each curing systems affected to the mechanical properties of NR vulcanizates, which can be discussed in the later part of this research. However, it should be noted that the cure time used in this study was the average value for each curing systems: CV systems (10 min), semi-EV systems (10 min) and EV systems (15 min) in order to keep the crosslink density constant in each sample. According to these results, it was confirmed that the incorporation of the cuttlebone particles did not prevent the sulfur cross-linking reaction of NR, regardless the curing systems.

4.4 Swelling Properties of the NR Vulcanizates

The influence of commercial $CaCO_3$ or cuttlebone particles addition on the swelling ratio values of the sulfur cross-linked NR vulcanizates in toluene is plotted against the filler contents at room temperature as presented in Figure 4.7. The weight of toluene absorbed per gram of rubber, Q (equation 3.4), for all three vulcanization systems, decreased with increasing loadings of both types of $CaCO_3$. As Q is inversely proportional to the degree of crosslinking [59], this supports that an increase in the crosslink density with increasing $CaCO_3$ contents in the NR vulcanizates, which then correlates with the increasing torque with increasing $CaCO_3$ contents in the NR vulcanizat (Figures 4.4 - 4.6). Moreover, the higher reinforcement of $CaCO_3$ in the NR matrix restricts the extensibility of the rubber chains induced by swelling. This made it difficult for the solvent to penetrate into the gaps between rubber molecules and hence decreases the Q value [60]. Generally, the rubber swelling is influenced by various factors, such as crosslink type, amount and type of filler and elastomer type [61]. The higher values of Q for the EV-system over those of both the CV and semi-EV systems could be ascribed to the different types of crosslinks resulting from these systems. It is assumed that the EV-system creates small amount of the mono- and disulphide (-S-, -S-S-) crosslinks types in the NR vulcanizates. On the other hand, the crosslink types in the NR vulcanizates cured by CV system or semi-EV system tended to be more polysulfides (-S_x-) due to the excess amount of sulfur in the system [62].
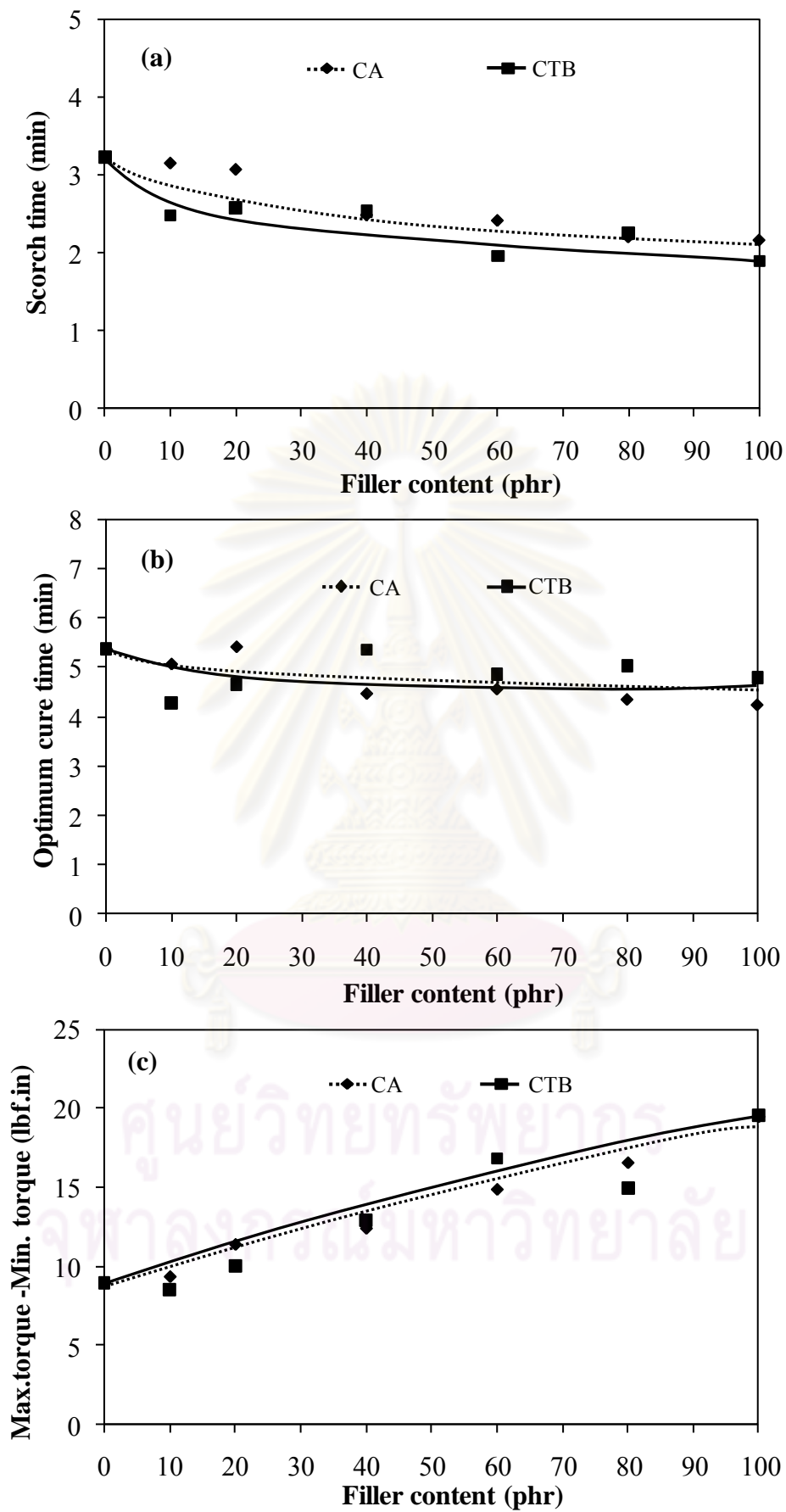
Figure 4.4 Effect of commercial $CaCO_3$ or cuttlebone particles loading on the (a) scorch time (b) optimum cure time and (c) maximum torque - minimum torque of the NR compounding in CV system.
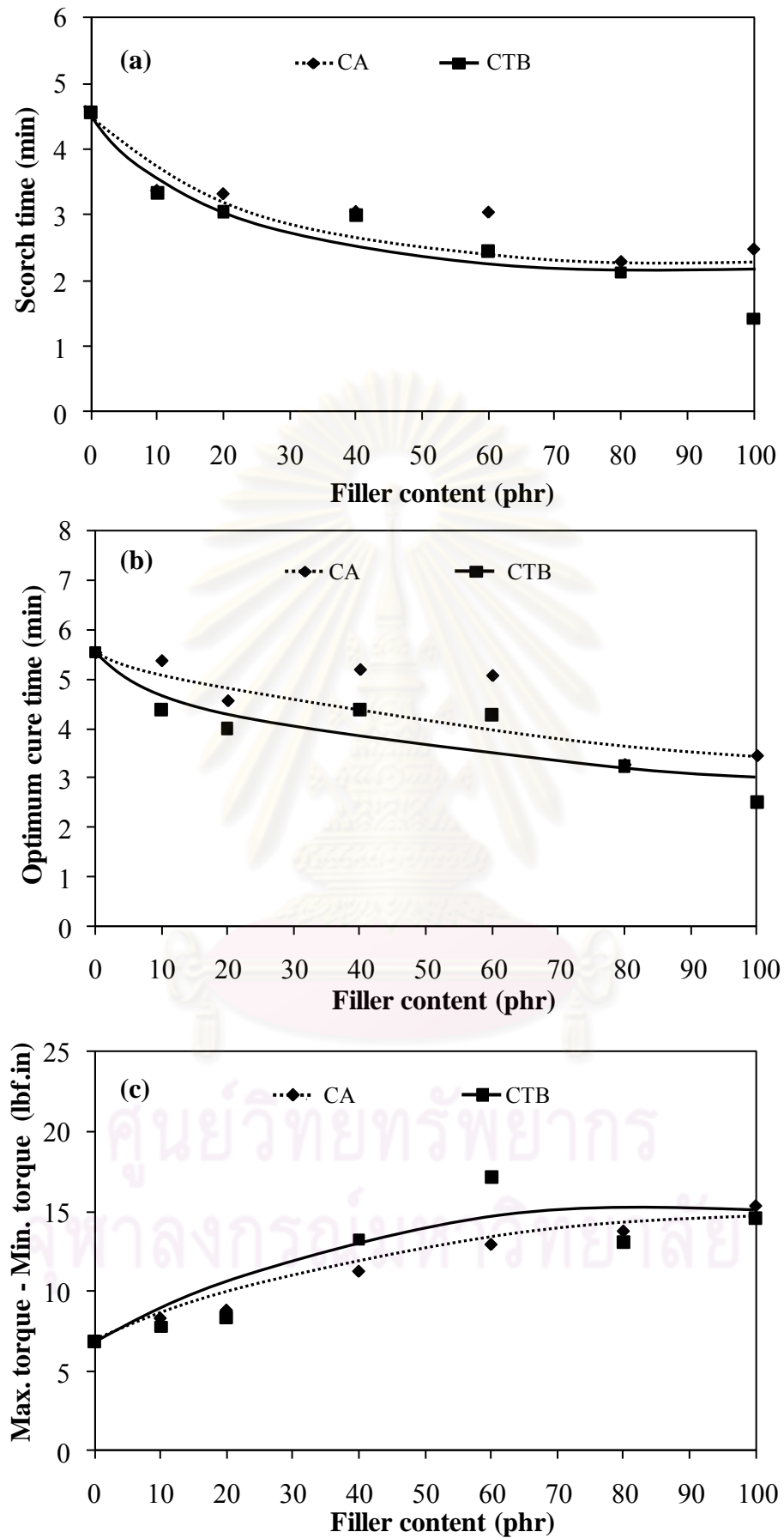
Figure 4.5 Effect of commercial CaCO$_3$ or cuttlebone particles loading on the (a) scorch time (b) optimum cure time and (c) maximum torque - minimum torque of the NR compounding in semi-EV system.
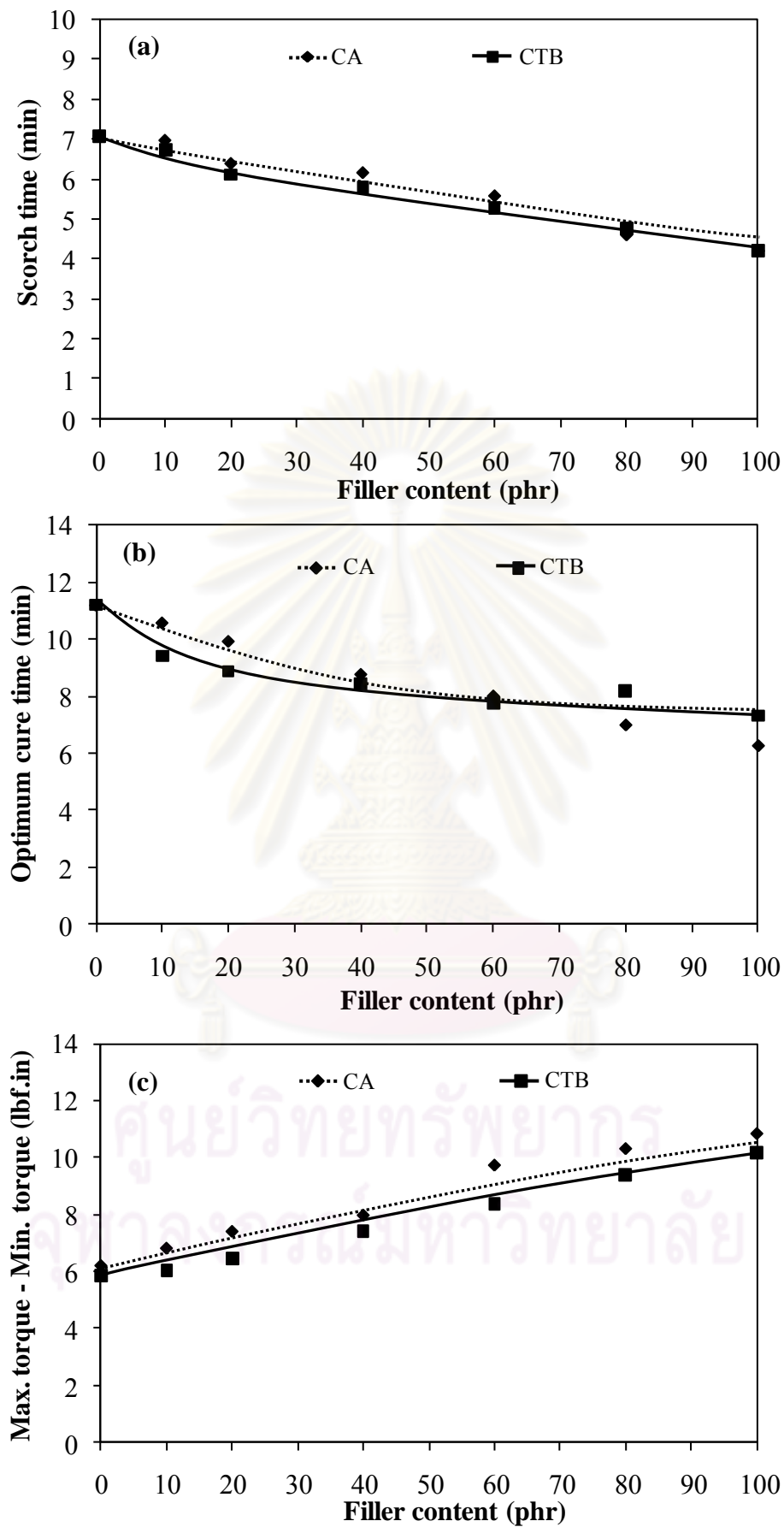
Figure 4.6 Effect of commercial CaCO₃ or cuttlebone particles loading on the
(a) scorch time (b) optimum cure time and (c) maximum torque -
minimum torque of the NR compounding in EV system.
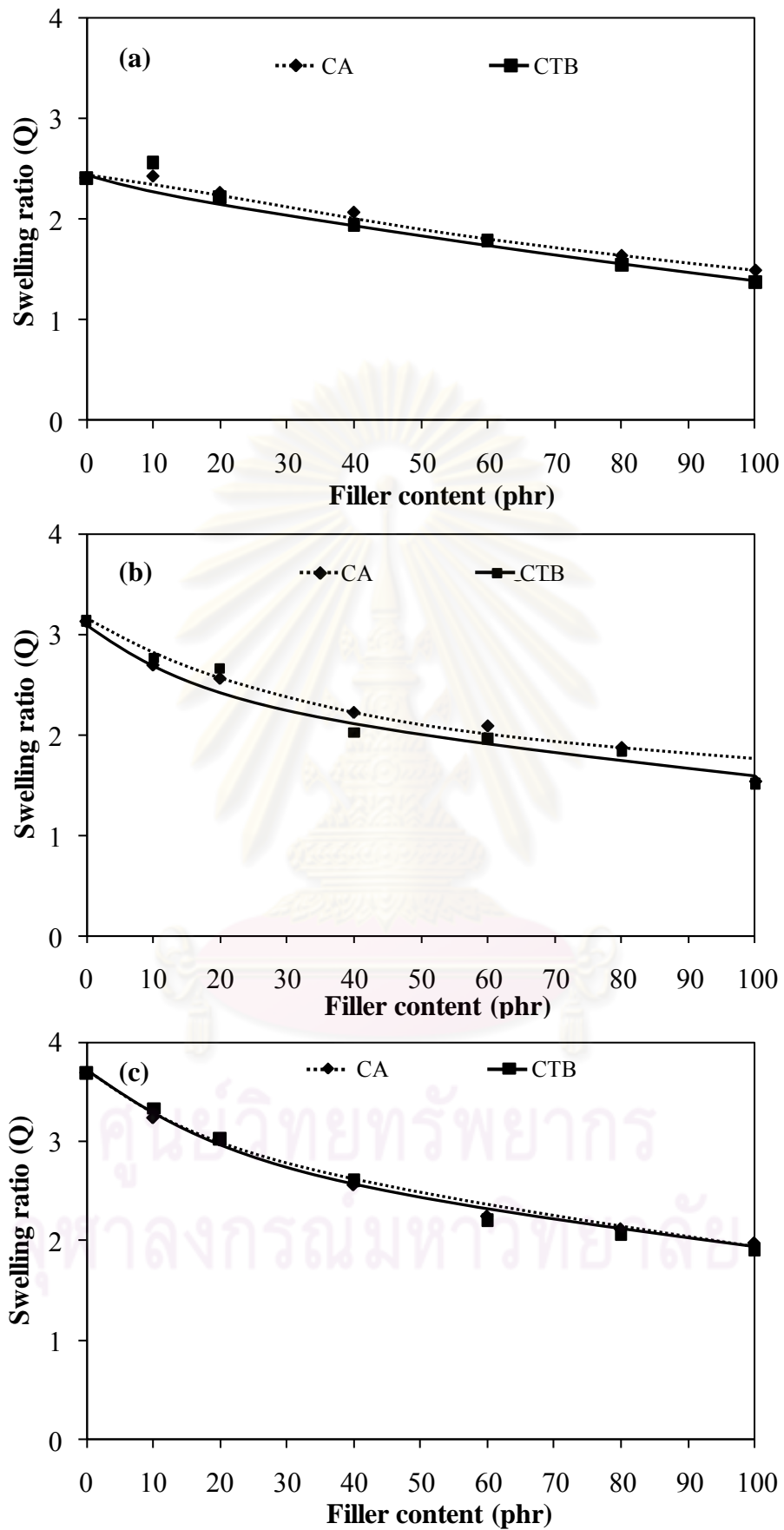
Figure 4.7 Swelling ratios (Q) of commercial CaCO$_3$ or cuttlebone particles filled

NR vulcanizates in various curing systems; (a) CV system (b) semi-EV

system and (c) EV system.

The excess amount of these sulfur increased the probability of formation of polysulphide crosslinks. This leads to a relative increase of the crosslinking reaction in NR vulcanizates resulted in the decreased of the Q values. According to these results, the presence of $CaCO_3$, hence cuttlebone particles, increased the crosslink density (reducing the swelling ratio) of the NR vulcanizates, regardless the curing system. Additionally, the experimental Q values of all samples for each curing system was lower than 5. It is in agreement with the theoretical value that if Q is lowers than 5 it confirms that the rubber chains are fully vulcanized.

4.5 Mechanical Properties of NR Vulcanizates

Mechanical properties of the NR vulcanizates using three types of vulcanizing system were measured in terms of moduli at 100% (M_{100}) and 300% (M_{300}) elongation, tensile strength (T_B), ultimate elongation (E_B), tear strength and hardness, respectively. All raw data of mechanical properties for filled NR vulcanizates with different curing systems were reported in Appendix C (Tables C-1 - C-3). The effect of commercial $CaCO_3$ or cuttlebone particles loading on the M_{100} and M_{300} of NR vulcanizates in various curing systems was exhibited in Figure 4.8. The results showed that the M_{100} and M_{300} increased significantly with increasing filler loading due to the reinforcing effect of $CaCO_3$ filler. The reinforcement effect by the cuttlebone particles was found to be comparable with the commercial $CaCO_3$. Generally, the smaller the size of filler is, the larger the reinforcement effect of the filler becomes [9]. In this research, however, the average size of the cuttlebone particles (106 μm) was about a hundred times larger than that of the commercial $CaCO_3$ (1.5 μm), but the reinforcement effect is comparable with that of the commercial filler. Probably, the presence of the organic components, such as protein and chitin, is speculated to give a good reinforcement effect of the cuttlebone particles to NR. Furthermore, the reinforcement of cuttlebone more than 40 phr in NR vulcanizates for all curing systems was found to be greater than those of commercial $CaCO_3$ filled ones. These results might be because the specific surface area (Table 4.3) of cuttlebone particle was higher than that of commercial $CaCO_3$, leading to a stronger rubber-filler interaction in the cuttlebone filled NR vulcanizates [60]. This result was also supported by SEM observation in the later section of this research.

Additionally, the mechanical behavior of an elastomer depends strongly on the crosslink density. The modulus increases monotonically with the crosslink density, and at the same time, networks become more elastic or less hysteretic [61]. The results in terms of modulus were correlated with the increase in the torque different (Figures 4.4 - 4.6) and the decrease in the swelling ratio (Figure 4.7) of the NR vulcanizates. According to the obtained results, the rigidity of the NR vulcanizates increased with increasing filler loading. This means that the cuttlebone particles behave like rigid fillers since they showed a higher modulus than the NR matrix. Rigid fillers are not easily deformed and their addition to a relatively soft matrix results the development local stretching in the matrix which exceed the overall strain of the composite. Thus, the rubber will respond with a higher stress when deformed. This phenomenon known as "strain amplification" resulted in a significant increase in modulus [60, 63-64]. When comparing the M_{100} and M_{300} values of the cuttlebone filled NR vulcanizates for the different curing systems, the moduli shows that the CV system are clearly greater than those from the semi-EV and EV system, respectively. The results indicated that the polysulfidic linkage makes the rubber chain more rigid and more crosslink formation compared to monosulfidic and disulfidic linkage, which were observed in the semi-EV and EV systems [65].

The mechanical properties of the commercial $CaCO_3$ or cuttlebone particles filled NR vulcanizates in terms of T_B, E_B and hardness of filled NR vulcanizates for three kinds of curing systems were illustrated in Figures 4.9 - 4.11. The T_B increased with increasing filler loading until a maximum level was reached about 20 phr of filler loading and decreased by further loading for all curing systems. This trend could be explained by two possible reasons. Firstly, when filler reinforced NR composites is subjected to load, the filler act as carriers of load and stress is transferred from matrix along the filler leading to effective and uniform stress distribution which results in a composite having good mechanical properties. Nevertheless, the incorporation of the cuttlebone particles into the NR matrix can improve the stiffness of the vulcanizates that is reduced the elasticity of the vulcanizates in the same time. Hence, this phenomenon is affected to the ability of the cuttlebone particles to support stress transferred from the elastomeric phase resulted in the decrease of T_B of the NR vulcanizates [4, 51, 60]. The results obtained were also associated with the E_B in Figure 4.9 (b) - 4.11 (b). The E_B was slightly decreased with an increase of the

quantity of cuttlebone particles. The hardness of the commercial $CaCO_3$ or cuttlebone particles filled NR vulcanizates increased continuously with increasing commercial $CaCO_3$ or cuttlebone particles loadings, regardless the curing systems as seen in Figures 4.9 (c) - 4.11 (c). As mentioned earlier, NR vulcanizates became stiffer and harder as the commercial $CaCO_3$ or cuttlebone particles loading increased, resulting in the increase of the hardness at high filler content. Apart from the reason as mentioned above, the other reason can be attributed to the aggregation of the filler in NR matrix. This occurrence can be discussed by the SEM investigation in the further part of this research.

Theoretically, NR inherently possesses high strength due to strain-induced crystallization. When fillers are incorporated into NR matrix, the regular arrangement of rubber molecules is disrupted and hence the ability for crystallization is lost. This is the reason why T_B and E_B of the filler filled NR vulcanizates decreased by increasing the filler loading that was contrasted with the synthetic rubber [51]. This is a common observation since many researchers [64-68] reported the effect of the incorporation of filler on the mechanical properties in terms of T_B and E_B of the NR and synthetic rubber. Additionally, the mechanical properties of the cuttlebone particles filled NR vulcanizates was found to be comparable with those of commercial filled ones, regardless the curing systems. However, the mechanical properties of cuttlebone particles filled NR vulcanizates with different curing systems showed the different results among them. The results revealed that the EV system imparts the NR vulcanizates with lowest mechanical properties value whereas the CV system imparts the NR vulcanizates with the highest mechanical properties. This is simply due to the fact that the NR vulcanizates with crosslinks which were predominantly polysulphidic exhibit properties i.e. T_B and hardness, superior to those of the corresponding mono- and disulphidic crosslinking vulcanizates [65].

Furthermore, it is important to know that the main component in the cuttlebone particles was approximately 90 % $CaCO_3$ and the remained content was the organic components ca. 10%. The mechanical properties of NR vulcanizates filled with the cuttlebone particles were greater than that of commercial $CaCO_3$ filled ones, although the commercial $CaCO_3$ is composed of almost 100% $CaCO_3$. These results referred that the organic components like protein and chitin in the cuttlebone particles was essentially affected to give a potential reinforcement to NR vulcanizates.
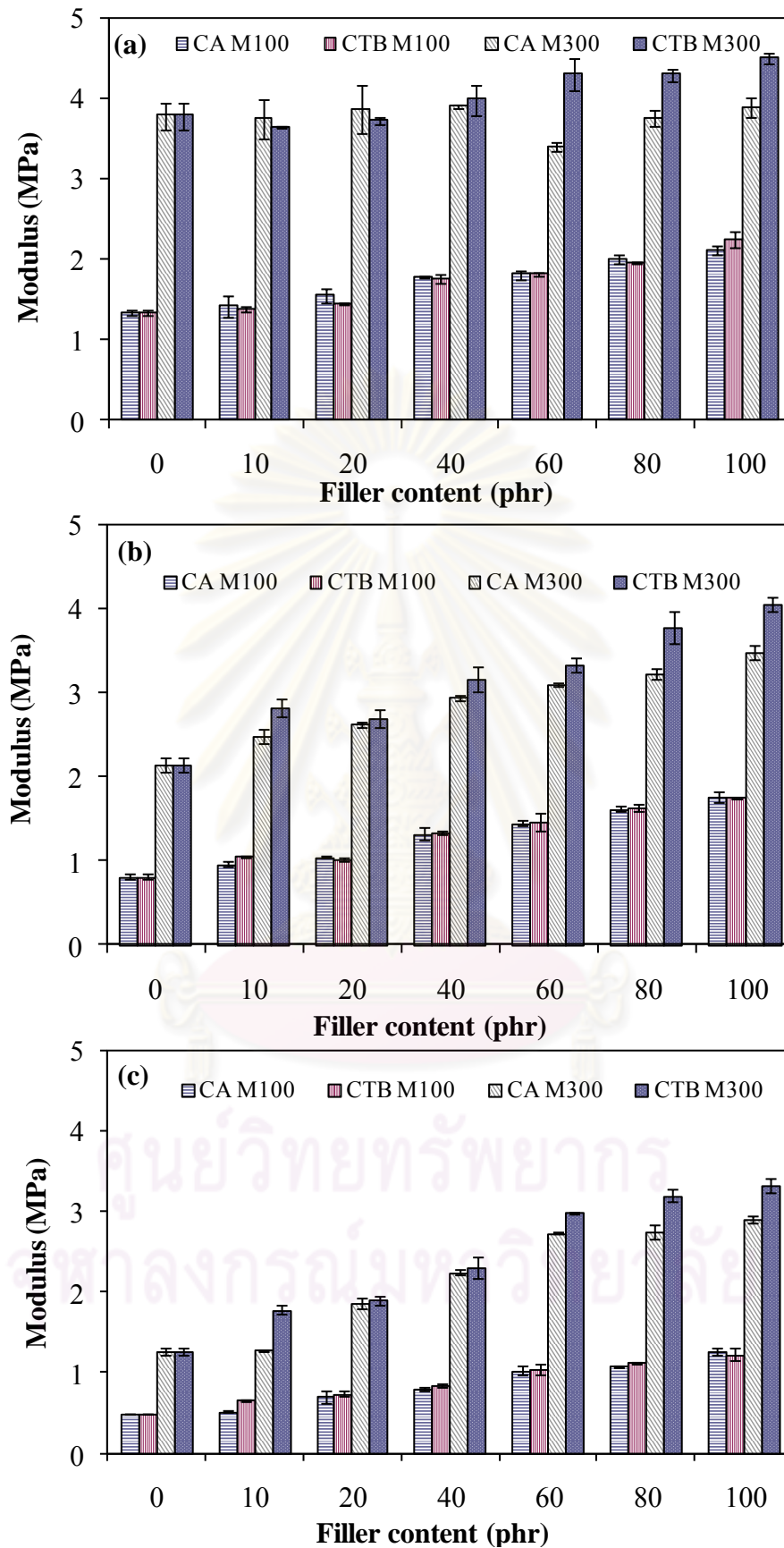
Figure 4.8 The effect of commercial CaCO$_3$ or cuttlebone particles on the modulus at

100 % and 300% elongation of NR vulcanizates in various curing systems;

(a) CV system (b) semi-EV system and (c) EV system.
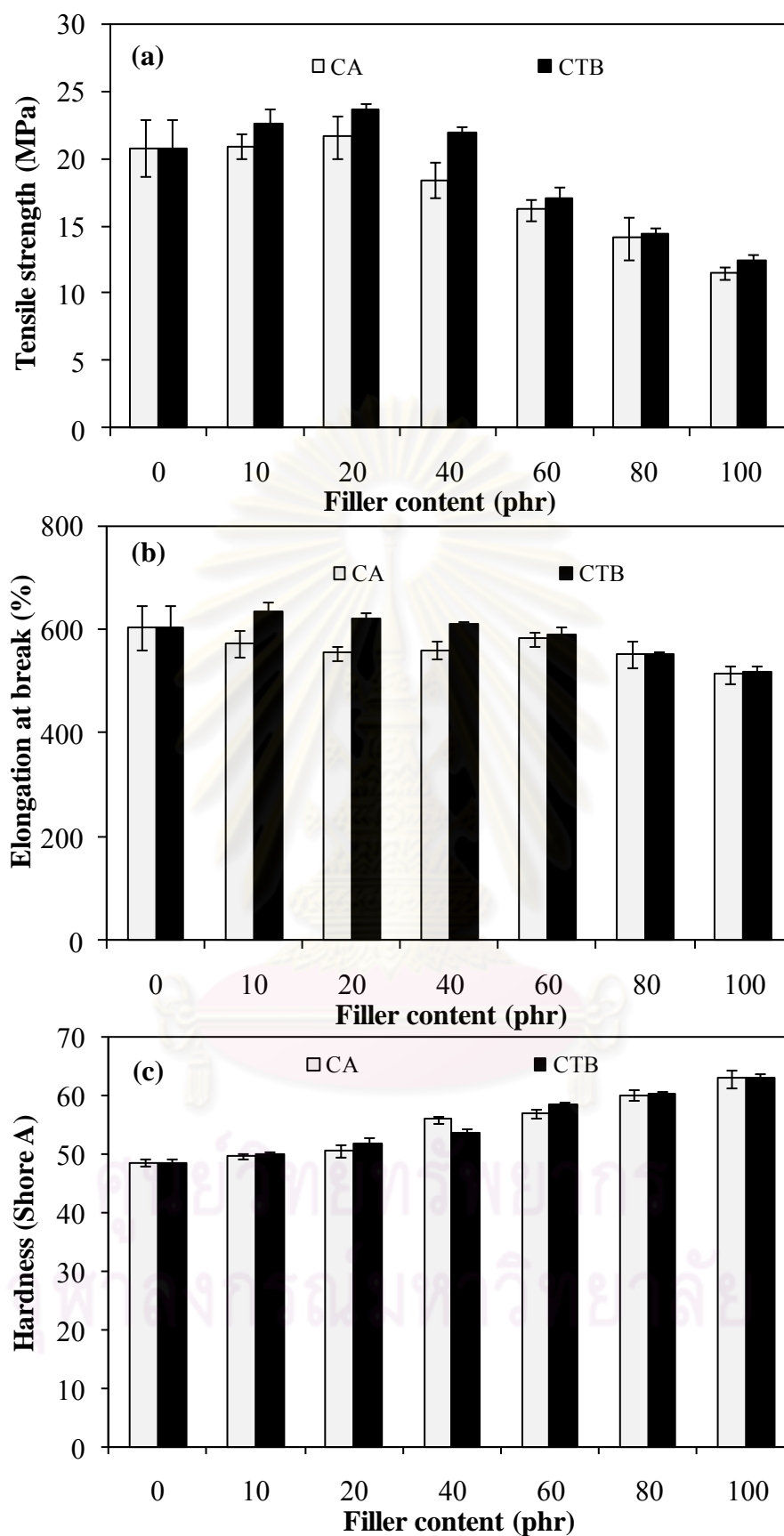
Figure 4.9 The effect of commercial CaCO₃ or cuttlebone particles on (a) tensile strength, (b) elongation at break and (c) hardness of NR vulcanizates in CV system.
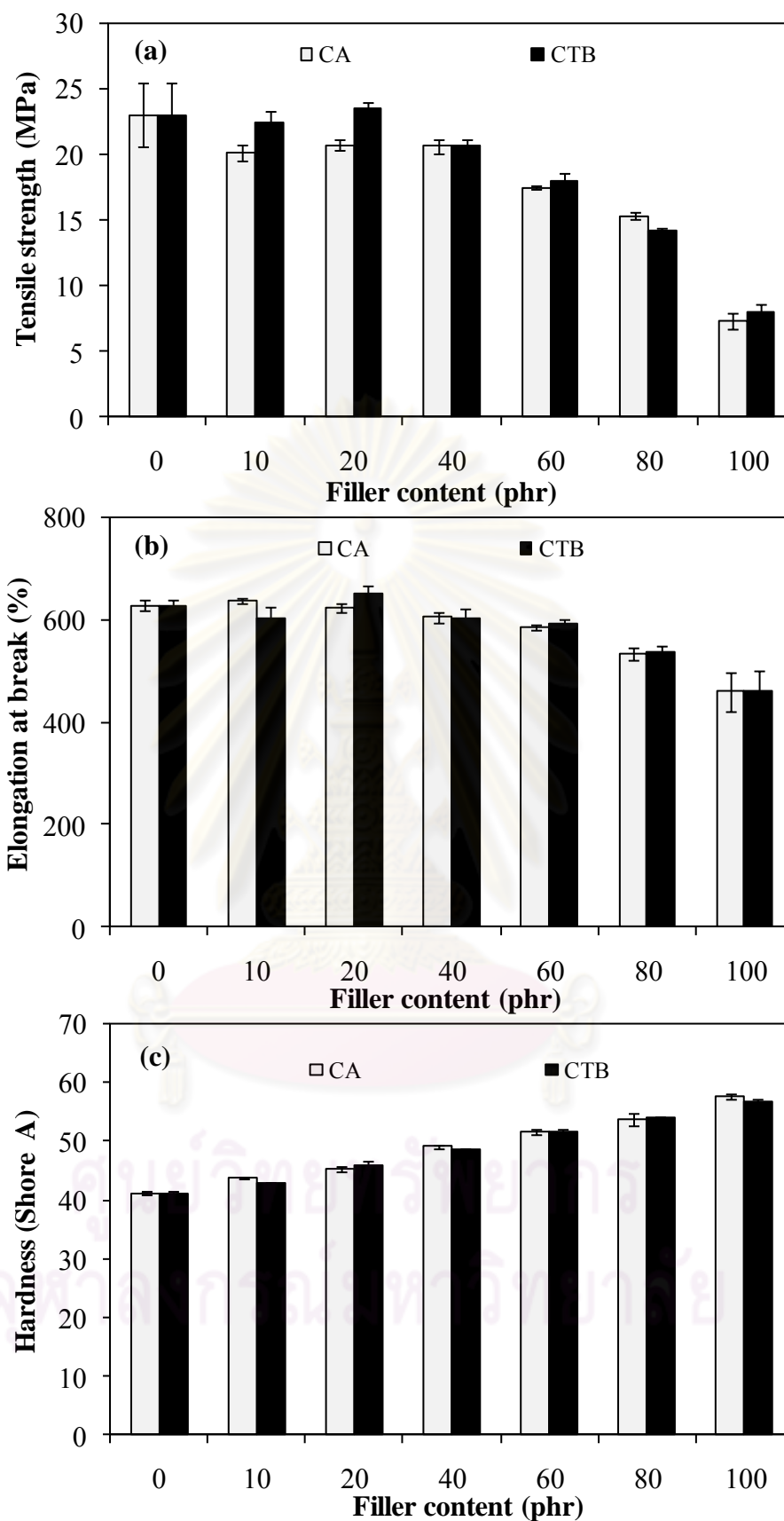
Figure 4.10 The effect of commercial $CaCO_3$ or cuttlebone particles on (a) tensile strength, (b) elongation at break and (c) hardness of NR vulcanizates in semi-EV system.
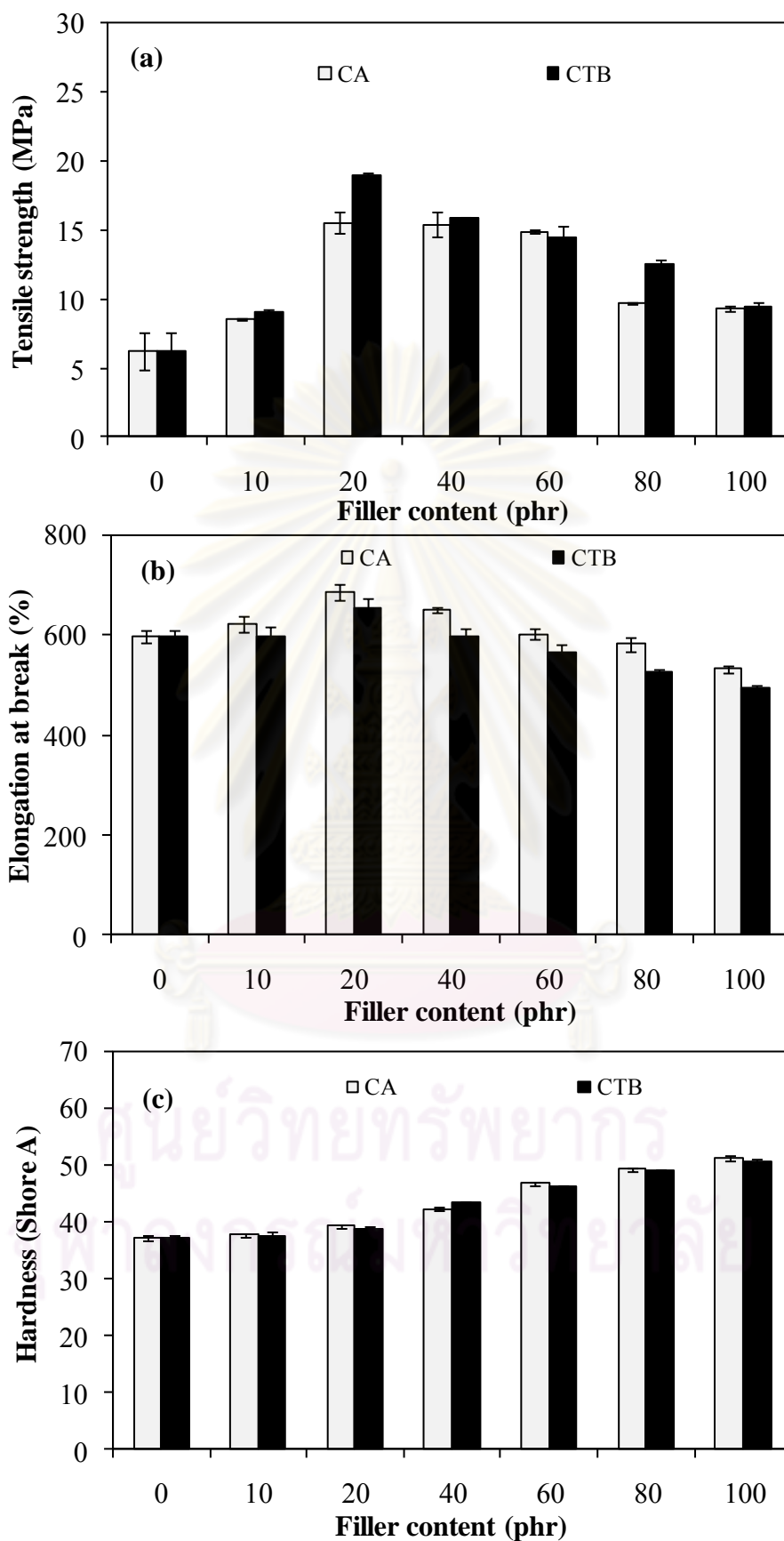
Figure 4.11 The effect of commercial CaCO$_3$ or cuttlebone particles on (a) tensile strength, (b) elongation at break and (c) hardness of NR vulcanizates in EV system.

Tear strength is the force per unit thickness used to initiate a rupture or tear of the materials. Table 4.5 shows the tear strength at various quantities of commercial $CaCO_3$ or cuttlebone particles in the NR vulcanizates with various curing systems. It can be seen that the dependence of tear strength on the both series of filler loading in NR vulcanizates was very similar to that of tensile strength. That is, tear strength for filled NR vulcanizates seemed to be decreased with increasing filler contents and its values trended to be lower than those of unfilled NR vulcanizate. This observation was associated with the inability of the filler molecules to transfer the tearing force [69], and also probably because of the rigid interface between the filler and rubber phase. Furthermore, it can be seen that tear strength of the CV vulcanizates was superior to the semi-EV and EV vulcanizates when comparing at the same filler content. These might be because the influences of crosslink structure, which were predominantly polysulphidic in the CV system, could be increased tear strength of NR vulcanizates cured with the CV system than those in semi-EV and EV systems.

Abrasion volume loss of commercial $CaCO_3$ or cuttlebone particles filled NR vulcanizates, which is inversely proportional to the abrasion resistance, was also shown in Table 4.5. The results revealed that the filler filled NR vulcanizates in CV curing system gave slightly higher abrasion resistance than NR vulcanizates in semi-EV and EV systems, respectively. According to Rattanasom *et al.* [65], they reported that crosslink density, hardness, modulus, and friction coefficient of the NR vulcanizates were important factors controlling the abrasion resistance. The greater crosslink density and, hence, the hardness and modulus gave rise to the enhancement of abrasion resistance. On the other hand, the lower the friction coefficient resulted in the higher the abrasion resistance. Although, the friction coefficient was not determined in this research, the results seemed to agree well with their modulus. From the results obtained in this experiment, the greater abrasion resistance of CV vulcanizates should be due to their higher closslinks as well as modulus. In addition, all samples for three kinds of curing systems exhibited a gradual decrease in abrasion resistance with increasing the commercial $CaCO_3$ or cuttlebone particles loading. According to these results, the $CaCO_3$ did not improve not only tear strength but also abrasion resistance of NR vulcanizates compared to the gum vulcanizates.

Table 4.5 Tear strength and DIN abrasion loss of commercial $CaCO_3$ or cuttlebone particles filled NR vulcanizates in various curing systems.

Sample code	Tear strength (N/mm)			Abrasion volume loss (mm^3)		
	CV	semi-EV	EV	CV	semi-EV	EV
NR	38.4	31.7	24.5	19.3	28.9	147.8
CA-10	32.0	28.8	24.7	22.3	31.2	189.2
CA-20	40.6	30.4	26.1	25.7	44.1	155.2
CA-40	34.0	28.9	26.6	49.5	53.6	68.6
CA-60	32.4	29.9	28.3	56.6	72.3	189.7
CA-80	31.3	26.5	26.8	85.5	85.5	205.3
CA-100	30.2	25.0	28.3	103.5	101.5	230.4
CTB-10	33.9	27.1	21.7	24.7	56.4	138.3
CTB-20	37.9	28.7	26.4	32.9	52.7	52.1
CTB-40	35.5	28.2	24.9	29.0	51.7	73.4
CTB-60	33.7	28.9	26.9	65.9	64.8	163.4
CTB-80	34.9	28.2	26.5	107.6	82.1	217.7
CTB-100	30.4	27.3	26.2	90.4	96.7	232.6

According to the previous study, Poompradub *et al.* [9] investigated the effect of the cuttlebone particles on the mechanical properties of NR vulcanizates in peroxide vulcanization. When compared the mechanical properties of composite materials in both sulfur and peroxide vulcanization systems, it is clearly seen that by using the different curing system, the mechanical properties of NR vulcanizates in sulfur vulcanization were superior to the NR vulcanizates in peroxide system as seen in Table D-1 (Appendix D). Accordingly, the cuttlebone particles can be effectively used as the reinforcing filler to improve the mechanical properties of NR vulcanizates in either sulfur or peroxide vulcanization systems.

4.6 Thermal Properties of NR Vulcanizates

    4.6.1 Effect of Thermal Aging on the Mechanical Properties of NR Vulcanizates

        The effects of commercial $CaCO_3$ or cuttlebone particles loading on the mechanical properties of NR vulcanizates and retention after thermal aging at 100 ^{0}C for 22 $\pm$ 2 h were investigated and the results are presented in Figures 4.12 – 4.14. The summarization of mechanical properties of NR vulcanizates after thermal aging was also shown in Appendix C (Tables C-1 - C-3). Generally, the mechanical properties in terms of T_B and E_B of the NR vulcanizates after thermal aging are two parameters often found to be the most direct and useful indicators of the remaining mechanical properties [70]. The results revealed that the mechanical properties of the NR vulcanizates in terms of T_B and E_B were decreased in both series (commercial $CaCO_3$ or cuttlebone filled NR vulcanizates). This result indicated that the vulcanization reaction has been completely occurred. According to Vinod *et al.* [71], they reported that the temperature caused two competing reactions namely cross-link formation and scission of chains. Further aging at the same temperature caused more polymer degradation than crosslink formation resulting in a decrease in T_B and E_B of NR vulcanizates. The higher retention (>100%) in T_B or the E_B of NR vulcanizates (EV system) could be due to the continuing cross-linking of the elastomer. However, the capability to retain the mechanical properties of the commercial $CaCO_3$ or cuttlebone particles filled NR vulcanizates after thermal aging had more resistance towards aging as compared with the NR vulcanizates without any filler as illustrated in Figures 4.12 – 4.14. The result showed that the thermal stability of the cuttlebone particles filled NR vulcanizates was found to be comparable with those of the commercial $CaCO_3$ filled ones and tended to increase with increasing filler contents. Nevertheless, it can be observed that the T_B and E_B retention of commercial $CaCO_3$ or cuttlebone particles filled NR vulcanizates at 10 phr (CV system) was slightly decreased in the comparison with the NR vulcanizates without any filler. This result was possibly associated with dilution effect caused by the amount of the filler filled NR vulcanizates.

Table 4.6 Thermal stability of commercial $CaCO_3$ or cuttlebone particles filled NR
vulcanizates.

Sample code	CV system		semi-EV system		EV system	
	$RT_B{}^a$ (%)	$RE_B{}^b$ (%)	$RT_B{}^a$ (%)	$RE_B{}^b$ (%)	$RT_B{}^a$ (%)	$RE_B{}^b$ (%)
NR	45.69	65	85.11	76	82.77	99
CA-10	22.99	59	61.98	92	108.50	95
CA-20	66.71	90	63.20	88	69.16	86
CA-40	74.78	92	63.41	81	85.47	93
CA-60	77.00	87	82.25	90	88.17	96
CA-80	80.01	91	39.07	86	121.36	91
CA-100	78.66	97	93.68	114	106.12	103
CTB-10	40.86	56	87.41	85	82.28	93
CTB-20	73.46	94	79.56	82	80.15	92
CTB-40	69.84	87	81.80	88	79.34	106
CTB-60	70.78	95	87.19	88	90.62	111
CTB-80	80.85	100	87.04	89	90.15	105
CTB-100	77.52	101	95.12	99	98.73	101

[a] Tensile strength retention
[b] Elongation at break retention
% Retention = (Mechanical properties after aging/ mechanical properties before aging) x 100
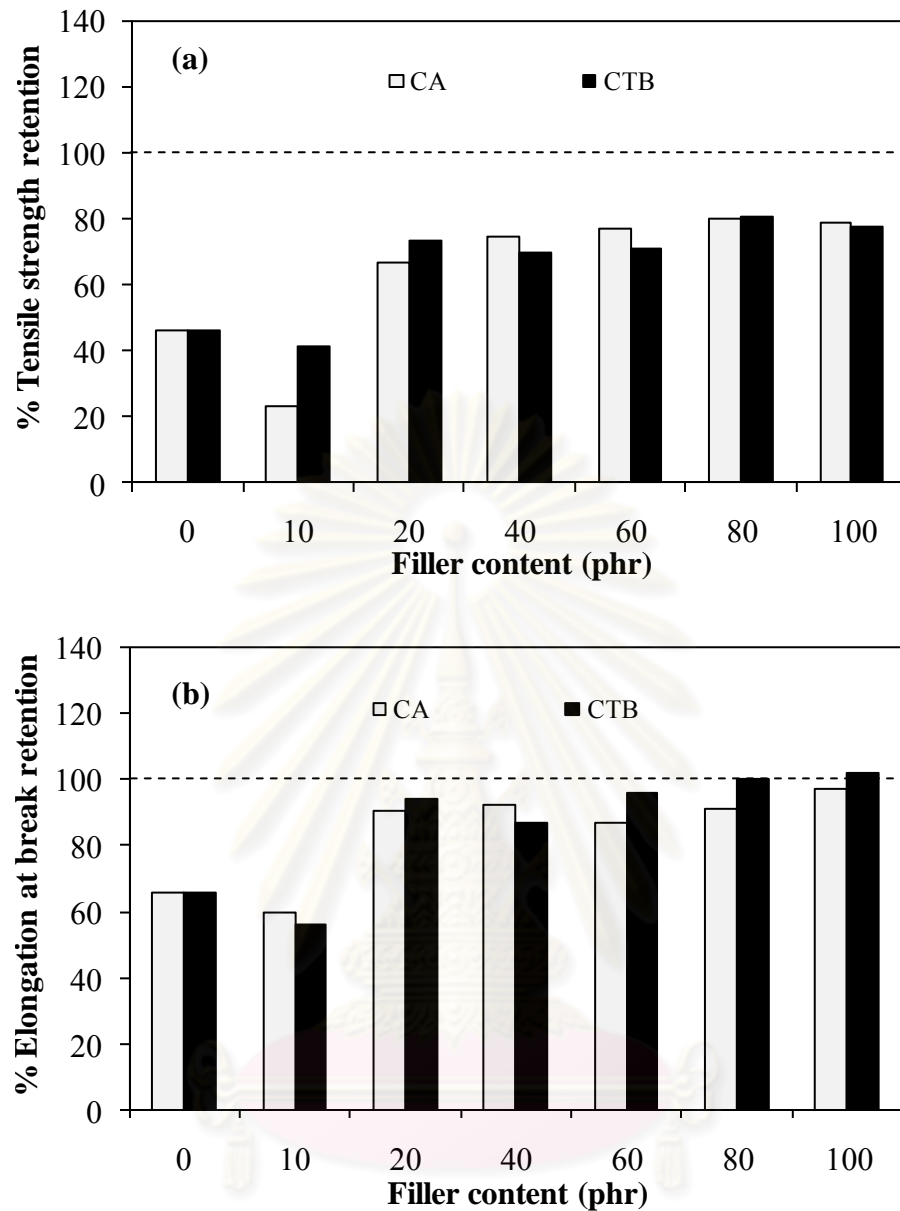
Figure 4.12 Retention values of mechanical properties of NR vulcanizates in CV system after thermal aging at 100 ^{0}C for 22 $\pm$ 2 h (a) tensile strength and (b) elongation at break.
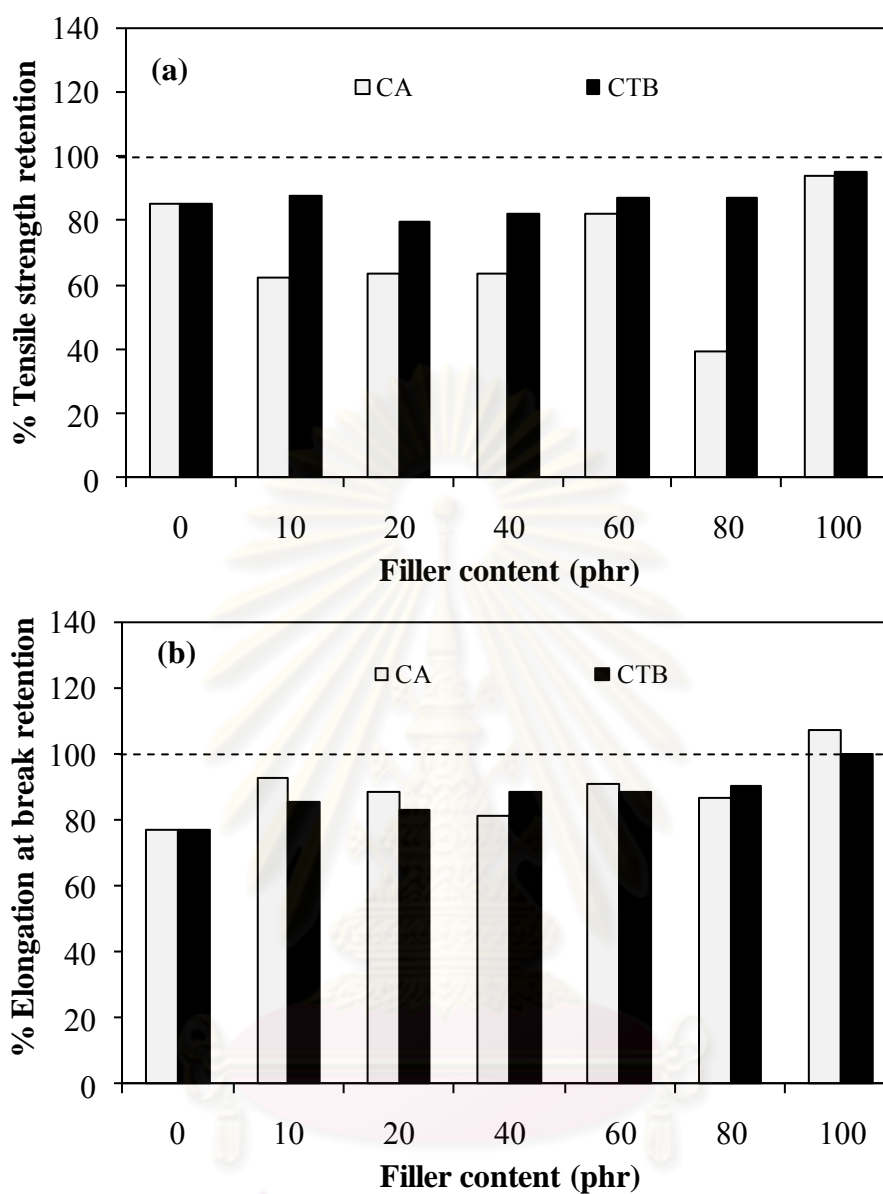
Figure 4.13 Retention values of mechanical properties of NR vulcanizates in semi-EV system after thermal aging at 100 ^{0}C for 22 $\pm$ 2 h (a) tensile strength and (b) elongation at break.
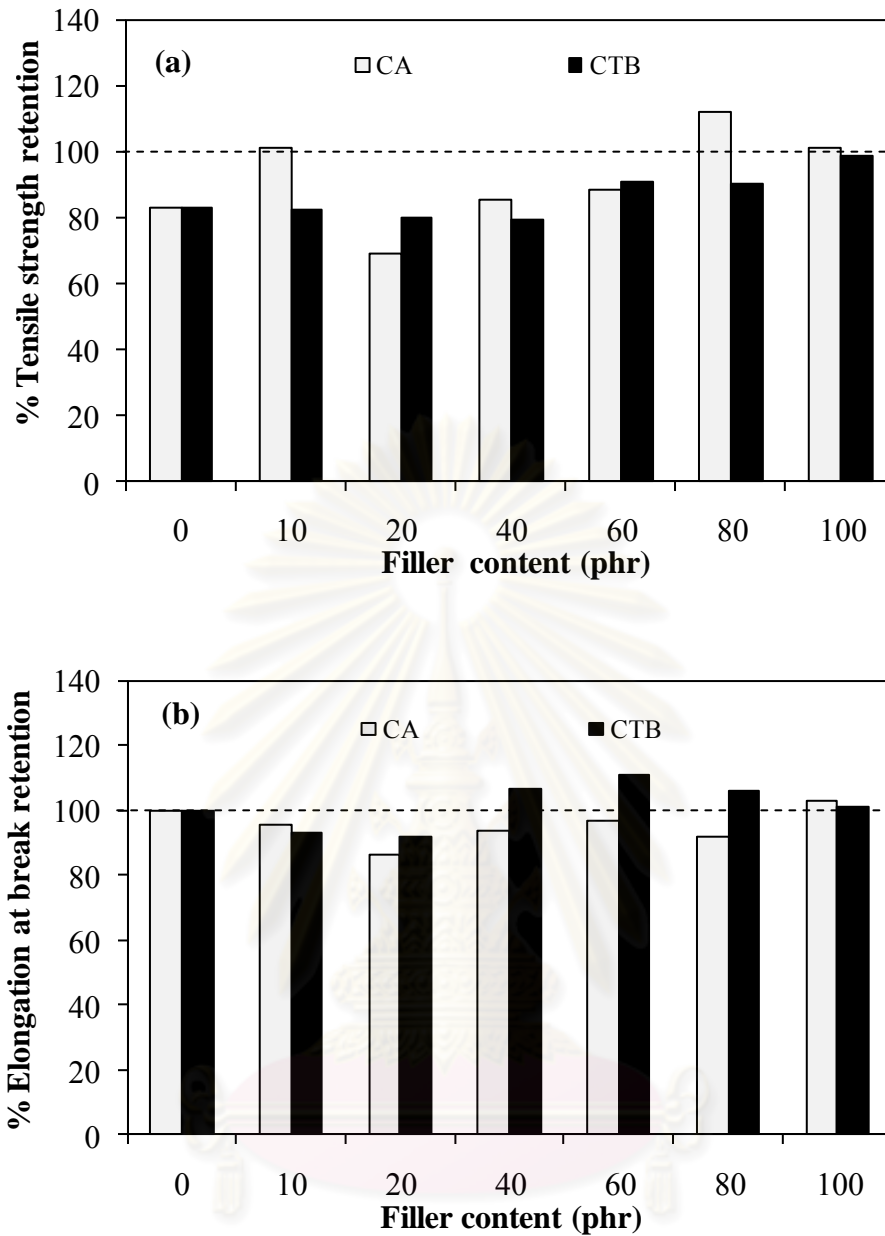
Figure 4.14 Retention values of mechanical properties of NR vulcanizates in EV system after thermal aging at 100 ^{0}C for 22 $\pm$ 2 h (a) tensile strength and (b) elongation at break.

The thermal stability of the cuttlebone particles filled NR vulcanizates in terms of the retention after aging can also be discussed in an aspect of the curing system. Figure 4.15 is shown the tensile retention of the NR vulcanizates after aging at 100 ^{0}C for 22 $\pm$ 2 h for three kinds of curing systems. As expected, the EV and semi-EV vulcanizates exhibited greater thermal stability (in term of tensile strength retention) than CV vulcanizates, when the cuttlebone particle content was increased beyond 20 phr. This is simply due to the fact that the crosslink structure in the EV and semi-EV system is mainly mono-sulfidic and di-sulfidic crosslink which is stronger and more thermally stable than polysulfidic crosslinks which are mainly found in the CV systems [59, 65].
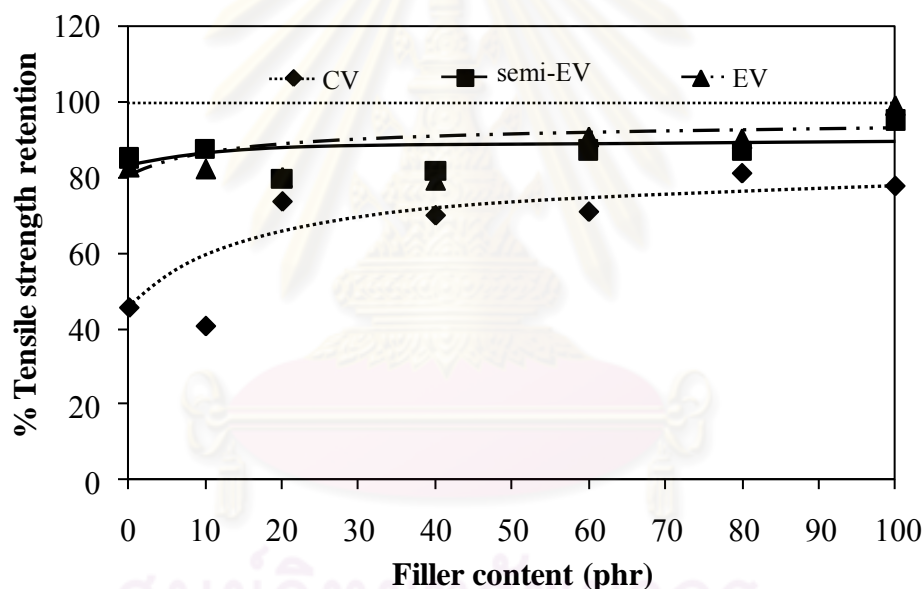
Figure 4.15 Tensile strength retention of NR vulcanizates in various curing systems as a function of cuttlebone particle content.

4.6.2 Ozone Resistance of the NR Vulcanizates

Atmospheric ozone usually causes the degradation of polymers under conditions that may be considered as normal, when other oxidative aging processes are very slow and the polymer retains its properties for a rather long time. Nowadays the ozone resistance of polymer products is of paramount importance, because the problem has worsened as atmospheric ozone concentrations have gradually increased, especially in industrialized areas [72]. In this study, the ozone resistance of commercial $CaCO_3$ or cuttlebone particles filled NR vulcanizates was investigated. The samples were exposed in a HAMPDEN ozone cabinet at 40 ^{0}C in an atmosphere containing 50 pphm by volume of ozone concentration for 24 and 48 h. A type of ozone cracking on the rubber surface was classified according to Table 3.4. The comparison of cracking for commercial $CaCO_3$ or cuttlebone particles filled NR vulcanizates cured by various systems was demonstrated in Table 4.7, Figures 4.16 – 4.18 and Figures E-1 – E-3 (Appendix E), respectively. It can be seen that the significant cracking (C-3 and C-4) appeared on the surface of not only commercial $CaCO_3$ filled NR vulcanizates but also cuttlebone particles filled ones. The mechanism of ozonolysis of NR is proposed in Scheme 4.1 [71]. The first step was a cycloaddition of ozone to the olefinic double bond to form an ozone–olefin adduct referred to as the primary ozonide. The primary ozonide was an unstable species, since it contained two very weak O–O bonds. Thus, the second step in the ozonolysis mechanism was the decomposition of the primary ozonide to carbonyl compounds and a carbonyl oxide. The carbonyl oxide was considered to be the key intermediate in the C=C bond ozonolysis mechanism which might be polymerized to yield polymeric peroxides but these products were relatively unstable (eventually decompose to give chain scission products). Thus, the third step in the ozonolysis mechanism was the fate of the carbonyl oxide, which depended on the presence of molecules containing active hydrogen such as alcohols and water, leading to the reactive products [71 - 73]. According to the results, it can be concluded that the incorporation of $CaCO_3$ filler could not prevent the initiation and propagation of ozone cracking on the surface of NR vulcanizates. The result illustrated that the NR vulcanizates had C-3 type and C-4 type of cracking (Table 4.7) after 24 and 48 h of ozonation, respectively. However, considering from the stretched surfaces of the

cuttlebone particles filled the NR vulcanizates compared with the commercial CaCO$_3$ filled ones, it can be postulated that the cuttlebone particles filled NR vulcanizates exhibited less amount of cracking than the commercial filled ones, regardless the curing systems as shown in Figures 4.16 – 4.18 and Figures E-1 – E-3, respectively.
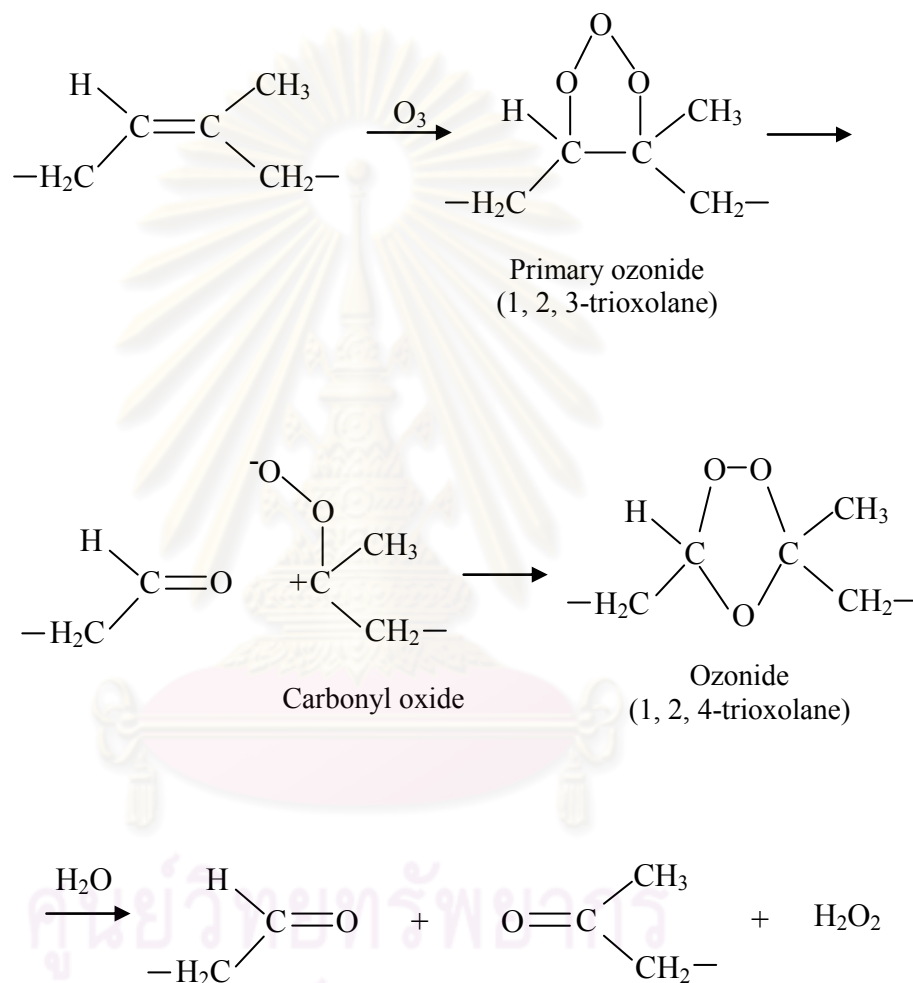
Scheme 4.1 The mechanism of the ozonolysis of NR [73].

Table 4.7 Ozone cracking of commercial $CaCO_3$ or cuttlebone particles filled NR
vulcanizates in various curing systems.

Sample code	Type of cracking					
	CV system		Semi-EV system		EV system	
	24 h	48 h	24 h	48 h	24 h	48 h
NR	C-3	C-4	C-3	C-4	C-4	C-4
CA-20	C-3	C-4	C-3	C-4	C-4	C-4
CA-40	C-3	C-4	C-3	C-4	C-4	C-4
CA-80	C-3	C-4	C-3	C-4	C-3	C-4
CTB-20	C-3	C-4	C-3	C-4	C-3	C-4
CTB-40	C-3	C-4	C-3	C-4	C-3	C-4
CTB-80	C-3	C-4	C-3	C-4	C-3	C-4

C-3: Numberless cracking, which is deep and comparatively long (below 1 mm).

C-4: Numberless cracking, which is deep and long (above 1 mm and below 3 mm).

ศูนย์วิทยทรัพยากร

จุฬาลงกรณ์มหาวิทยาลัย
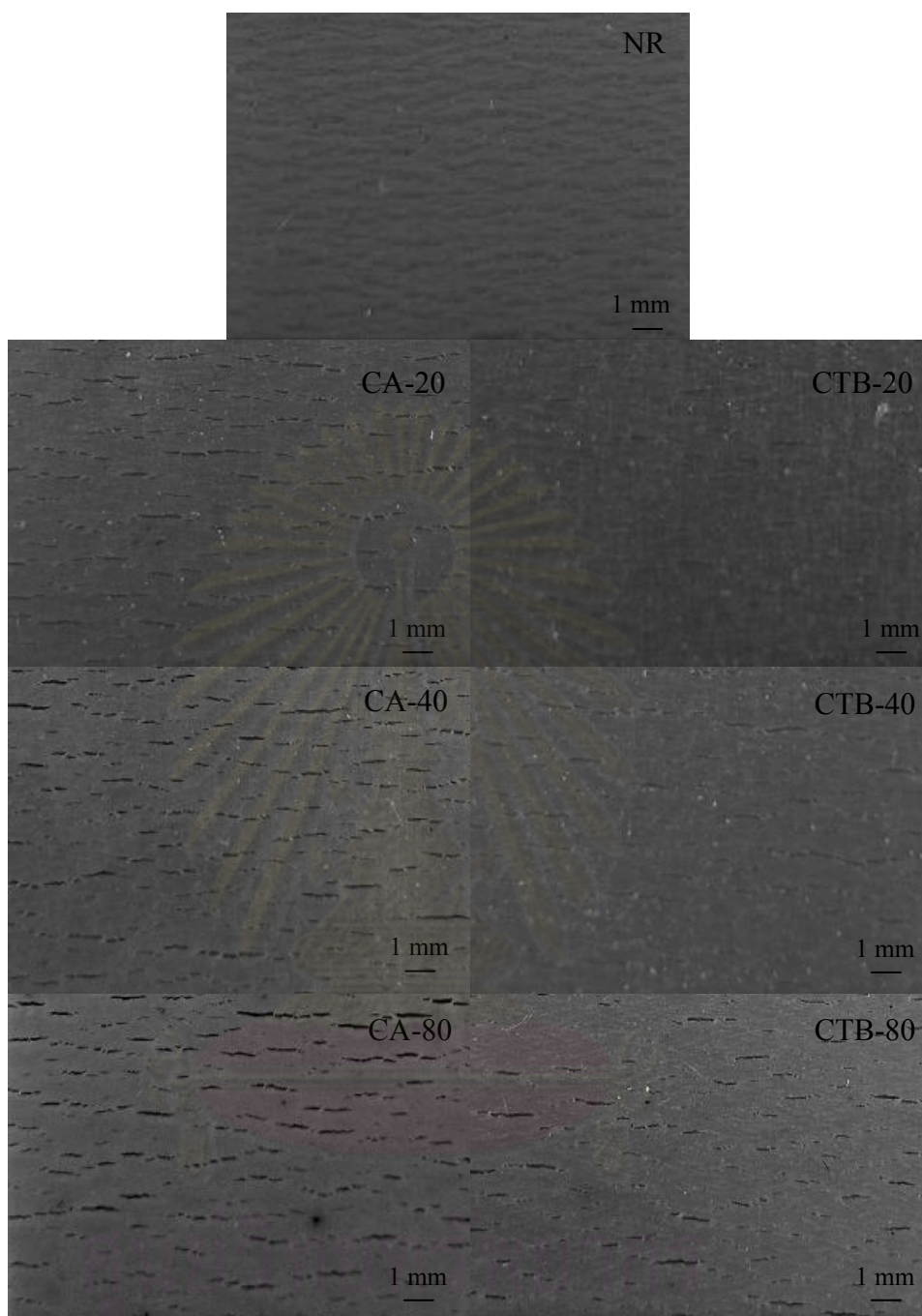
Figure 4.16 Stretched surfaces of commercial CaCO$_3$ and cuttlebone particles filled NR vulcanizates in CV systems after exposure to ozone (50 pphm) at 40 ^{0}C for 48 h.
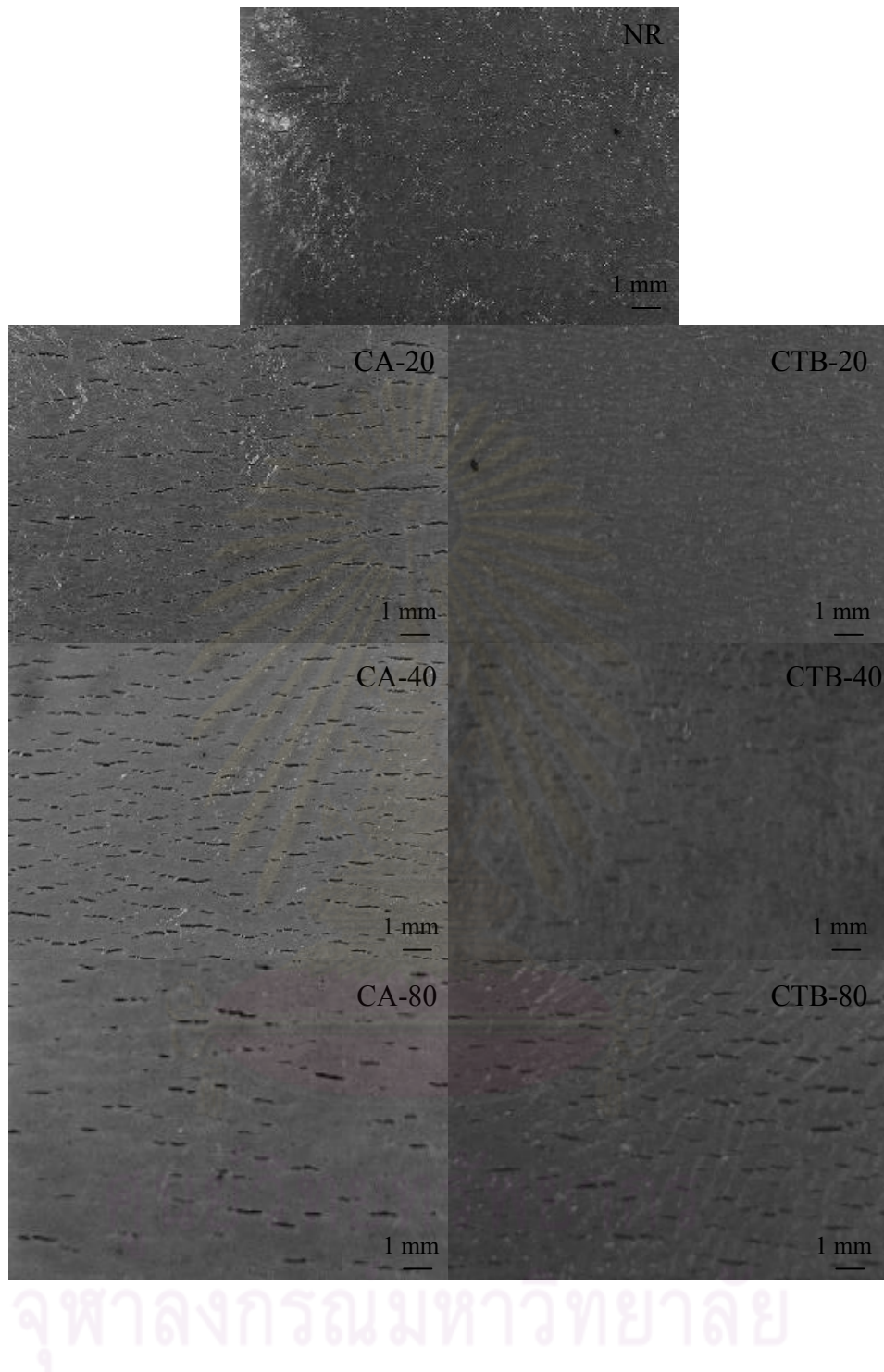
Figure 4.17 Stretched surfaces of commercial CaCO$_3$ and cuttlebone particles filled
NR vulcanizates in semi-EV systems after exposure to ozone (50 pphm)
at 40 ^{0}C for 48 h.
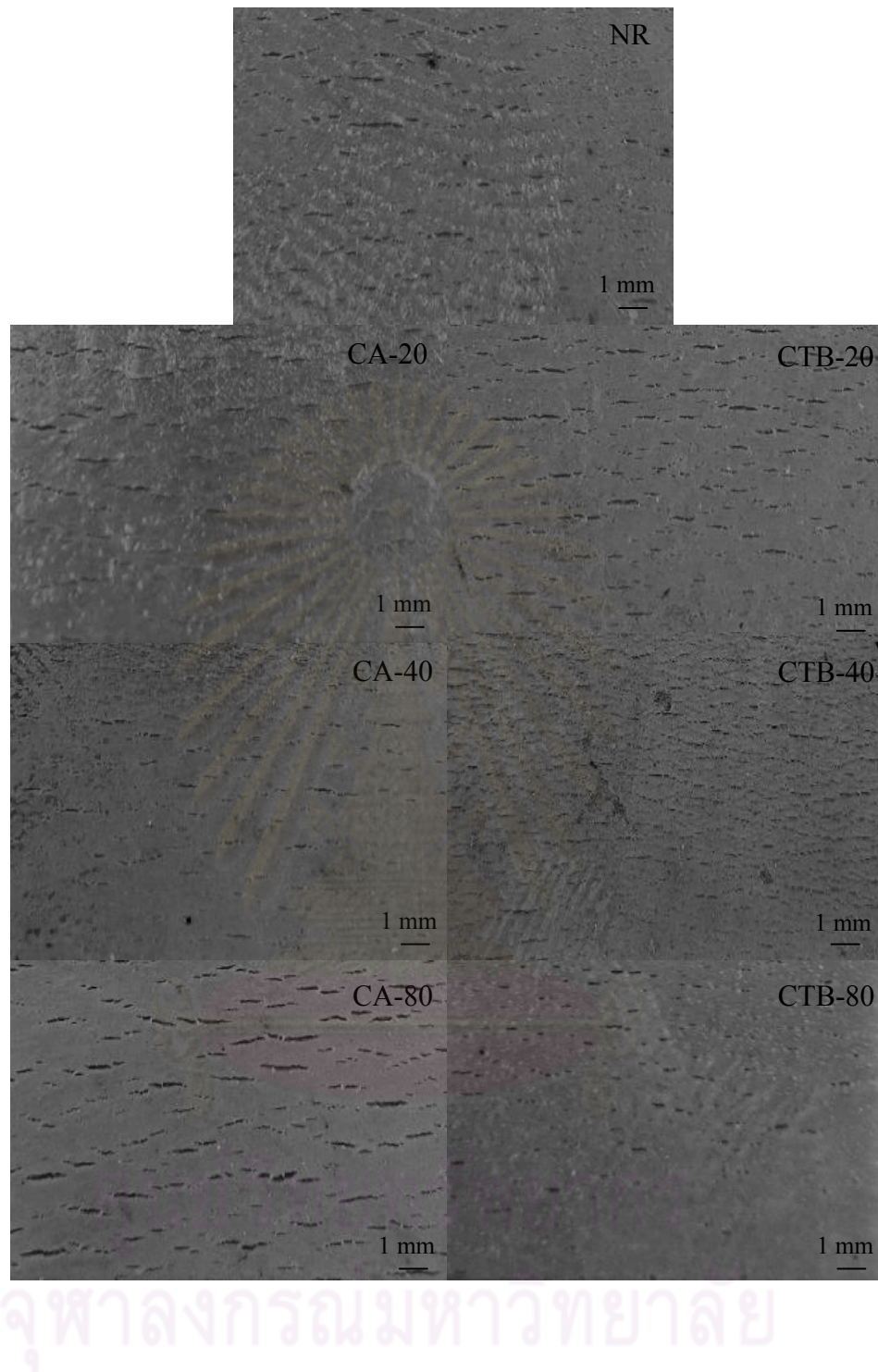
Figure 4.18 Stretched surfaces of commercial $CaCO_3$ and cuttlebone particles filled
NR vulcanizates in EV systems after exposure to ozone (50 pphm) at
40 ^{0}C for 48 h.

4.7 Dynamic Mechanical Properties of NR Vulcanizates

In general, rubbers show both elastic and damping behaviors because they are viscoelastic materials. When they are deformed by a sinusoidal stress within the linear viscoelastic region, the resulting strain will also be sinusoidal but will be out of phase with the applied stress [74]. The dynamic mechanical analysis (DMA) method determines elastic modulus or storage modulus (E′), viscous modulus or loss modulus (E″) and damping coefficient (tan δ) as a function of temperature, frequency or time. Dynamic losses are usually associated with hysteresis and specific mechanisms of molecular or structural motion in polymer materials. The damping in the system or the energy loss per cycle can be measured from the tangent of the phase angle or loss tangent (tan δ) and defined by tan δ = E″/E′ where E′ is the storage modulus due to the stored elastic energy in the materials and recovered during each cycle and it also indicates the stiffness of the material, while E″ is the loss modulus or damping factor due to energy dissipation in the system per cycle.

In this study, the dynamic mechanical properties of NR vulcanizates reinforced by commercial $CaCO_3$ or cuttlebone particles only for CV system are shown in Figure 4.19. The E′ at 25 ^{0}C and height and temperature of maximum tan δ peak of the NR vulcanizates are also summarized in Table 4.8. Figure 4.19 (a) shows the temperature dependence of E′ of NR vulcanizates at various filler loading. The results revealed that the E′ decreased with increasing temperature due to the decrease in stiffness of the NR vulcanizates. The curves for all the samples had the following three distinct regions: a glassy region, a transition region and a rubbery region. For temperature around the glassy region, NR matrix was in the glassy state: the E′ values were slightly decreased as a function of temperature. In this glassy region (approximately -120 ^{0}C to -60 ^{0}C), thermal energy was insufficient to surmount the potential barriers for rotational and translation motions of segments of the rubber chains. The entire molecular chains of NR vulcanizates were completely frozen resulted in the higher degree of modulus than the other region. Subsequently, the dramatically decreased of the E′ values of NR vulcanizates was observed around the transition region (approximately -60 ^{0}C to -20 ^{0}C). This incident is due to the increasing mobility of rubber chain segment when the temperature increased.

This modulus drop was corresponded to an energy dissipation phenomenon displayed in the concomitant relaxation process [43], where tan δ passed through a maximum values. Then, the modulus reached a plateau around 1 MPa, corresponding to the rubbery state. The broad temperature range from -10 ^{0}C to 80 ^{0}C of the rubbery state was demonstrated that the deformation of rubber chain tended to straighten out or disentanglement of rubbery chains. As seen in the Figure 4.19 (a), it can be seen that the modulus remained constant for the entire samples. This result can be explained by the viscoelastic responses of the crosslinked polymer through the rubbery plateau region. As temperature is increased, the crosslinks consisting of primary chemical bonds remain intact, preventing the chains from translating relative to one another until up to temperature where chemical degradation begins to occur [75]. The result also affirmed that the cuttlebone particles did not prevent the crosslinking reaction in NR vulcanizates and the reaction had been completely occurred well. Furthermore, DMA is an effective tool in order to determine the dynamic glass transition temperature (T_g). The dynamic T_g is defined as the temperature at which (i) maximum of the tan δ occurs or (ii) maximum of the E″ occurs or (iii) the middle point of E′ vs. temperature curve [3]. Figure 4.19 (b) exhibits the tan δ as a function of temperature. It can be observed that maxima in tan δ of both fillers (commercial $CaCO_3$ or cuttlebone particles) reinforced NR vulcanizates did not coincide with the unfilled NR vulcanizates. The maximum of tan δ values decreased with increasing filler loading, indicating that the complexity of dynamic mechanical behavior of these filled NR vulcanizates arising from the restricted movement of NR molecules due to the addition of rigid particle of reinforcing filler resulted in the high energy input required for the motion of the molecular chains of the rubber. According to Geethamma *et al*. [3], they reported that DMA was an effective method to evaluate the interfacial bonding in NR vulcanizates. The NR vulcanizates with poor interfacial bonding between the filler and NR matrix tended to dissipate more energy than those with good interfacial bonding. In Figure 4.19 (b), it was observed that the maximum of tan δ values decreased with increasing filler loading, indicating that the NR composites possessed low damping and so good interfacial bonding characteristics in the rubbery matrix. This observation could also be observed by the SEM investigation.

The variations of E' value of NR vulcanizates at 25 ^{0}C were shown in Figure 4.19 (a). It can be observed that the E' value increased with increasing filler loading and there were same in both series (commercial $CaCO_3$ or cuttlebone particles). The results revealed that the NR without any filler showed the lowest modulus across the temperature zone above -20 ^{0}C. With the same ratio, the E' value at 25 ^{0}C of NR vulcanizates increased in the following order: CA-80 > CA-40 > CA-20 > NR and CTB-80 > CTB-40 > CTB-20 > NR. These indicated that the elastic modulus of filler filled NR vulcanizates was higher than the unfilled NR vulcanizates [1]. This result was corresponded to analysis on the mechanical properties in term of M_{100} and M_{300} as shown in Table C-1 (Appendix C). Furthermore, the presence of reinforcing filler in the NR matrix was also found to lower the peak height of tan δ compared with that for the unfilled NR vulcanizates. The results suggested that the commercial $CaCO_3$ or cuttlebone particles filled NR vulcanizates would be increased an elastic behavior of the NR vulcanizates resulted in the decrease of the peak height of tan δ. The temperatures at the maximum of tan δ peak, which are ascribed to the dynamic T_g, were almost equal among the samples as reported in Table 4.8. In fact, as the filler content was increased, the dynamic T_g was usually shifted to the higher temperature. This is possibly due to the filler behaved like a rigid particles resulted in the increase in the stiffness of the NR vulcanizates. Nevertheless, in the case of cuttlebone particles reinforced NR vulcanizates showed that the dynamic T_g was almost constant. This means that the filler-to-rubber interaction in cuttlebone particle filled NR vulcanizates was predominant. However, such temperatures for commercial $CaCO_3$ filled ones were shifted to the higher temperature compared to unfilled NR vulcanizates due to the strong filler-to-filler interaction. The obtained results were confirmed by SEM images in the latter section.

Table 4.8 Dynamic mechanical properties of NR vulcanizates.

Sample code	E′ at 25 ^{0}C (MPa)	Height of tanδ peak	Temperature of maximum tan δ peak (^{0}C)
NR	0.70	2.3	-45.0
CA-20	0.83	2.1	-44.0
CA-40	1.11	2.1	-44.0
CA-80	1.51	1.6	-42.4
CTB-20	0.88	2.2	-45.8
CTB-40	1.03	2.0	-46.1
CTB-80	1.48	1.6	-45.4
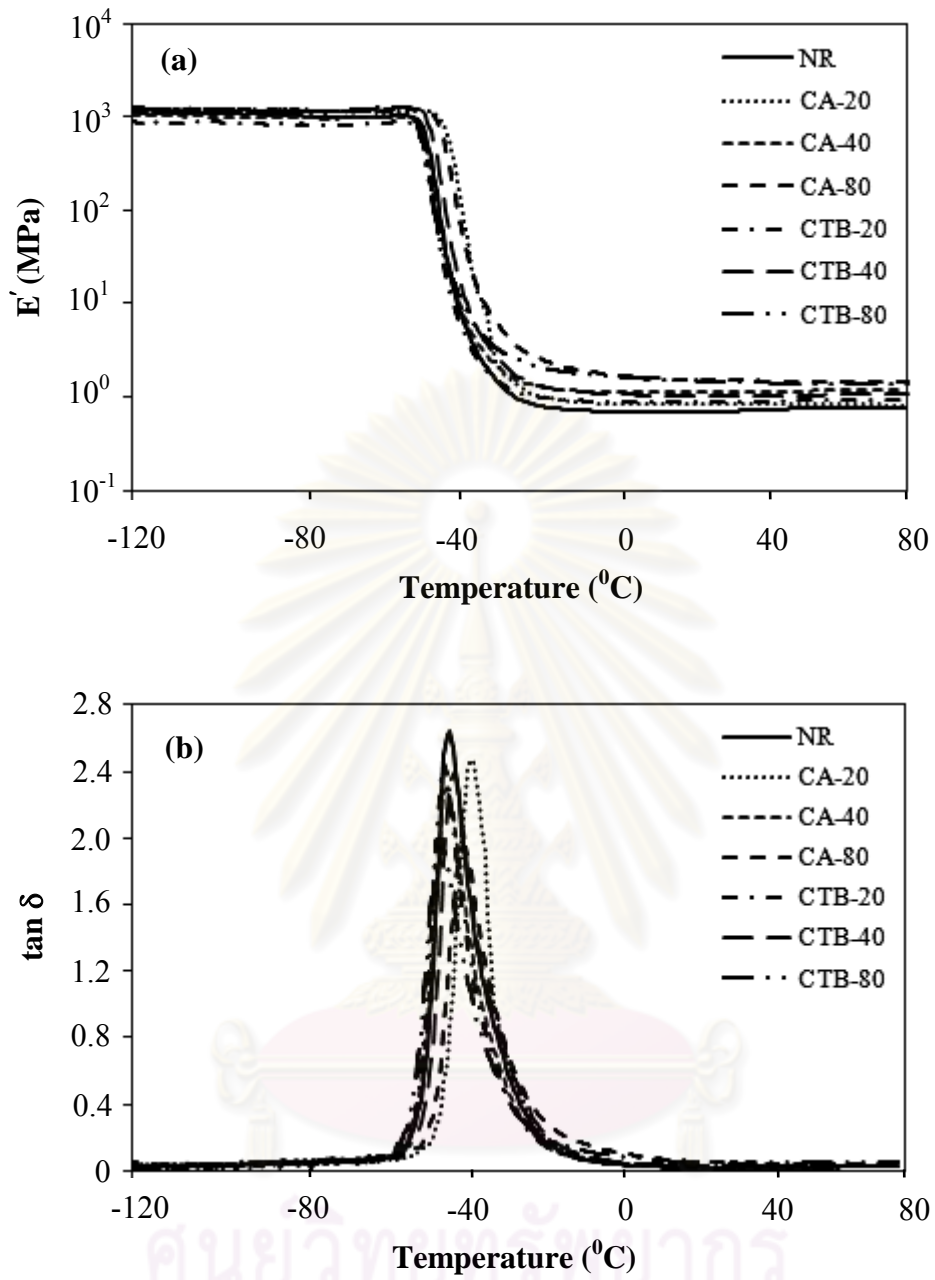
Figure 4.19 Dynamic mechanical property analysis of commercial $CaCO_3$ or cuttlebone particles filled NR vulcanizates as described by (a) the storage modulus (E′) and (b) tan δ.

4.8 Morphology of NR Vulcanizates

The SEM micrographs of the tensile fracture surface of the commercial $CaCO_3$ or cuttlebone particles reinforced NR vulcanizates in various curing systems are shown in Figures 4.20 – 4.22, where the white circular representing commercial $CaCO_3$, while rod shape representing cuttlebone particles which were dispersed in the rubbery matrix (grey-toned color). It can be seen that the both fillers had a good distribution in the rubbery matrix at lower filler loading. The particles size of the commercial $CaCO_3$ and the cuttlebone particles, which was estimated from the SEM micrograph, was ca. 15 μm and 30 μm, respectively. At the high filler loading in both types of reinforcing filler, the cluster of filler agglomerate was clearly observed. This result could support that the increase of the maximum torque might be due to the filler agglomeration (Figures 4.4 (b) - 4.6 (b)) [64]. The agglomeration leads to the formation of weak point in the rubbery matrix, accordingly reducing the elastomeric strength. Thus, the reduction in mechanical properties might be due to agglomeration of the filler particles to form a domain that acts like a foreign body or is simply the result of physical contact between adjacent aggregates [60]. Consequently, it is clearly observed that the black holes, which could act as initial defects leading to localized stress concentration during deformation [60], in the case of cuttlebone particles filled NR vulcanizates were less than those of commercial $CaCO_3$ filled ones. The appearance was associated with the rubber–filler interaction as a result of detachment of the filler from the rubbery matrix. That is to say, the interaction between cuttlebone particles and NR matrix must be stronger than that between commercial $CaCO_3$ and NR matrix. These results supported that the presence of the organic components such as protein and chitin give a good reinforcement effect of cuttlebone particles to NR, to obtain the superior mechanical properties than commercial $CaCO_3$ filled ones.
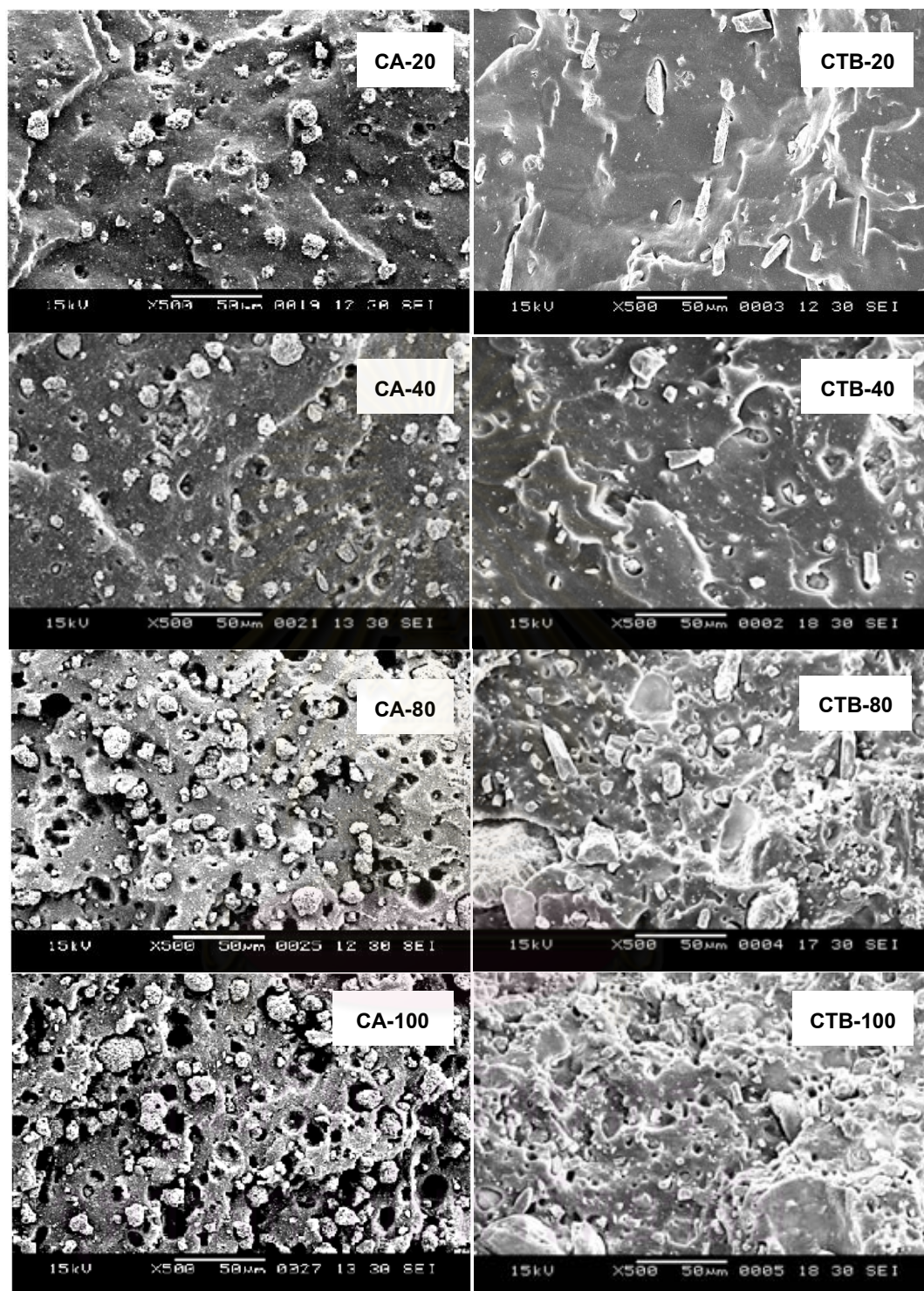
Figure 4.20 SEM micrographs of tensile fracture surface of the commercial CaCO$_3$ or cuttlebone particles filled NR vulcanizates cured by CV system (magnification: 500 x).
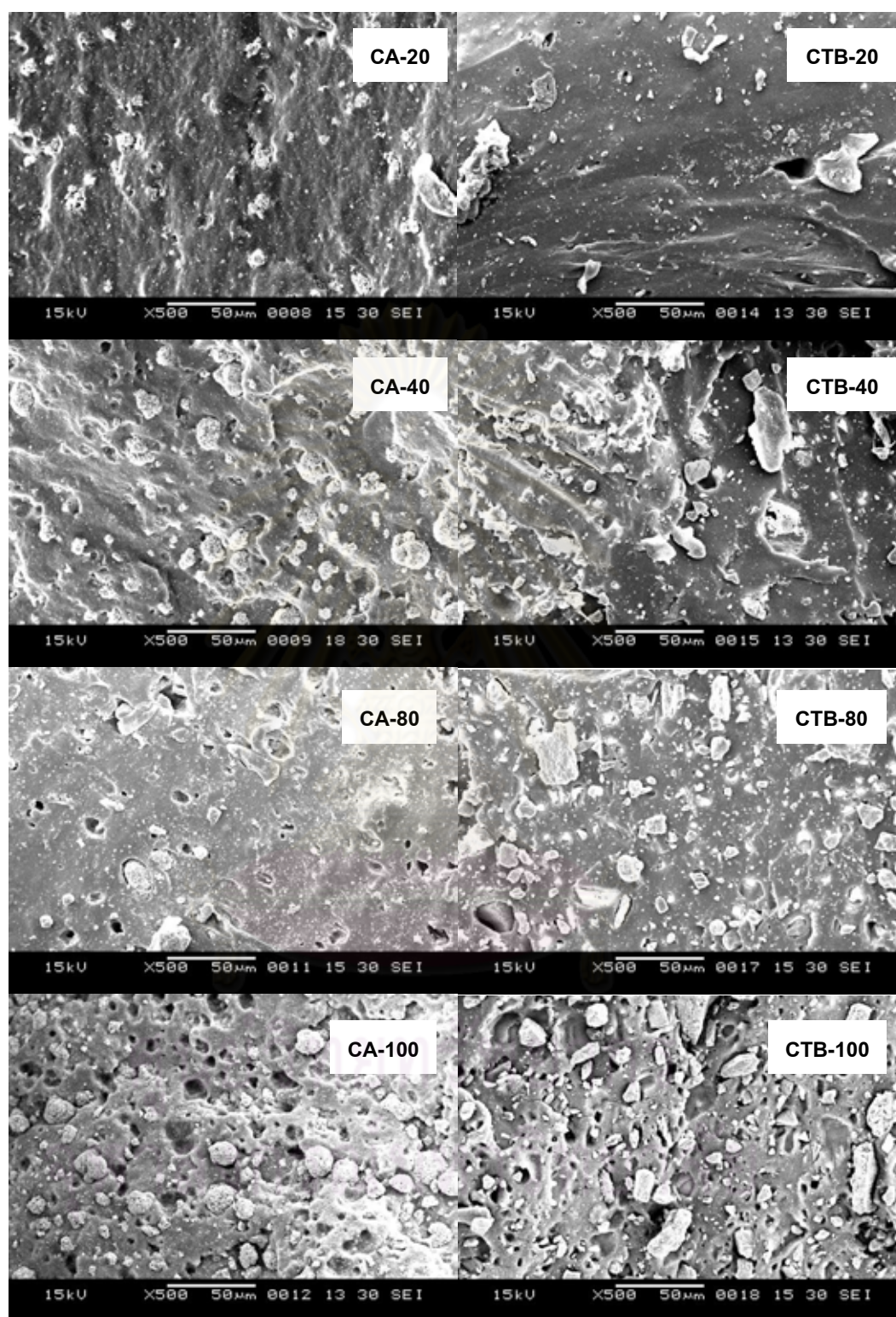
Figure 4.21 SEM micrographs of tensile fracture surface of the commercial CaCO$_3$ or cuttlebone particles filled NR vulcanizates cured by semi-EV system (magnification: 500 x).
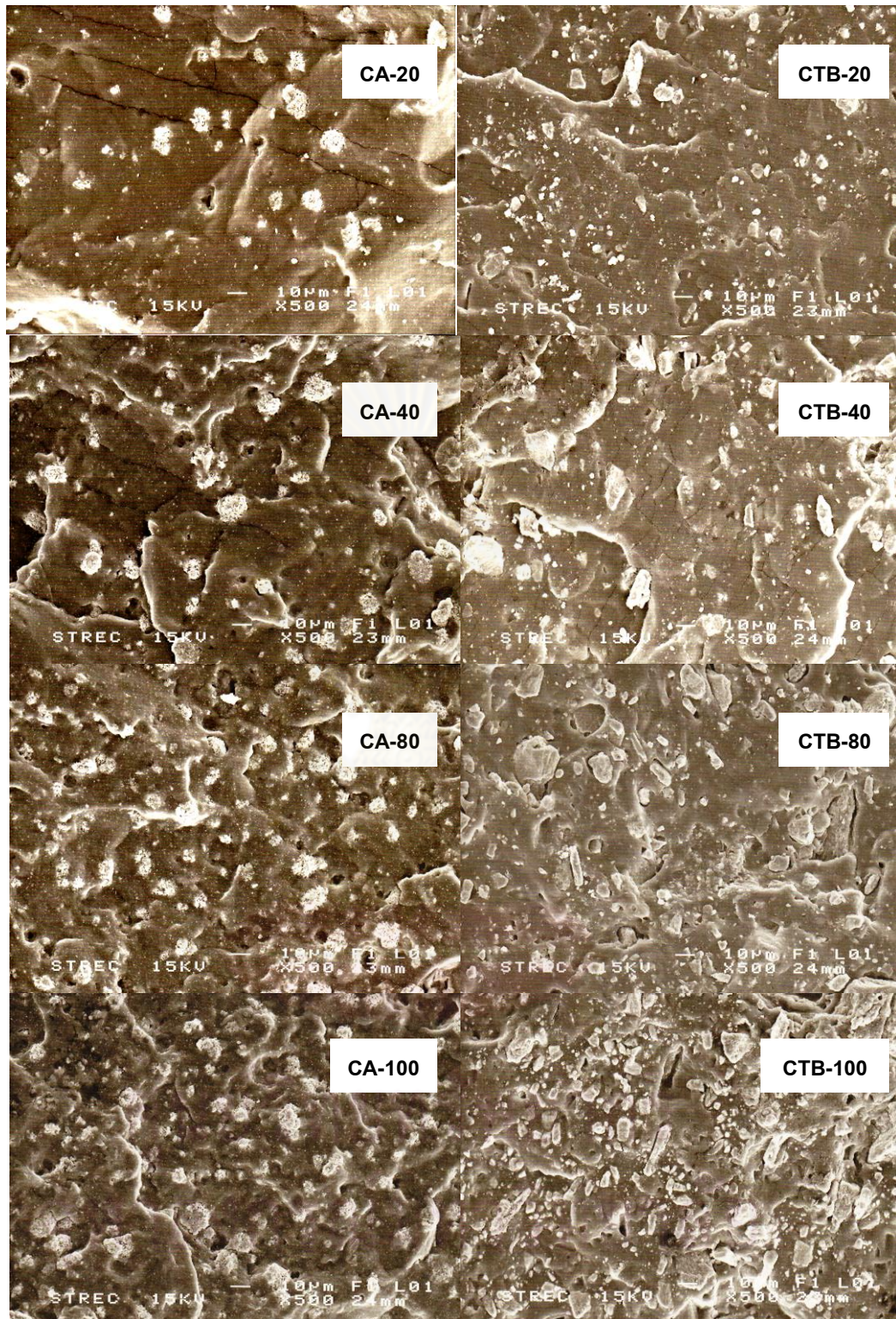
Figure 4.22 SEM micrographs of tensile fracture surface of the commercial $CaCO_3$ or cuttlebone particles filled NR vulcanizates cured by EV system (magnification: 500 x).

CHAPTER V

CONCLUSION AND FUTURE DIRECTION

5.1 Conclusion

In this study, the NR vulcanizates based on cuttlebone natural material as a reinforcing filler were successfully prepared. The major conclusions of this study can be elaborated as follows:

The characteristics and the essential components of the inner cuttlebone shell were similar to the outer cuttlebone shell. Therefore, the both parts of the cuttlebone (so-called the "cuttlebone particles") were combined in order to use as a reinforcing filler for NR vulcanizates. The crystal structure, density, average size and BET surface area of cuttlebone particles were an aragonite form of $CaCO_3$ (orthorhombic shape), 2.50 g/cm^3, 106 μm and 11.0 m^2/g, while those of commercial $CaCO_3$ were a calcite form of $CaCO_3$ (hexagonal-rhombohedral shape), 2.54 g/cm^3, 1.5 μm and 5.5 m^2/g, respectively. The thermal degradation of cuttlebone particles occurred in two steps. The first step of degradation was due to the decomposition of organic materials and the latter was associated with the burning of $CaCO_3$. The organic components in the cuttlebone particles were extracted by using the demineralization and deproteinization methods. It was found that the cuttlebone particles were consisted of an inorganic part of $CaCO_3$ (89 - 94 %) and an organic parts of protein (3 - 7 %) and β-chitin (3 - 4 %).

The NR composites with cuttlebone particles were successfully prepared via three kinds of sulfur vulcanizations, i.e., conventional vulcanization (CV), semi-efficiency vulcanization (semi-EV) and efficiency vulcanization (EV) systems. The curing properties, i.e., the scorch time and optimum cure time, of NR compounding tended to decrease with increasing filler loading. The swelling behavior of NR composite materials showed that the cuttlebone particles did not prevent a sulfur cross-linking reaction of NR vulcanizates and the results were similar to commercial $CaCO_3$ filled NR vulcanizates. The mechanical properties such as the M_{100} and M_{300} of NR composites via three kinds of sulfur vulcanizations increased with increasing filler loading that was associated with the decreases in the T_B and E_B of NR composite

materials. The mechanical properties of cuttlebone filled NR vulcanizates were found to be comparable with those of commercial $CaCO_3$ filled ones. Comparing among three kinds of vulcanization systems, the EV system imparted the NR vulcanizates with lowest mechanical properties values whereas the CV system imparted the NR vulcanizates with the highest mechanical properties. Nevertheless, the $CaCO_3$ filler did not improve tear strength, abrasion and ozone resistance of the composites materials. The incorporation of the $CaCO_3$ filler could improve the thermal stability of the NR composite materials compared with the gum vulcanizate without any filler content. Dynamic mechanical properties of cuttlebone particles filled NR vulcanizates were comparable with those of the commercial $CaCO_3$ filled ones. From the SEM micrographs, the presence of the organic component plays a role in providing a good rubber-filler interaction of the cuttlebone particles to NR matrix. Accordingly, the cuttlebone can be a candidate as a biomass for filler of rubber materials, and it can be useful for decreasing the waste products of cuttlefish from the environmental issues.

5.2 Future Direction

1. Study in more detail on the biodegradable behavior of cuttlebone filled NR vulcanizates by environmental or microbial bacteria.

2. Explore the use of cuttlebone particles to the other rubber types e.g. butadiene rubber, butyl rubber and nitrile rubber.

REFERENCES

[1] Tang, H., *et al.* Reinforcement of elastomer by starch. Macromol. Mater. Eng. 291 (2006): 629-637.

[2] Ismail, H., Edyham, M.R., and Wirjosentono, B. Bamboo fibre filled natural rubber composites: the effects of filler loading and bonding agent. Polym. Test. 21 (2002): 139–144.

[3] Geethamma, V.G., Kalaprasad, G., Groeninckx, G., and Thomas, S. Dynamic mechanical behavior of short coir fiber reinforced natural rubber composites. Compos.: Part A 36 (2005): 1499–1506.

[4] Ismail, H., Nasaruddin, M.N., and Rozman, H.D. The effect of multifunctional additive in white rice husk ash filled natural rubber compounds. Eur. Polym. J. 35 (1999): 1429-1437.

[5] Nair, K.G., and Dufresne, A. Crab shell chitin whisker reinforced natural rubber nanocomposites. 2. Mechanical behavior. Biomacromol. 4 (2003): 666–674.

[6] Ismail, H., and Jaffri, R.M. Physico-mechanical properties of oil palm wood flour filled natural rubber composites. Polym. Test. 18 (1999): 381–388.

[7] Abdelmouleh, M., Boufi, S., Belgacem, M.N., and Dufresne, A. Short natural-fibre reinforced polyethylene and natural rubber composites: Effect of silane coupling agents and fibers loading. Compos. Sci. Tech. 67 (2007): 1627–1639.

[8] Birchall, J.D., and Thomas, N.L. On the architecture and function of cuttlefish bone. J. Mater. Sci. 18 (1983): 2081–2086.

[9] Poompradub, S., Ikeda, Y., Kokubo, Y., and Shiono, T. Cuttlebone as reinforcing filler for natural rubber. Eur. Polym. J. 44 (2008): 4157-4164.

[10] Fong, C.L. Introduction to Natural Rubber Latex, RRIM Training Manual on Natural Rubber Processing. Kaula lumphur; 1992 (reprinted)

[11] Dictionary and Encyclopedia Directory [Online]. Available from http://www.wordiq.com/definition/Rubber [2010, September 16].

[12] Chemistry explained: Foundations and Applications [Online]. Available from http://www.chemistryexplained.com/Ru-Sp/Rubber.html [2010, September 18].

[13] Brydson, J. A. Rubber Chemistry. London: Applied science, 1978.

[14] Nagdi, K. Rubber as an Engineering material: Guideline for user. New York: Henser Plublisher, 1993.

[15] Hoffmann, W. Rubber Technology Handbook. New York: Hanser Plublisher, 1989.

[16] Richard, F.G. The Mixing of Rubber. London: Chapman & Hall, 1997.

[17] Gupta, B.R. Rubber Processing on a Two-Roll Mill. New Delhi: Allied Publishers, 1998.

[18] Rodgers, B. Rubber compounding: Chemistry and application. New York: Marcel Dekker, 2004.

[19] Properties of natural rubber [Online]. Available from http://www.tutor vista.com/content/chemistry/chemistry-ii/carbon-compounds/natural-rubber.php [2010, October 3]

[20] Mortan, M. Rubber Technology. 2nd ed. New York: Van Nostrand Reinhold, 1973.

[21] Odian, G. Principles of Polymerization. 4th ed. New Jersey: Wiley & Sons, 2004.

[22] Bateman, L., Moore, C.G., Porter, M. and Saville, B. The Chemistry and Physics of Rubber-Like Substances. New York: John Wiley & Sons, 1963.

[23] Hofmann, W. Vulcanization and Vulcanizing Agents. London: Maclaren, 1967.

[24] Coran, A.Y. Science and Technology of Rubber. New York: Academic Press, 1978.

[25] Mark, J.E., Erman, B., and Eirich, F. Science and Technology of Rubber. 3rd ed. London: Academic Press, 2005.

[26] Marzocca, A.J., Garraza, A.L.R., Sorichetti, P., and Mosca, H.O. Cure kinetics and swelling behavior in polybutadiene rubber. Polym. Test. 29 (2010): 477–482.

[27] ASTM D395 Method B, Test performed either on plied up specimens from actual hose or standard ASTM slabs cure to similar cure conditions as hose. 2002.

[28] Schapp, A.A, and Peters M.W.G.M. Twaron para-aramid fiber in knitted hoses; influence of the yarn properties on the hose performance. Meeting of ACS Rubber Division, Cleveland, OH, October 1997, Paper 50.

[29] Keller, RC. Advances in ethylene-propylene elastomer compounding for hose applications. Rubber World 188 (1983): 33.

[30] Loan, L.D., and Winslow, F.H. Macromolecules: An Introduction to Polymer Science. New York: Academic Press, 1979.

[31] Roberts, A.D. Natural Rubber Science and Technology. New York: Oxford University Press, 1990.

[32] Elliot, D.J. Developments with Natural Rubber in Developments in Rubber Technology. London: Applied Science Publisher, 1979.

[33] Blow, C.M., and Hepburn, C. Rubber Technology and Manufacture. 2nd ed. London: Butterworth Scientific, 1982.

[34] Ciesielski, A. An Introduction to Rubber Technology. England: Rapra Technology, 2000.

[35] Ciullo, P.A., and Hewitt, N. The rubber formulary. New York: Noyes / William Andrew, 1999.

[36] Ciullo, P.A. Industrial Minerals and Their Uses A Handbook and Formulary. New Jersey: Noyes Publication, 1996.

[37] Castano, N., Greiff, M.D., and Naranjo, A.C. Applied Rubber Technology. Munich: Carl Hanser Verlag, 2001.

[38] Karak, N. Fundamentals of Polymers: Raw Materials to Finish Products. New Delhi: PHI Learning Private, 2009.

[39] Leblanc, J.L. Filled Polymers: Science and Industrial Application. USA: Taylor & Francis, 2010.

[40] Rothon, R.N. Particulate-Filled Polymer Composites. 2nd ed. England: Rapra Technology, 2003.

[41] Harper, C. Handbook of Plastics Technologies: The Complete Guide to Properties and Performance. USA: McGraw-Hill, 2006.

[42] Whelan, T. Polymer Technology Dictionary. London: Chapman & Hall, 1994.

[43] Thomas, S., and Stephen, R. Rubber Nanocomposites: Preraration, Properties and Application. Singapore: Wiley & Sons, 2010.

[44] Ishida, H. Polymer Composite Processing. Cleveland: Case Western Reserve University, 1997.

[45] Gibson, R.F. Principles of Composite Material Mechanics. New York: McGrew-Hill, 1994.

[46] Kogel, J.E., Trivedi, N.C., Barker, J.M., and Krukowski, S.T. Industrial Minerals & Rocks: Commodities, Markets and Uses. Colorado: Society for Mining, Metallurgy and Exploration, 2006.

[47] Xanthos, M. Functional Fillers for Plastics. 2nd ed. Germany: Wiley-VCH, 2010.

[48] Vansant, E.F., Van Der Voort, P., and Vrancken, K.C. Characterization and Chemical Modification of the Silica Surface. Amsterdam: Elsevier Science, 1995.

[49] Hepburn, C. Rubber Compounding Ingredients Need: Theory and Innovation part I. England: Rapra technology, 1981.

[50] Katz, H.S., and Milewski, J.V. Handbook of Fillers and Reinforcements for Plastics. New York: Van Nostrand Reinhold, 1978.

[51] Jacob, M., Thomas, S., and Varughese, K.T. Mechanical properties of sisal/oil palm hybrid fiber reinforced natural rubber composites. Compos. Sci. Technol. 64 (2004): 955–965.

[52] Wang, Z.F., et al. The impact of esterification on the properties of starch/natural rubber composite. Compos. Sci. Technol. 69 (2009): 1797–1803.

[53] Al Sagheer, F.A., Al-Sughayer, M.A., Muslim, S., and Elsabee, M.Z. Extraction and characterization of chitin and chitosan from marine sources in Arabian Gulf. Carbohyd. Polym. 77 (2009): 410-419.

[54] Lavall, R.L., Assis, O.B.G., Sergio, P., and Filho, C. β-chitin from the pens of Loligo sp.: Extraction and characterization. Bioresource Technol. 98 (2007): 2465–2472.

[55] Nishi, T., and Nagano, F. The Physical Testing Standard of Rubber. Rubber research centre. Document number 117 (1983): 114-121.

[56] Abdou, E.S., Nagy, K.S.A., and Elsabee, M.Z. Extraction and characterization of chitin and chitosan from local sources. Bioresource Technol. 99 (2008): 1359–1367.

[57] Hu, X., *et al.* Solubility and property of chitin in NaOH/urea aqueous solution. Carbohyd. Polym. 70 (2007): 451–458.

[58] Geethamma, V.G., Joseph, R., and Thomas, S. Short coir fiber-reinforced natural rubber composites: Effects of fiber length, orientation, and alkali treatment. J. Appl. Polym. Sci. 55 (1995): 583-594.

[59] Sae-oui, P., Thepsuwan, U., and Hatthapanit, K. Effect of curing system on reinforcing efficiency of silane coupling agent. Polym. Test. 23 (2004): 397–403.

[60] Pal, K., *et al.* Effect of epoxidized natural rubber–organoclay nanocomposites on NR/high styrene rubber blends with fillers. Mater. Design 30 (2009): 4035–4042.

[61] Ismail, H., and Chia, H.H. The effects of multifunctional additive and vulcanization systems on silica filled epoxidized natural rubber compounds. Eur. Polym. J. 34 (1998): 1857-1863.

[62] El-Salam, F.A., El-Salam, M.H.A., and Mohamed, M.I. Vulcanizing system dependence of the rubbery swelling, dielectric and doppler shift characteristics of IIR/EPDM blends. Egypt. J. Solids 29 (2006): 181-192.

[63] Ishiaku, U.S., Chong, C.S., and Ismail, H. Cure characteristics and vulcanizate properties of a natural rubber compound extended with convoluted rubber powder. Polym. Test. 19 (2000): 507–521.

[64] Nagajima, M. The Science and Practice of Rubber Mixing. England: Rapra technology, 2000.

[65] Rattanasom, N., Poonsuk, A., and Makmoon, T. Effect of curing system on the mechanical properties and heat aging resistance of natural rubber/tire tread reclaimed rubber blends. Polym. Test. 24 (2005): 728–732.

[66] Chaichua, B., Prasassarakich, P., and Poompradub, S. In situ silica reinforcement of natural rubber by sol–gel process via rubber solution. J. Sol-Gel Sci. Tech. 52 (2009): 219–227.

[67] Jin, F.L., and Park, S.J. Thermo-mechanical behaviors of butadiene rubber reinforced with nano-sized calcium carbonate. Mater. Sci. Eng. A 478 (2008): 406–408.

[68] Zhou, Z.W., Zhu, Y.F., and Liang, J. Preparation and properties of powder styrene–butadiene rubber composites filled with carbon black and carbon nanotubes. Mater. Res. Bull. 42 (2007): 456–464.

[69] Nakason, C., Kaesaman, A., and Eardrod, K. Cure and mechanical properties of natural rubber-g-poly(methyl methacrylate) -cassava starch compounds. Mater. Lett. 59 (2005): 4020 – 4025.

[70] Mostafa, A., Abouel-Kasem, A., Bayoumi, M.R., and El-Sebaie, M.G. The influence of CB loading on thermal aging resistance of SBR and NBR rubber compounds under different aging temperature. Mater. Design 30 (2009): 791–795.

[71] Vinod, V.S., Varghese, S., and Kuriakose, B. Degradation behaviour of natural rubber–aluminium powder composites: effect of heat, ozone and high energy radiation. Polym. Degrad. Stab. 75 (2002): 405–412.

[72] Allen, N.S., et al. Influence of ozone on styrene–ethylene–butylene–styrene (SEBS) copolymer. Polym. Degrad. Stab. 79 (2003): 297–307.

[73] Mykhaylyk, T.A., Collins, S., Jani, C., and Hamley, I.W. Ozone etching of a highly asymmetric triblock copolymer with a majority polydiene component. Eur. Polym. J. 40 (2004): 1715–1721.

[74] Kumnuantip, C., and Sombatsompop, N. Dynamic mechanical properties and swelling behaviour of NR/reclaimed rubber blends. Mater. Lett. 57 (2003): 3167– 3174.

[75] Montgomery, T.S., and William, J.M. Introduction to Polymer Viscoelasticity. 3rd. New Jersey: Wiley & Sons, 2005.

APPENDICES

Appendix A

Table A-1 Material specification of commercial calcium carbonate (Silver-W).

Properties	Specification
Particle shape	Spindle
Appearance	White powder
Whiteness (Kett), %	92
BET surface area, m^2/g	5.5
pH	10.3
Surface coating agents	-
Diameter of a primary particle, nm	1500

Appendix B

Data of Cure Characteristics of NR Compounding

Table B-1 Optimum cure time (t_{c90}), scorch time (t_{s2}) and M_{HR}-M_L (maximum torque
- minimum torque) of commercial $CaCO_3$ or cuttlebone particles filled
NR vulcanizates cured with the CV system.

Sample code	M_L (lbf-in)	M_{HR} (lbf-in)	M_{HR}-M_L (lbf-in)	T_{s2} (min)	T_{c90} (min)	Cure Time[*] (min)	Curing Temperature (^{0}C)
NR	0.15	9.09	8.94	3.23	5.38	10	155
CA-10	0.14	9.49	9.35	3.15	5.08	10	155
CA-20	0.15	11.54	11.39	3.07	5.43	10	155
CA-40	0.20	12.61	12.41	2.49	4.48	10	155
CA-60	0.22	15.10	14.88	2.42	4.57	10	155
CA-80	0.19	16.76	16.57	2.21	4.36	10	155
CA-100	0.25	19.74	19.49	2.17	4.25	10	155
CTB-10	0.16	8.68	8.52	2.48	4.27	10	155
CTB-20	0.17	10.21	10.04	2.58	4.65	10	155
CTB-40	0.23	13.18	12.95	2.54	5.36	10	155
CTB-60	0.19	17.02	16.83	1.96	4.86	10	155
CTB-80	0.22	15.20	14.98	2.25	5.03	10	155
CTB-100	0.19	19.76	19.57	1.89	4.79	10	155

* The average cure time was used in order to keep the crosslink density constant in each sample.

Table B-2 Optimum cure time (t_{c90}), scorch time (t_{s2}) and M_{HR}-M_L (maximum torque
- minimum torque) of commercial $CaCO_3$ or cuttlebone particles filled
NR vulcanizates cured with the semi-EV system.

Sample code	M_L (lbf-in)	M_{HR} (lbf-in)	M_{HR}-M_L (lbf-in)	T_{s2} (min)	T_{c90} (min)	Cure Time* (min)	Curing Temperature (^{0}C)
NR	0.11	6.96	6.85	4.56	5.54	10	155
CA-10	0.10	8.41	8.31	3.37	5.38	10	155
CA-20	0.07	8.88	8.81	3.32	4.57	10	155
CA-40	0.14	11.37	11.23	3.05	5.20	10	155
CA-60	0.17	13.07	12.90	3.04	5.08	10	155
CA-80	0.11	13.84	13.73	2.29	3.28	10	155
CA-100	0.15	15.45	15.30	2.48	3.46	10	155
CTB-10	0.13	7.89	7.76	3.34	4.39	10	155
CTB-20	0.13	8.47	8.34	3.04	4.01	10	155
CTB-40	0.13	13.38	13.25	3.00	4.39	10	155
CTB-60	0.17	17.3	17.13	2.45	4.29	10	155
CTB-80	0.17	13.25	13.08	2.12	3.23	10	155
CTB-100	0.17	14.78	14.61	1.42	2.52	10	155

* The average cure time was used in order to keep the crosslink density constant in each sample.

Table B-3 Optimum cure time (t_{c90}), scorch time (t_{s2}) and M_{HR}-M_L (maximum torque - minimum torque) of commercial $CaCO_3$ or cuttlebone particles filled NR vulcanizates cured with the EV system.

Sample code	M_L (lbf-in)	M_{HR} (lbf-in)	M_{HR}-M_L (lbf-in)	T_{s2} (min)	T_{c90} (min)	Cure Time[*] (min)	Curing Temperature (^{0}C)
NR	0.34	6.18	5.84	7.06	11.20	15	155
CA-10	0.37	6.79	6.42	6.95	10.58	15	155
CA-20	0.36	7.38	7.02	6.37	9.93	15	155
CA-40	0.26	7.95	7.69	6.14	8.77	15	155
CA-60	0.31	9.71	9.40	5.56	8.01	15	155
CA-80	0.18	10.29	10.11	4.58	6.99	15	155
CA-100	0.14	10.82	10.68	4.18	6.26	15	155
CTB-10	0.31	6.36	6.05	6.74	9.42	15	155
CTB-20	0.30	6.77	6.47	6.11	8.87	15	155
CTB-40	0.26	7.69	7.43	5.80	8.43	15	155
CTB-60	0.24	8.61	8.37	5.28	7.76	15	155
CTB-80	0.20	9.58	9.38	4.77	8.19	15	155
CTB-100	0.16	10.33	10.17	4.22	7.32	15	155

* The average cure time was used in order to keep the crosslink density constant in each sample.

Appendix C

Data of Mechanical Properties of Vulcanized Rubber

Table C-1 Mechanical properties of commercial $CaCO_3$ or cuttlebone particles filled NR vulcanizates before and after thermal aging at 100 ^{0}C

for 22 $\pm$ 2 h in conventional vulcanized system (CV).

Sample code	Before aging					After aging				
	M^a_{100} (MPa)	M^b_{300} (MPa)	T_B^c (MPa)	E_B^d (%)	Hardness (Shore A)	M^a_{100} (MPa)	M^b_{300} (MPa)	T_B^c (MPa)	E_B^d (%)	Hardness (Shore A)
NR	1.33+0.04	3.78+0.17	20.77+2.10	604+43	48.6+0.54	1.46+0.07	4.42+0.1	9.49+3.38	397+46	47.6+1.08
CA-10	1.40+0.13	3.74+0.24	20.92+0.91	571+25	49.8+0.45	1.21+0.01	3.08+0.55	4.81+0.97	343+55	49.6+0.54
CA-20	1.54+0.09	3.86+0.30	21.30+1.60	554+13	50.6+1.14	1.74+0.11	4.39+0.59	14.21+1.03	500+29	50.4+0.65
CA-40	1.77+0.01	3.90+0.02	18.40+1.31	559+16	56.0+0.70	1.79+0.09	3.78+0.15	13.76+1.18	518+5	53.2+0.44
CA-60	1.80+0.06	3.39+0.06	16.22+0.77	581+13	57.0+0.79	1.94+0.07	3.58+0.07	12.49+0.24	506+74	55.4+0.65
CA-80	1.99+0.05	3.74+0.10	14.46+0.14	552+26	60.2+0.83	2.00+0.21	3.76+0.18	11.57+0.70	504+5	58.1+0.74
CA-100	2.11+0.05	3.88+0.12	11.53+0.42	513+17	63.0+1.51	1.88+0.05	3.25+0.25	9.07+0.48	499+20	59.5+0.35
CTB-10	1.37+0.04	3.63+0.01	22.57+1.11	633+19	50.0+0.44	1.67+0.04	-	9.22+0.51	355+7	49.5+0.50
CTB-20	1.44+0.01	3.72+0.05	23.67+0.38	620 +12	52.0+0.83	1.37+0.09	3.76+0.19	17.39+1.08	583+16	51.6+0.54
CTB-40	1.75+0.06	3.98+0.19	21.95+0.47	610+4	53.6+0.89	1.55+0.12	3.78+0.24	15.33+0.68	531+24	53.6+0.41
CTB-60	1.80+0.02	4.29+0.20	17.01+0.84	588+16	58.5+0.50	1.61+0.06	3.76+0.13	12.04+2.67	563+44	54.9+0.54
CTB-80	1.95+0.01	4.29+0.08	14.47+0.42	551+6	60.4+0.54	1.97+0.14	4.10+0.22	11.70+0.33	551+17	58.4+0.41
CTB-100	2.24+0.09	4.50+0.07	12.37+0.49	518+10	63.0+0.70	2.01+0.07	3.91+0.23	9.59+1.84	529+67	63.2+0.44

[a] Stress at 100% elongation.
[b] Stress at 300% elongation.
[c] Tensile strength at break.
[d] Elongation at break.
- : means no data obtained because of rupture of the rubber sample at that elongation.

Table C-2 Mechanical properties of commercial $CaCO_3$ or cuttlebone particles filled NR vulcanizates before and after thermal aging at 100 ^{0}C

        for 22 $\pm$ 2 h in semi-efficient vulcanized system (semi-EV).

Sample code	Before aging					After aging				
	M^a_{100} (MPa)	M^b_{300} (MPa)	T_B^c (MPa)	E_B^d (%)	Hardness (Shore A)	M^a_{100} (MPa)	M^b_{300} (MPa)	T_B^c (MPa)	E_B^d (%)	Hardness (Shore A)
NR	0.81±0.03	2.14±0.09	22.97±2.45	628±9	41.2±0.27	1.11±0.01	3.71±0.12	19.55±0.88	483±14	42.0±0.00
CA-10	0.96±0.03	2.48±0.09	24.12±0.57	637±5	43.8±0.27	0.88±0.02	2.40±0.02	14.95±1.78	591±23	45.0±0.00
CA-20	1.04±0.02	2.62±0.03	20.71±0.45	623±8	45.3±0.44	0.88±0.01	2.49±0.04	13.09±1.00	552±6	47.7±0.27
CA-40	1.32±0.07	2.94±0.04	20.61±0.52	604±10	49.1±0.22	1.06±0.02	2.77±0.10	13.07±2.08	490±0	48.5±0.50
CA-60	1.45±0.03	3.10±0.03	17.47±0.20	585±5	51.7±0.44	1.48±0.01	3.52±0.21	14.37±0.37	531±10	50.7±0.44
CA-80	1.62±0.01	3.23±0.07	15.28±0.30	533±11	53.8±1.15	1.48±0.03	2.59±0.11	5.97±0.84	460±23	55.8±0.57
CA-100	1.76±0.06	3.48±0.09	7.29 ±0.59	460±38	57.6±0.41	1.45±0.01	2.38±0.09	6.83±0.59	493±1	57.7±0.57
CTB-10	1.05±0.01	2.82±0.10	22.41±0.86	603±21	42.9±0.22	1.23±0.03	3.35±0.06	19.59±2.13	515±29	43.1±0.41
CTB-20	1.01±0.02	2.70±0.11	23.49±0.43	652 ±12	45.9±0.74	1.19±0.05	3.10±0.22	18.69±2.88	540±2	45.9±0.22
CTB-40	1.34±0.02	3.16±0.15	20.67±0.49	604±17	48.6±0.22	1.34±0.03	3.35±0.03	16.91±0.04	533±9	48.8±0.27
CTB-60	1.46±0.10	3.33±0.09	17.96±0.59	590±9	51.7±0.44	1.51±0.00	3.75±0.01	15.66±0.28	521±5	50.9±0.22
CTB-80	1.64±0.04	3.78±0.19	14.20±0.21	537±10	54.0±0.35	1.70±0.01	3.96±0.04	12.36±0.52	483±22	54.0±0.35
CTB-100	1.75±0.00	4.06±0.08	8.00±0.59	461±39	56.9±0.22	1.42±0.05	3.39±0.23	7.61±0.76	460±23	56.2±0.27

[a] Stress at 100% elongation.
[b] Stress at 300% elongation.
[c] Tensile strength at break.
[d] Elongation at break.

Table C-3 Mechanical properties of commercial $CaCO_3$ or cuttlebone particles filled NR vulcanizates before and after thermal aging at 100 ^{0}C

for 22 $\pm$ 2 h in efficient vulcanized system (EV).

Sample code	Before aging					After aging				
	M^a_{100} (MPa)	M^b_{300} (MPa)	T_B^c (MPa)	E_B^d (%)	Hardness (Shore A)	M^a_{100} (MPa)	M^b_{300} (MPa)	T_B^c (MPa)	E_B^d (%)	Hardness (Shore A)
NR	0.49±0.00	1.26±0.04	6.27±1.34	569±11	37.1±0.41	0.55±0.02	1.38±0.02	5.19±0.32	568±14	35.4±0.41
CA-10	0.52±0.01	1.28±0.01	8.54±0.01	622±15	37.7±0.27	0.84±0.01	2.04±0.09	8.62±0.56	593±3	37.9±0.96
CA-20	0.70±0.07	1.86±0.07	15.50±0.78	686±15	39.3±0.27	0.89±0.02	2.16±0.08	10.72±0.47	593±10	38.7±0.83
CA-40	0.80±0.02	2.25±0.03	15.42±0.93	648±6	42.3±0.27	0.93±0.01	2.45±0.05	13.18±0.33	606±6	43.1±0.54
CA-60	1.03±0.06)	2.73±0.01	14.89±0.17	601±11	46.7±0.27	1.17±0.03	2.80±0.06	13.13±0.35	583±6	45.8±0.44
CA-80	1.08±0.01	2.75±0.08	9.73±0.06	581±13	49.2±0.27	1.42±0.03	3.28±0.03	10.89±0.60	534±14	47.8±0.44
CA-100	1.26±0.05	2.91±0.04	9.31±0.15	531±5	51.1±0.41	1.61±0.04	3.07±0.06	9.41±0.63	548±9	53.7±0.57
CTB-10	0.66±0.01	1.78±0.06)	9.03±0.17	597±18	37.5±0.70	0.73±0.00	1.79±0.08	7.43±0.08	555±20	38.1±0.54
CTB-20	0.74±0.03	1.90±0.05	18.90±0.25	654±18	38.8±0.27	0.79±0.02	2.00±0.13	15.15±0.16	602±15	39.7±0.27
CTB-40	0.84±0.02	2.31±0.13	15.83±0.16	595±17	43.3±0.27	0.94±0.03	2.30±0.07	12.56±0.40	634±3	42.0±0.35
CTB-60	1.04±0.06	2.99±0.01	14.51±0.74	564±17	46.2±0.27	1.07±0.06	2.53±0.02	13.15±0.95	628±8	46.3±0.27
CTB-80	1.13±0.01	3.20±0.08	12.49±0.36	527±5	49.1±0.22	1.17±0.03	3.00±0.04	11.26±0.33	557±2	49.8±0.44
CTB-100	1.23±0.07	3.32±0.09	9.51±0.29	494±3	50.5±0.50	1.46±0.03	3.40±0.07	9.39±0.01	501±17	52.9±0.54

[a] Stress at 100% elongation.
[b] Stress at 300% elongation.
[c] Tensile strength at break.
[d] Elongation at break.

Appendix D

Comparing of the Mechanical Properties of NR Composite Materials in both Sulfur and Peroxide Vulcanization System

Table D-1 Mechanical properties of commercial $CaCO_3$ or cuttlebone particles filled NR vulcanizates in sulfur and peroxide vulcanization systems.

Sample code	CV system				semi-EV system			
	M^a_{100} (MPa)	M^b_{300} (MPa)	T_B^c (MPa)	E_B^d (%)	M^a_{100} (MPa)	M^b_{300} (MPa)	T_B^c (MPa)	E_B^d (%)
NR	1.33±0.04	3.78±0.17	20.77±2.10	604±43	0.81±0.03	2.14±0.09	22.97±2.45	628±9
CA-10	1.40±0.13	3.74±0.24	20.92±0.91	571±25	0.96±0.03	2.48±0.09	24.12±0.57	637±5
CA-20	1.54±0.09	3.86±0.30	21.30±1.60	554±13	1.04±0.02	2.62±0.03	20.71±0.45	623±8
CA-40	1.77±0.01	3.90±0.02	18.40±1.31	559±16	1.32±0.07	2.94±0.04	20.61±0.52	604±10
CA-60	1.80±0.06	3.39±0.06	16.22±0.77	581±13	1.45±0.03	3.10±0.03	17.47±0.20	585±5
CA-80	1.99±0.05	3.74±0.10	14.46±0.14	552±26	1.62±0.01	3.23±0.07	15.28±0.30	533±11
CA-100	2.11±0.05	3.88±0.12	11.53±0.42	513±17	1.76±0.06	3.48±0.09	7.29±0.59	460±38
CTB-10	1.37±0.04	3.63±0.01	22.57±1.11	633±19	1.05±0.01	2.82±0.10	22.41±0.86	603±21
CTB-20	1.44±0.01	3.72±0.05	23.67±0.38	620±12	1.01±0.02	2.70±0.11	23.49±0.43	652±12
CTB-40	1.75±0.06	3.98±0.19	21.95±0.47	610±4	1.34±0.02	3.16±0.15	20.67±0.49	604±17
CTB-60	1.80±0.02	4.29±0.20	17.01±0.84	588±16	1.46±0.10	3.33±0.09	17.96±0.59	590±9
CTB-80	1.95±0.01	4.29±0.08	14.47±0.42	551±6	1.64±0.04	3.78±0.19	14.20±0.21	537±10
CTB-100	2.24±0.09	4.50±0.07	12.37±0.49	518±10	1.75±0.00	4.06±0.08	8.00±0.59	461±39

| Sample code	EV system				Peroxide system			
	M^a_{100} (MPa)	M^b_{300} (MPa)	T_B^c (MPa)	E_B^d (%)	M^a_{100} (MPa)	M^b_{300} (MPa)	T_B^c (MPa)	E_B^d (%)
NR	0.49±0.00	1.26±0.04	6.27±1.34	569±11	0.7±0.01	2.1±0.02	7.0±0.05	575±3
CA-10	0.52±0.01	1.28±0.01	8.54±0.01	622±15	0.7±0.00	2.0±0.01	11.2±0.06	635±6
CA-20	0.70±0.07	1.86±0.07	15.50±0.78	686±15	0.8±0.01	2.3±0.03	11.3±0.08	615±6
CA-40	0.80±0.02	2.25±0.03	15.42±0.93	648±6	1.0±0.00	3.0±0.02	13.2±0.07	615±2
CA-60	1.03±0.06	2.73±0.01	14.89±0.17	601±11	-	-	-	-
CA-80	1.08±0.01	2.75±0.08	9.73±0.06	581±13	1.6±0.03	4.4±0.03	12.5±0.06	580±8
CA-100	1.26±0.05	2.91±0.04	9.31±0.15	531±5	1.9±0.03	4.5±0.01	7.5±0.06	500±7
CTB-10	0.66±0.01	1.78±0.06	9.03±0.17	597±18	0.7±0.01	2.2±0.04	11.4±0.04	616±3
CTB-20	0.74±0.03	1.90±0.05	18.90±0.25	654±18	0.8±0.01	2.6±0.03	11.5±0.02	596±0
CTB-40	0.84±0.02	2.31±0.13	15.83±0.16	595±17	1.0±0.00	3.0±0.02	11.0±0.04	579±3
CTB-60	1.04±0.06	2.99±0.01	14.51±0.74	564±17	-	-	-	-
CTB-80	1.13±0.01	3.20±0.08	12.49±0.36	527±5	1.5±0.01	4.1±0.01	8.4±0.03	511±1
CTB-100	1.23±0.07	3.32±0.09	9.51±0.29	494±3	1.8±0.01	5.2±0.02	8.8±0.07	490±2

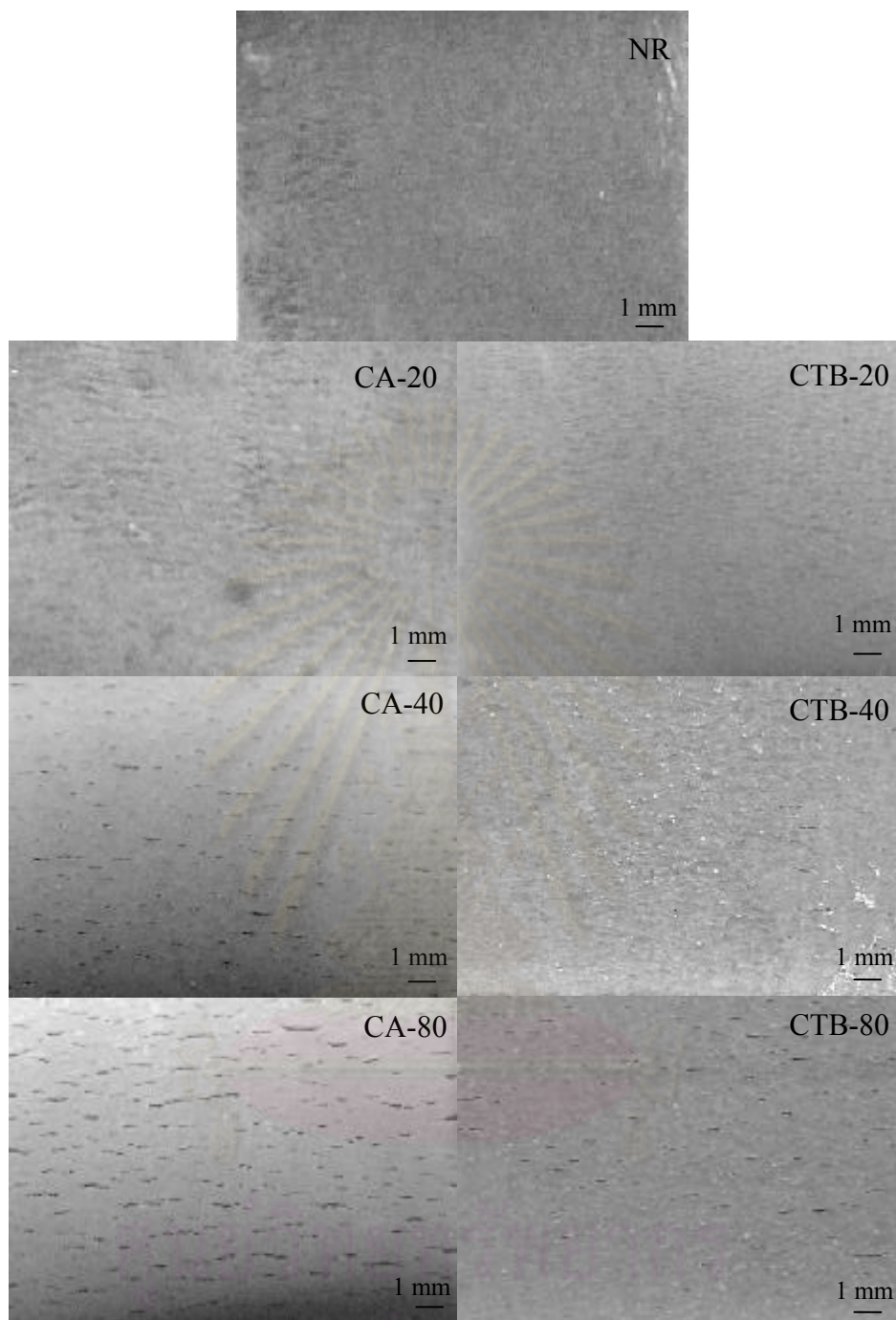[a] Stress at 100% elongation.
[b] Stress at 300% elongation.
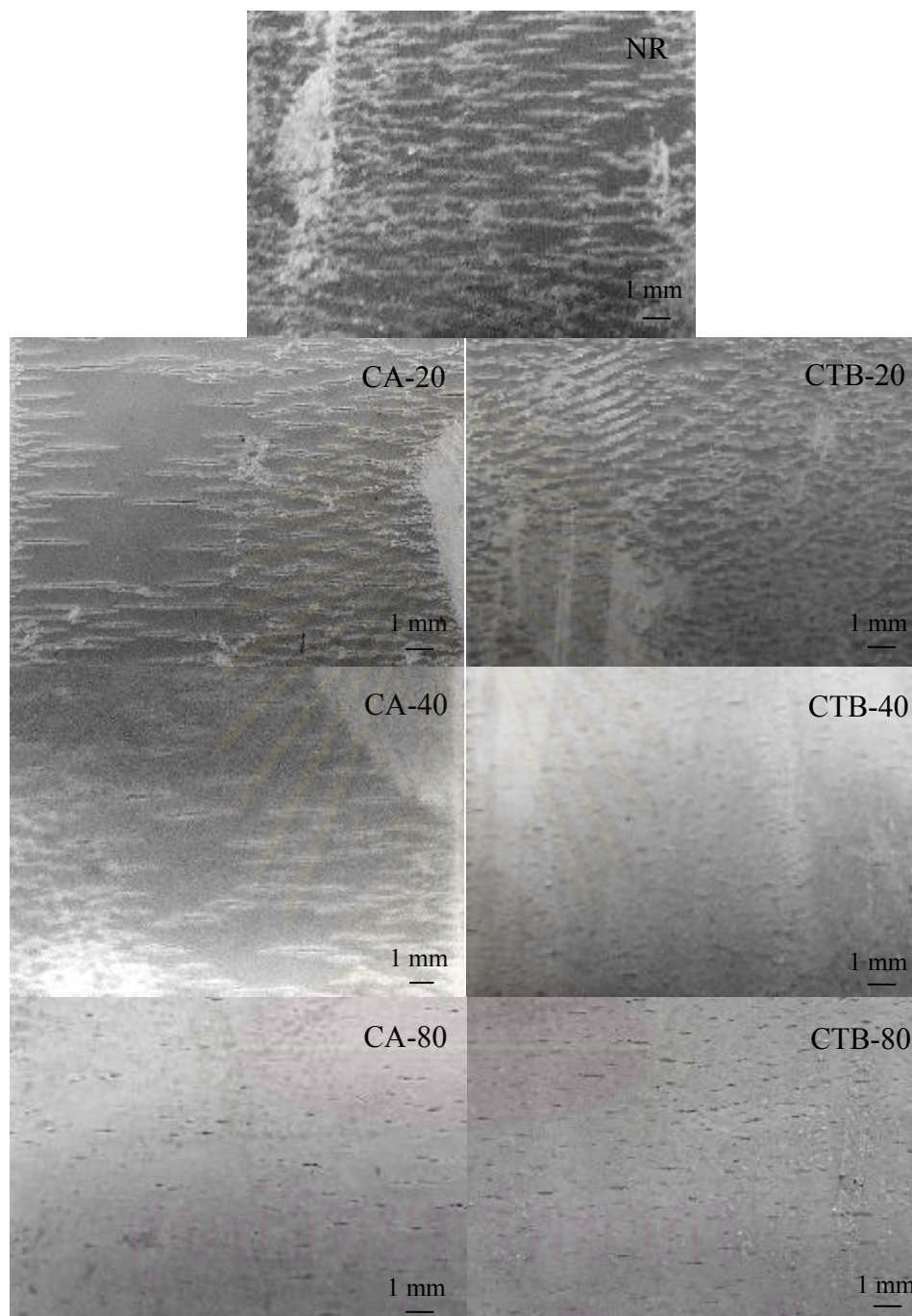[c] Tensile strength at break.
[d] Elongation at break.

Appendix E
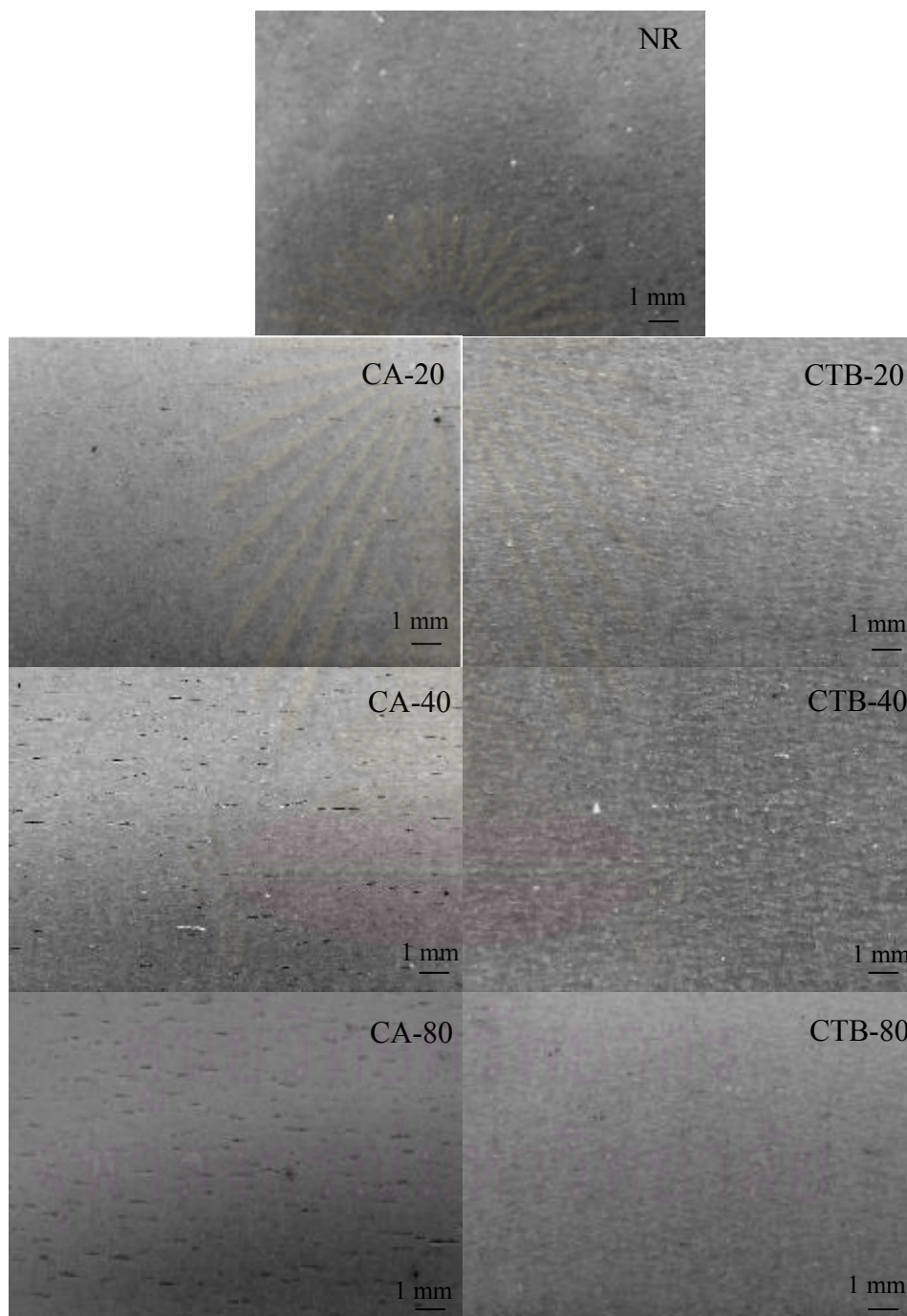
Figure E-1 Stretched surfaces of commercial CaCO₃ and cuttlebone particles filled
NR vulcanizates in CV systems after exposure to ozone (50 pphm) at
40 °C for 24 h.

Figure E-2 Stretched surfaces of commercial CaCO₃ and cuttlebone particles filled
NR vulcanizates in semi-EV systems after exposure to ozone (50 pphm)
at 40 °C for 24 h.

Figure E-3 Stretched surfaces of commercial CaCO$_3$ and cuttlebone particles filled
NR vulcanizates in EV systems after exposure to ozone (50 pphm) at
40 ^{0}C for 24 h.

Appendix F

Table F-1 The calculation of the total cost of the NR composites filled with commercial $CaCO_3$ or cuttlebone particles in the CV system.

Chemical	Quantity per batch (g)	Chemicals cost (Baht / kg.)	Electricity charge (Baht / batch)			Chemicals and electricity cost (baht / 100 g) (e = a+b+c)	Total cost (Baht / kg.) (e+f)1000 / 100, CA[h] (e+g)1000 / 100 , CTB[i] (e+d+g)1000 / 100 , CTB[j]	
			Two-roll mill	Compression molding	Vibratory mill machine			
Natural rubber (STR 5L)	100	102						
ZnO	5	83						
Stearic acid	2	40						
CBS	1	205						
Sulfur	3	24						
Total chemical cost		**11.63**[a]	6.46[*, b]	8.23[**, c]		26.32[e]		
Commercial $CaCO_3$ (CA)	10	50				0.5[f]	268.20[h]	
	20	50				1.0[f]	273.20[h]	
	40	50				2.0[f]	283.20[h]	
	80	50				4.0[f]	303.20[h]	
	100	50				5.0[f]	313.20[h]	
Cuttlebone (CTB)	10	0			4.79[***, d]	0[g]	263.20[i]	312.00[j]
	20	0			10.18[d]	0[g]	263.20[i]	365.90[j]
	40	0			20.35[d]	0[g]	263.20[i]	467.60[j]
	80	0			40.10[d]	0[g]	263.20[i]	665.10[j]
	100	0			49.68[d]	0[g]	263.20[i]	760.90[j]

[*] 16.4 kW*0.25 h = 4.10 kWh (1kWh = 1.575 baht)
$\qquad$ = 4.10 kWh*1.575 = 6.46 baht

[**] 15.84 kW*0.33 h = 5.23 kWh (1kWh = 1.575 baht)
$\qquad$ = 5.23 kWh*1.575 = 8.23 baht

[***] 380 kW*0.008 h = 3.04 kWh (1kWh = 1.575 baht)
$\qquad$ = 3.04 kWh*1.575 = 4.79 baht

[i] The cuttlebone particle was crushed without the machine.
[j] The cuttlebone particle was crushed by using the Vibratory mill machine.

ศูนย์วิทยทรัพยากร

จุฬาลงกรณ์มหาวิทยาลัย

VITAE

Mr. Pontawit Klungsuwan was born on February 11, 1986 in Bangkok, Thailand. He received a Bachelor's degree of Engineering, majoring in Petrochemical and Polymeric materials from Silpakorn University in 2008. He has pursued Master's degree in Petrochemistry and Polymer Science, Faculty of Science, Chulalongkorn University, Bangkok, Thailand since 2008 and finished his study in 2011.

Presentations

1. 11-12 March 2010 Oral presentation "Effect of cuttlebone on mechanical properties for natural rubber composites" The 18th Science Forum 2010 at Chulalongkorn University, Bangkok, Thailand.

2. 26-27 August 2010 Oral presentation "Green Filler for Natural Rubber Vulcanizate" International Conference for a Sustainable Greater Mekong Subregion at The Imperial Queen's Park Hotel, Bangkok, Thailand.

3. 6-8 November 2010 Oral presentation "Smart green composite: Effect of cuttlebone particle on the mechanical properties of NR vulcanizates" International Conference on Advances in Materials and Manufacturing Processes (ICAMMP 2010) at Shenzhen, China.

4. 10-11 March 2011 Oral presentation "The Reinforcement of NR Composites by Cuttlebone as Green Reinforcing Filler" The 19th Science Forum 2011 at Chulalongkorn University, Bangkok, Thailand.